Chemical and mechanical activation of hybrid fly ash cement

by

Grizelda du Toit

Submitted in partial fulfilment of the requirements for the degree

Philosophiae Doctor (PhD in Chemistry)

In the Faculty of Natural and Agricultural Sciences

University of Pretoria

Pretoria

October 2018

~ Declaration ~

I, Grizelda du Toit, declare that the thesis, which I hereby submit for the degree, PhD in Chemistry (Thesis), at the University of Pretoria, is my own work and has not previously been submitted by me for a degree at this, or any other tertiary institution.

Name of student: Grizelda du Toit Student number: 14320942

Signature:

Date: 25 October 2018

~ Acknowledgement ~

I wish to express my gratitude to:

- AfriSam (South Africa) Pty Ltd, for the financial aid and study opportunity, and also for making their laboratory resources and equipment available to me.

- My supervisor, Dr E.M (Liezel) van der Merwe, for agreeing to work with me in an unfamiliar discipline, but never giving up on me. For all the red track changes, all the e-mails, all the meetings and definitely all the coffee.

- To my co-supervisors, Prof. E.P. Kearsley for all your guidance, input and ideas, Prof. R.A. Kruger for sharing your invaluable experience with me, and finally, Mr. Mike Mc Donald, for continually supporting my studies while working, and making this process as easy on me and my family as possible.

- Ms Wiebke Grote (University of Pretoria) for the XRD analyses.

- The University of Pretoria Laboratory for Microscopy and Microanalysis for assistance with FESEM.

- Mr André Botha (University of Pretoria) for his time spent in assuring I have superb quality SEM micrographs.

- The National Research Foundation of South Africa for financial support (NRF; Grant No. TP14072580026).

- Last but definitely not least, my husband (Edwin du Toit). There would be no thesis without your never-ending love, encouragement and support. Also, thank you to my little Owen for making sure I didn't get too serious.

~ Summary ~

Hybrid fly ash cement is a binder with a composition between that of pozzolanic fly ash cement and alkali activated fly ash cement. Its production requires less cement clinker than ordinary Portland cement, facilitating a much needed reduction in the carbon dioxide footprint related to the production of high clinker-containing cement. Research on activation methods is required to overcome the low early age strength and slow strength development in hybrid fly ash cements. In this study the activation of a South African siliceous fly ash (70%) for use along with Portland cement (30%) in a hybrid alkaline binder was investigated. Both chemical (the addition of sodium sulfate) as well as mechanical (milling) activation of fly ash was studied.

This type of hybrid product falls outside of the scope of the accepted national standard, SANS 50197, which is adopted from the European standard EN 197, making it very important to understand as much as possible about the behaviour of this type of cement in the expectation of having it accepted by the standards bodies as well as the construction industry.

The literature tends to discuss the compressive strength of fly ash-lime systems (calcium hydroxide or calcium oxide) rather than fly ash-cement systems, even though a few studies have been published on hybrid cements. More emphasis is also placed on early age strength development (2 days up to 28 days) as opposed to the evolution of strength over a protracted time of up to a year. This study therefore aims to fill the gap by presenting and discussing compressive strength and characterisation results of hydrated fly ash hybrid cements over an extended curing period of up to a year. This will provide much needed and valuable information required for the production of cementitious products with a low carbon footprint.

It has been proven before that chemical activation in the form of sodium sulfate addition and mechanical activation via milling can both be used as effective activation methods for high fly ash containing hybrid cements. It is however not clear what effect the two activation techniques will have on compressive strength development over an extended curing period. Since fly ash chemistry (and to a certain extent cement chemistry) varies globally and even locally, it was imperative to test the effect of these activation techniques and the possible advantages they might present on local materials from South Africa.

The results obtained from this study showed that a fly ash hybrid cement containing 70% of a siliceous South African fly ash and 30% ordinary Portland cement, can reach mortar compressive strengths that comply with the national standard prescriptions i.e. a 32.5R (rapid early strength gain) when a combination of chemical (sodium sulfate) and mechanical activation is applied.

Characterisation and analytical techniques such as X-ray fluorescence (XRF), X-ray powder diffraction (XRD), Particle size distribution (PSD) analysis, Field emission scanning electron microscopy (FESEM), Thermogravimetric analysis (TGA), Fourier transform infrared spectroscopy (FTIR) and microcalorimetry (heat of hydration) of the raw and hydrated materials proved invaluable to some of the major findings regarding ettringite and pozzolanic reactivity of this study. Not only did the above mentioned activation techniques (especially the combination of chemical and mechanical activation) provide stable ettringite formation, but it also accelerated the pozzolanic reaction between fly ash and cement, which led to an improvement in early age strengths and strength development, resulting in hybrid cements that comply with the EN 197 cement strength requirements.

~ Table of contents ~

Chapter 1 - Introduction, objectives and scope

1.1. Introduction 1

1.2. Background 1

1.3. Aims and objectives of the study 4

1.4. Scope and limitations of the study 5

1.5. Methodology 6

1.6. Layout of the thesis 7

Chapter 2 - Review of the South African cement and fly ash *status quo* and hydration chemistry of hybrid fly ash cement

2.1. Introduction 9

2.2. Fly ash 9

2.2.1. Production and characteristics of South African fly ash 9

2.2.2. Fly ash classification according to EN 450 / SANS 50450 11

2.2.3. Global perspective of fly ash production and utilization 12

2.2.4. South African perspective on fly ash production and utilization 14

2.3. Fly ash as a component in the production of blended cement 15

2.3.1. The restrictions of fly ash-containing cements in the cement market (locally and globally) according to EN 197-1:2011 Edition 2 15

2.3.2. A short review on the hydration chemistry of ordinary Portland cement 16

2.3.3. A short review on the hydration chemistry of typical fly-ash (pozzolana) containing cement 18

2.4. Hybrid cement 20

2.4.1. What is hybrid cement? 20
2.4.2. Activation and production of high fly ash-containing hybrid cements 22
2.4.3. Hydration chemistry of high fly ash-containing hybrid cements 25
2.5. Conclusion 27

Chapter 3 - Experimental program

3.1. Introduction 29
3.2. Chemical characterisation techniques 32
3.2.1 X-ray fluorescence (XRF) 32
3.2.2 X-ray powder diffraction (XRD) 32
3.2.3 Particle size distribution (PSD) 33
3.2.4 Field emission scanning electron microscopy (FESEM) 34
3.2.5 Thermogravimetric analysis (TGA) 34
3.2.6 Fourier transform infrared spectroscopy (FTIR) 37
3.3. Characteristics of the fly ash surface reactivity exposed to a calcium hydroxide environment 39
3.4. Sulfate optimisation of a hybrid cement produced from unclassified fly ash (UFA) and cement (MC) 40
3.4.1 Introduction 40
3.4.2 Setting time 41
3.4.3 Early age strength development 41
3.5. Hybrid fly ash cement paste 43
3.5.1 Characterisation techniques 43
3.5.2 Setting time 45
3.5.3 Heat of hydration 45
3.5.4 Expansion (soundness) 48
3.6. Hybrid fly ash mortar tests 49

3.7. Hybrid fly ash concrete testing 50
3.7.1 Mix composition 50
3.7.2 Workability (Slump retention) 52
3.7.3 Strength behaviour 54
3.8. Overview of experimental program 55

Chapter 4 - Characterisation of raw cementitious materials

4.1 Introduction 56
4.2 X-ray fluorescence (XRF) 56
4.3 X-ray powder diffraction (XRD) 57
4.4 Particle size distribution (PSD) 59
4.5 Field emission scanning electron microscopy (FESEM) 61
4.6 Thermogravimetric analysis (TGA) 64
4.7 Fourier transform infrared spectroscopy (FTIR) 65
4.8 Conclusion 66

Chapter 5 - Investigation into the effect of chemical and mechanical activation

5.1 Introduction 67
5.2 Characteristics of the fly ash surface reactivity exposed to a calcium hydroxide environment 67
5.3 Sulfate optimisation study of a hybrid cement produced from unclassified fly ash (UFA) and cement 73
5.3.1. Setting time 74
5.3.2. Strength behaviour 76
5.4 Conclusion 82

Chapter 6 - Characterisation of hydrating hybrid fly ash cement paste

6.1 Introduction 85
6.2 Setting time 86
6.3 Heat of hydration 87
6.4 Chemical characterisation 91
6.4.1. X-ray powder diffraction (XRD) analysis 91
6.4.2. Thermogravimetric analysis (TGA) 95
6.4.3. Fourier transform infrared spectroscopy (FTIR) 101
6.5 The effect of chemical and mechanical activation on the pozzolanic reactivity of fly ash in a high fly ash hybrid cement 106
6.6 The effect of chemical and mechanical activation on stable ettringite formation in a high fly ash hybrid cement 108
6.7 Expansion (soundness) 111
6.8 Conclusion 114

Chapter 7 - Mortar test results and discussion of hybrid fly ash cement

7.1 Introduction 116
7.2 Strength of mortars 116
7.3 Conclusion 124

Chapter 8 - Concrete test results and discussion of hybrid fly ash cement

8.1 Introduction 125
8.2 Slump retention of concrete 125
8.3 Strength of concrete 126
8.4 Conclusion 131

Chapter 9 - Conclusions and recommendations for future work

9.1. Introduction.....132

9.2. Conclusions.....134

9.3. Recommendations for future work 138

References..... 140

~ List of tables ~

Table 2.1. Classification system of the European (and RSA) standards bodies for fly ash used in concrete according to EN 450 and SANS 50450. 12
Table 2.2. The 27 products in the family of common cements as published in EN 197 / SANS 50197 (CEN, 2011). 16

Table 3.1. The most prominent dehydration, dehydroxylation and decarbonation temperature regions for cement and hydrated cement. 35
Table 3.2. Typical FTIR characteristic transmission bands for species occurring in cement and hydrated cement (cm^{-1}). 38
Table 3.3. Mechanical and physical requirements from EN 197 given as characteristic values (CEN, 2011). 41
Table 3.4. Grading analysis of CEN sand complying with EN 196 / SANS 50196. 42
Table 3.5. Chemical composition (XRF, wt %) of the aggregates used in the concrete mixes. 51
Table 3.6. Grading analysis of the 22.4 mm stone and crusher sand used in the concrete mixes. 51
Table 3.7. Target mix design for hybrid fly ash concrete mixes. 52
Table 3.8. Slump limits according to SABS 1200 G 1982 and accepted in South Africa (SABS, 1982). 53

Table 4.1. Chemical composition (XRF, wt. %) of the starting materials. 57
Table 4.2. Mineralogical composition (XRD, wt. % normalised) of the starting materials. 58
Table 4.3. The particle size distribution (µm) of the raw materials at 10%, 50% and 90% of the respective sample size. 59

Table 5.1. Setting time of the UFA hybrid cement when Na_2SO_4 is added in dry powder form (n = 1). 75
Table 5.2. Compressive strength (MPa) of the UFA hybrid cement when Na_2SO_4 is added in dry powder form compared to Na_2SO_4 added in dissolved form. 77

Table 6.1. Mortar hybrid setting times (minutes) at different Na_2SO_4 additions for FCFA, UFA and MUFA hybrids. 86
Table 6.2. Numerical data for the total heat output for FCFA, UFA and MUFA at 0% and 5% Na_2SO_4, after 48 hours and 7 days. 90
Table 6.3. Heat released (Joule/gram) for the 4 hybrid cements at 41 hours of hydration. ...113

Table 8.1. Slump retention (mm) at different Na_2SO_4 additions for FCFA, UFA and MUFA hybrids....126

~ List of figures ~

Figure 2.1. Mineral matter transformation mechanism during combustion of coal to produce fly ash (Tomeczec & Palugniok, 2002). 10
Figure 2.2. Coal combustion products (CCP) and pulverised fly ash (PFA) production statistics for America, UK and Australia for the year 2014. 13
Figure 2.3 The position of hybrid fly ash cements relative to pozzolanic fly ash cements on the pure Portland cement (PC)-pure alkali activation of fly ash (AAFA) spectrum (Garcia-Lodeiro *et al.*, 2016b). 21

Figure 3.1. TGA and DTG of a hydrating Portland cement at different curing ages, illustrating typical decomposition processes of solids occurring in cementitious systems (Lothenbach *et al.*, 2016). 36
Figure 3.2. (a) The steel moulds in which mortar prims are cast and (b) the compressive strength testing equipment for mortar prisms. 43
Figure 3.3. Example of the EPS moulds used (left) and neat pastes cast in the EPS moulds (right) for analytical characterisation. 44
Figure 3.4. Example of a heat of hydration curve, presenting the typical five stages of heat evolution for ordinary Portland cement (Hu *et al.*, 2014).....46
Figure 3.5. Early age calorimetric data. Initial (In.) and final (Fi) setting times are indicated on the graphs. FAN4 is the considered scenario. (Donatello et al., 2013).....47
Figure 3.6. Example of an (a) ampule and syringes and (b) the TAM Air microcalorimeter. 48
Figure 3.7. The slump test, also illustrating the difference between the different practices (Domone, 2003). 53
Figure 3.8. Diagram providing an overview of the experimental program. 55

Figure 4.1. Particle size distribution of the three FA samples: (a) volume % and (b) cumulative undersize volume 60
Figure 4.2. Scanning electron micrographs representing the morphology of untreated (a-b) FCFA, (c-d) UFA and (e-f) MUFA at 3000x and 50000x magnification respectively. 62

Figure 4.3. Scanning electron micrographs representing the morphology of the unhydrated Portland cement sample (MC). 63
Figure 4.4. TGA (a) and DTG (b) data for the unhydrated, raw cementitious materials MC, UFA and MUFA. 64
Figure 4.5. FTIR transmission spectra of the cementitious materials used as starting material: (a) MC, (b) UFA and MUFA. 65

Figure 5.1. Morphology of FCFA after exposure (1 to 56 days) to a saturated solution of calcium hydroxide, with and without 5% sodium sulfate addition (50000x). 68
Figure 5.2. Morphology of UFA after exposure (1 to 56 days) to a saturated solution of calcium hydroxide, with and without 5% sodium sulfate addition (50000x). 69
Figure 5.3. Morphology of MUFA after exposure (1 to 56 days) to a saturated solution of calcium hydroxide, with and without 5% sodium sulfate addition (50000x). 70
Figure 5.4. XRD phase identification of the untreated fly ash samples and 56 day fly ash specimens exposed to a calcium hydroxide environment, with and without 5% sodium sulfate addition. 72
Figure 5.5. Initial and final time of the UFA hybrid cement when Na_2SO_4 is added in dry powder form (n = 1). 76
Figure 5.6. Sulfate optimisation - 1 day mortar compressive strengths. 78
Figure 5.7. Sulfate optimisation - 2 days mortar compressive strengths. 78
Figure 5.8. Sulfate optimisation - 7 days mortar compressive strengths. 81
Figure 5.9. Sulfate optimisation - 28 days mortar compressive strengths. 81

Figure 6.1. Graphical representation of the mortar hybrid setting times (minutes) at different Na_2SO_4 additions for FCFA, UFA and MUFA hybrids. 86
Figure 6.2. Heat evolution curves (heat flow rate (a,c) and cumulative heat (b,d)) for FCFA, UFA and MUFA at 0% and 5% Na_2SO_4, after 48 hours and 7 days. 88
Figure 6.3. XRD diffractograms of anhydrous cement, UFA and hydrated (a) UFA and (b) UFA5 hybrid cement, at all curing ages tested. 92
Figure 6.4. XRD diffractograms of anhydrous cement, MUFA and hydrated (a) MUFA and (b) MUFA5 hybrid cement, at all curing ages tested. 93
Figure 6.5. DTG and TGA data of anhydrous UFA, cement and hydrated UFA hybrid cement with no chemical activation applied, at all curing ages tested. 96

Figure 6.6. DTG and TGA data of anhydrous UFA, cement and hydrated UFA5 hybrid cement with chemical activation applied, at all curing ages tested. 97
Figure 6.7. DTG and TGA of anhydrous MUFA, cement and hydrated MUFA hybrid cement when mechanical activation is applied, at all curing ages tested. 98
Figure 6.8. DTG and TGA data of anhydrous MUFA, cement and hydrated MUFA5 hybrid cement when combined activation is applied, at all curing ages tested. 99
Figure 6.9. FTIR transmission spectra between wavenumbers 530-2000 cm^{-1} obtained for the (a) UFA and (b) UFA5 hybrid cements at all hydration ages tested. 102
Figure 6.10. FTIR transmission spectra between wavenumbers 530-2000 cm^{-1} obtained for the (a) MUFA and (b) MUFA5 hybrid cements at all hydration ages tested. 103
Figure 6.11. FTIR transmission spectra for portlandite between wavenumbers 3600-4000 cm^{-1} presented at 1 day and 28 days of hydration, for UFA, UFA5, MUFA and MUFA5 hybrid cement pastes. 105
Figure 6.12. Summary of XRD and DTG data presenting the occurrence of portlandite as an indication of the pozzolanic reaction of hydrated fly ash hybrid cement upon chemical and mechanical activation. 107
Figure 6.13. Summary of XRD and DTG data presenting the presence of ettringite in hydrated fly ash hybrid cement specimens upon chemical and mechanical activation. 109
Figure 6.14. Well crystallized ettringite needles in the UFA hybrid with 5% Na_2SO_4 at 180 days of curing. 111

Figure 7.1. Mortar compressive strength of the reference fly ash cement hybrids (without Na_2SO_4) produced from FCFA, UFA and MUFA (n = 6). 117
Figure 7.2. Mortar compressive strength of the fly ash cement hybrids (with and without Na_2SO_4) produced from (a) FCFA, (b) UFA and (c) MUFA for up to 1 year of curing (n=6). 118
Figure 7.3. The (a) 7 day and (b) 28 day compressive strengths for the FCFA, UFA and MUFA hybrids versus the amount of Na_2SO_4 added to the blend. 120
Figure 7.4. The 1 day strength expressed as a percentage of the 28 day strength of the fly ash cement hybrids, produced from FCFA, UFA and MUFA. 121
Figure 7.5. Total heat versus strength at 1, 2 and 7 days of hydration for (a) FUFA & FUFA5, (b) UFA & UFA5 and (c) MUFA and MUFA 5 hybrid cement mortars. 123

Figure 8.1. Concrete compressive strength of the reference fly ash concrete hybrids (without Na_2SO_4) produced from FCFA, UFA and MUFA (n = 2). 127
Figure 8.2. Concrete compressive strength of the fly ash concrete hybrids (with and without Na_2SO_4) produced from (a) FCFA, (b) UFA and (c) MUFA for up to 1 year of curing (n=2). 128
Figure 8.3. The (a) 7 day and (b) 28 day compressive strengths for the FCFA, UFA and MUFA concrete hybrids versus the amount of Na_2SO_4 added to the blend. 130

Figure 9.1. Overview of the experimental program. 133

~ List of abbreviations ~

AFm*	Monocarboaluminate ($3CaO{\cdot}Al_2O_3{\cdot}CaCO_3{\cdot}11H_2O$)
AFt†	Ettringite ($3CaO{\cdot}Al_2O_3{\cdot}3CaSO_4{\cdot}32H_2O$)
ATR	Attenuated total reflection
C-(A)-S-H; C-A-S-H	Calcium-aluminate-silicate-hydrate
C_2S	Belite ($2CaO.SiO_2$)
C_3A	Tricalcium aluminate ($3CaO.Al_2O_3$)
C_3S	Alite ($CaSiO_5$)
C_4AF	Tetracalcium aluminoferrite ($4CaO.Al_2O_3.Fe_2O_3$)
$Ca(OH)_2$	Calcium hydroxide or Portlandite
CFA	Coal fly ash
$C\underline{S}$	Gypsum ($CaSO_4{\cdot}2H_2O$)
CSH / C-S-H	Calcium silicate hydrate
DEF	Delayed ettringite formation
DTG	Derivative thermogravimetric analysis
EN	European Standard

* AFm is listed as Monocarboaluminate ($3CaO{\cdot}Al_2O_3{\cdot}CaCO_3{\cdot}11H_2O$) as this is the only AFm-type phase relevant to the findings of this study.

† AFt is listed as Ettringite ($3CaO{\cdot}Al_2O_3{\cdot}3CaSO_4{\cdot}32H_2O$) as this is the only AFt-type phase relevant to the findings of this study.

EPS	Expanded polystyrene
FA	Fly ash
FCFA	Fine Classified Fly Ash
FESEM	Field Emission Scanning Electron Microscopy
FTIR	Fourier Transform Infrared Spectroscopy
IEA	International Energy Agency
MC	ordinary Portland cement (used in this study)
MUFA	Mechanically Activated Unclassified Fly Ash
Na_2SO_4	Sodium sulfate
N-A-S-H; (N,C)-A-S-H)	Sodium-calcium-aluminate-silicate-hydrate
OPC	Ordinary Portland Cement
PFA	Pulverised fuel ash (Bottom ash + Fly ash)
PSD	Particle size distribution
SABS	South African Bureau of Standards
SANS	South African National Standard
SCM	Supplementary cementitious material
TEA	Triethanolamine
TGA	Thermogravimetric analysis
UFA	Unclassified Fly Ash
XRD	X-ray powder diffraction

~ Chapter 1 ~

Introduction, objectives and scope

1.1. Introduction

This chapter presents the reader with a short introduction providing background information regarding the holistic theme of this thesis. The overall and individual objectives, as well the novelty of this work is described. The scope, methodology and layout presented will give the reader a clear understanding as to what was covered in the planning and content of this thesis.

1.2. Background

Hybrid fly ash cement is a binder with a composition between that of pozzolanic fly ash cement and alkali activated fly ash cement (Donatello et al., 2013; Donatello et al., 2014a; Garcia-Lodeiro et al., 2015). The production of hybrid cement requires less clinker than that for ordinary Portland cement, and therefore produces less CO_2. Portland cement accounts for approximately 7-8% of the total CO_2 emitted globally (approximately 0.8 tonnes of CO_2 is released per tonne of clinker manufactured) (Duchesne *et al.*, 2010; Garcia-Lodeiro *et al.*, 2016c; Olivier *et al.*, 2015; Palomo *et al.*, 2007). The inherent advantage of hybrid alkaline cements, over their alkali activated counterparts is that they do not require the addition of highly alkaline (and usually expensive) chemicals, but rely on a safe source of alkali formed in situ to facilitate both the dissolution of any amorphous (glassy) phases present in the source materials, as well as hydration at ambient temperature (Donatello et al., 2013; Donatello et al., 2014b; Kovtun et al., 2015; Shekhovtsova et al., 2016).

The particular material under consideration in this specific study, is siliceous coal fly ash with pozzolanic properties from a coal-fired power station in South Africa. The aim of this study is to go beyond the maximum level of 55% replacement of clinker with fly ash, as specified in the current South African National Standard (SANS 50197-1:2013), and investigate the activation and performance of hybrid cement containing up to 70% fly ash.

During the production of blended cement, the maximum fly ash content is constrained due to insufficient early strength and slow strength development ascribed to the rate of the pozzolanic reaction between cement and fly ash (Blanco *et al.*, 2006; Heinz *et al.*, 2010). It is also well known that both the degree of hydration and the early age compressive strength tend to decrease along with an increase in level of fly ash (Al-Zahrani *et al.*, 2006). The lowest strength class of cementitious binder specified by EN 197 viz 32.5N, requires a minimum compressive strength of 16.0 MPa after 7 days, and 32.5 MPa after 28 days. Typically hybrid cements contain at least 70% fly ash by mass (Garcia-Lodeiro *et al.*, 2016b; Palomo *et al.*, 2014), and therefore do not meet the requirements as set by the current cement standards. If commercially viable fly ash based hybrid cements are to be developed, it would be necessary to enhance the reactivity of the fly ash so that strength develops at an acceptable rate and adequate strength values are achieved.

Fly ash is a by-product produced during coal-fired power generation and it is extracted by electrostatic precipitators or bag filters from the flue gases of furnaces fired with pulverised coal (Institute, 2009). The chemical composition of South African fly ash mainly consists of SiO_2, Al_2O_3 and CaO, with CaO being the less abundant oxide of the three, since calcareous coal fly ash which exhibits hydraulic properties is not produced locally.

The generation of electricity (with fly ash as by-product) in South Africa is dominated by coal-fired power stations attributable to significant coal reserves. Eskom, one of the largest utilities in the world, is the state-owned power utility and supplies approximately 95% of the electricity consumed in the country. In the 2014/15 financial year, Eskom consumed 119.2 million tons of coal and produced 34.4 million tons of total coal ash from their coal-fired stations (Reynolds-Clausen & Singh, 2017). Currently, two new supercritical coal-fired 6 x 794 MW (gross) power stations are being constructed, and are the largest ever ordered by Eskom. Once these utilities are completed, Eskom will generate an estimated 45 million tons of coal ash per year (Kruger, 2013).

Fly ash reactivity can be improved either by chemical or mechanical activation or a combination of these two techniques (Donatello *et al.*, 2013; Donatello *et al.*, 2014b; Fernández-Jiménez *et al.*, 2011; Garcia-Lodeiro *et al.*, 2016c; Kumar *et al.*, 2007; Kumar & Kumar, 2011; Qian *et al.*, 2001; Qiao *et al.*, 2006; Temuujin *et al.*, 2009; Velandia *et al.*, 2016). The pozzolanic reactivity of fly ash can be considered as the rate of reaction occurring between

its amorphous phase and calcium hydroxide prevalent in moisture laden cementitious materials (Kaur *et al.*, 2017; Velandia *et al.*, 2016).

The early age hydration of hybrid cement activated with Na_2SO_4 as an alkali activator has previously been studied (Donatello *et al.*, 2013; Pacheco-Torgal *et al.*, 2015). When evaluating the acceleration of the reactivity of fly ash by means of chemical activation with sodium sulfate, the rate at which strength increased improved significantly, especially during the early stages (Shi & Day, 1995; Velandia *et al.*, 2016).

Besides the chemical activation option described above, it is also of merit to consider the mechanical activation of fly ash by means of milling. It has been reported that mechanical activation of fly ash leads to increased reactivity, especially when the median particle size (d_{50}) is reduced to less than 5-7 µm; the critical particle size for silicates below which mechanical activation begins to manifest itself (Balaz, 2008; Kumar & Kumar, 2011; Temuujin *et al.*, 2009).

Qian *et al.* proved that the combination of grinding and the addition of Na_2SO_4 produced higher compressive strength compared to any single method of activation for lime-fly ash systems (Qian *et al.*, 2001).

It is evident that either sodium sulfate addition (chemical activation) or milling of fly ash (mechanical activation) are effective activation methods for high fly ash – containing cement/lime systems. However the literature tends to discuss the compressive strength of fly ash-lime systems (calcium hydroxide or calcium oxide) rather than fly ash-cement systems. More emphasis is also placed on early age strength development (2 days up to 28 days) as opposed to the evolution of strength over a protracted time of up to a year. Hence, it is not clear what effect the two activation techniques will have on compressive strength over an extended curing period.

This study aims to fill the gap by presenting and discussing compressive strength and characterisation results of hydrated fly ash hybrid cements cured for up to 1 year. This will provide much needed and valuable information required for the production of cementitious products with a low carbon footprint.

1.3. Aims and objectives of the study

In an effort to reduce CO_2 emission by reducing clinker factors, and optimally utilize stockpiled South African fly ash in blended cements, the principal aim of the study was to evaluate the reaction products, performance and suitability of both chemically and mechanically activated, high fly ash cement blends (hybrid cements). Specific objectives include:

1) Evaluation and comparison of the physical surface effect of chemical activation at four different curing ages, on three different siliceous fly ashes, differentiated by fineness and/or particle shape (due to mechanical activation) (Chapter 5).

2) Determination of the effect of the quantity of sodium sulfate addition (chemical activation) on fly ash-based hybrid cement specimens, with regard to mortar compressive strength gain at three different curing ages. The effect of dry addition of Na_2SO_4 to the hybrid specimens as well as addition of the Na_2SO_4 in solution form was studied (Chapter 5).

3) Evaluation of the setting times and heat evolution of fly ash hybrid pastes containing 70% of fly ash , as well as expansion on the hybrid cement containing the highest amount (5%) of Na_2SO_4 (Chapter 6).

4) Characterisation and discussion of the hydration products resulting from combined (chemical and mechanical) activation of fly ash, when used to produce hybrid cement paste containing 70% fly ash, at different curing ages over a period of one year (Chapter 6).

5) Reporting and discussion of strength behaviour of fly ash-based hybrid mortar cements containing 70% of the three fly ashes, differentiated by fineness and/or particle shape (due to mechanical activation), at different sulfate additions and curing ages (up to one year) (Chapter 7).

6) Reporting and discussion of the slump retention and strength behaviour of concrete made with fly ash-based hybrid cement containing 70% of the three fly ashes, differentiated by

fineness and/or particle shape (due to mechanical activation), at different sulfate additions and curing ages (up to one year) (Chapter 8).

The aim of this thesis is to contribute to the development of new environmentally friendly binders in concrete, specifically for application in the South African market. The effect of combined chemical and mechanical activation on the formation of hydration products and the properties of very high fly ash containing cementitious systems is poorly understood and literature in this regard is exceedingly limited.

The utilisation of South African fly ash via combined activation, in an effort to consume more stockpiled fly ash, as well as a reduction in the clinker factor which will result in lower CO_2 emissions by the cement industry, adds value to the novelty of the study.

1.4. Scope and limitations of the study

In order to limit variability within this study, the three siliceous fly ashes (classified, unclassified and milled unclassified) used during this research, were produced at the same power station. This enabled comparison of the physical properties and especially chemical behaviour, so that the effect of combined activation could be realized for unclassified fly ash, which formed the main subject under investigation during this research.

In order to produce hybrid systems, the relevant fly ash included for this study was added consistent at a ratio of 70% fly ash to 30% Portland cement. The chemical activator was added at different concentrations to determine its effect on the hybrid systems. Mechanical activation of a single batch of unclassified ash was carried out in a laboratory mill to produce the mechanically activated fly ash.

Characterisation and reaction behaviour were analysed using the following analytical techniques: Isothermal Calorimetry, X-Ray Powder Diffractometry (XRD), Thermogravimetric Analysis (TGA), Fourier Transform Infrared spectroscopy (FT-IR) and Field Emission Scanning Electron Microscopy (SEM). In order to investigate the physical behaviour of the hybrid systems, mortar compressive strength and setting time, as well as

concrete compressive strength and workability was assessed. The research was principally based on laboratory test work.

This study does not include investigation or discussion regarding the following topics:

- An optimisation study of hybrid cement systems produced with different percentages of fly ash addition.
- An investigation of hybrid cement systems produced with fly ash from different power stations.
- Physical and chemical properties of blends mixed at different water-to-cement ratios.
- Setting behaviour and flexural strength of concrete specimens.
- Pore water analysis of the cement paste specimens.
- An investigation into delayed ettringite formation or alkali-silica reaction (ASR) of hydrated cement and concrete
- Deterioration of paste due to chemical attack.

1.5. Methodology

The effect of a combination of chemical and mechanical activation on the production of a high volume fly ash containing hybrid cement, and its different characteristics and technological properties was studied.

For the purpose of this thesis, hybrid cement refers to a cementitious binder containing 70% of a South African fly ash produced at the same power utility, be it classified fly ash, unclassified fly ash, or milled unclassified fly ash (mechanically activated). The remainder of the binder consists of 30% ordinary Portland cement.

Chemical activation refers to commercially available Na_2SO_4 that was added to the dry hybrid blend in different concentrations, and calculated as a percentage of the fly ash content. Mechanical activation refers to a single batch of unclassified ash that was milled in a laboratory mill, to produce a mechanically activated fly ash with a d_{50} particle size of about 7 µm.

The following approach was used to validate the objectives of this study:

- Identify the test methods pertinent to this investigation.
- Determine the surface effect of chemical and mechanical activation at different dosages on pure fly ash systems, hydrated in calcium hydroxide.
- Perform a sulfate optimisation study to determine the effect of Na_2SO_4 activation on the compressive strength of mortar.
- Investigate the setting time, heat of hydration and expansion of hybrid cement pastes; also characterise the hydration products produced in hybrid cement pastes using a combination of analytical techniques
- Investigate the influence of chemical and mechanical activation on the compressive strength behaviour of fly ash hybrid mortar; and workability and compressive strength of hybrid fly ash concrete.

1.6. Layout of the thesis

This thesis consist of the following chapters:

Chapter 1 The problem statement and objectives for this investigation is introduced.

Chapter 2 Literature review on the South African cement and fly ash *status quo* and hydration chemistry of hybrid fly ash cement.

Chapter 3 The experimental procedures, materials and methods are presented.

Chapter 4 Characterisation of all the raw cementitious materials used in this study (cement and fly ash).

Chapter 5 A study on the surface effect of chemical and mechanical activation on pure fly ash hydrated in calcium hydroxide, as well as sulfate optimisation study based on compressive strength of fly ash hybrid cement mortars.

Chapter 6 A report and discussion on the results of all of the characterisation techniques applied to the hydrated hybrid fly ash cement pastes.

Chapter 7 A report and discussion of the results of the physical test work performed on hybrid fly ash mortars.

Chapter 8 A report and discussion of the results of the physical test work performed on hybrid fly ash concrete.

Chapter 9 Conclusions and recommendations for future work based on the findings of this study are reported.

~ Chapter 2 ~

Review of the South African cement and fly ash *status quo* and hydration chemistry of hybrid fly ash cement

2.1. Introduction

This chapter provides a review on the production, hydration kinetics and properties of fly ash based hybrid cements, activated using different approaches. Fly ash and cement chemistry, as well as the status quo of fly ash production and utilization in South Africa is presented. Literature that aims at assisting the reader to understand certain test methods, results or discussions, are not provided here but rather in the relevant chapters.

The information in this chapter furthermore aims to emphasize the need for research providing valuable information regarding the hydration chemistry of high fly ash containing hybrid cements. These hybrid cements are produced with siliceous fly ash from a South African source and activated and hydrated at ambient temperature, thereby supplying a possible alternative to the millions of tons of fly ash being stockpiled. With the upcoming implementation of carbon taxes in South Africa the successful production and application of fly ash hybrid cement will also lead to the reduction in carbon emissions.

"…*cement science should firmly and boldly aim toward that horizon, intensifying its efforts to undertake a technological transition that is long overdue. Alternative cements are not an illusion, but a reality*." (Palomo et al., 2014).

2.2. Fly ash

2.2.1. Production and characteristics of South African fly ash

Fly ash and metakaolin are the low-calcium aluminosilicates most commonly used in alkaline hybrid cement and concrete, although the latter is used very sparingly in the cement industry due its high cost (Palomo *et al.*, 2014).

Coal fly ash (CFA) is a by-product of coal combustion in thermal coal-fired power plants, and if not put to beneficial use, is recognised as an environmental pollutant (Blissett & Rowson, 2012; Rashad, 2014; Yao *et al.*, 2015). It is generated at 1200-1700 °C from various organic and inorganic constituents of the feed coal. Due to the scale of variety in its components, CFA is deemed to be one of the most complex anthropogenic materials to be characterised, resulting in the identification of approximately 316 individual minerals and 188 mineral groups in CFA specimens from around the world (Blissett & Rowson, 2012). The non-combustible material (ash) leaving the furnaces during coal combustion is called pulverised fuel ash (PFA) and it is the sum total of bottom ash (BA) and fly ash (FA). Bottom ash consists of fused and agglomerated fly ash and drops to the bottom troughs on leaving the furnaces, from where it is removed. Fly ash is a powdery residue, which leaves the furnaces with the flue gases and is collected by either electrostatic precipitators or filter bags. When FA is collected by electrostatic precipitators, 70% by mass is collected in the first field, 20% in the second field, 6% in the third field and 3% in the fourth field in a four-field precipitator, with less than 1-2% escaping through the chimney stack in an efficiently operated power station. In power stations with more than four precipitator fields, the increased collection efficiency results in even less ash escaping through the chimney stack (Krüger, 2003). Figure 2.1 provides a simplified representation of the formation of fly ash particles as presented by Tomeczec and Palugniok (Tomeczec & Palugniok, 2002).

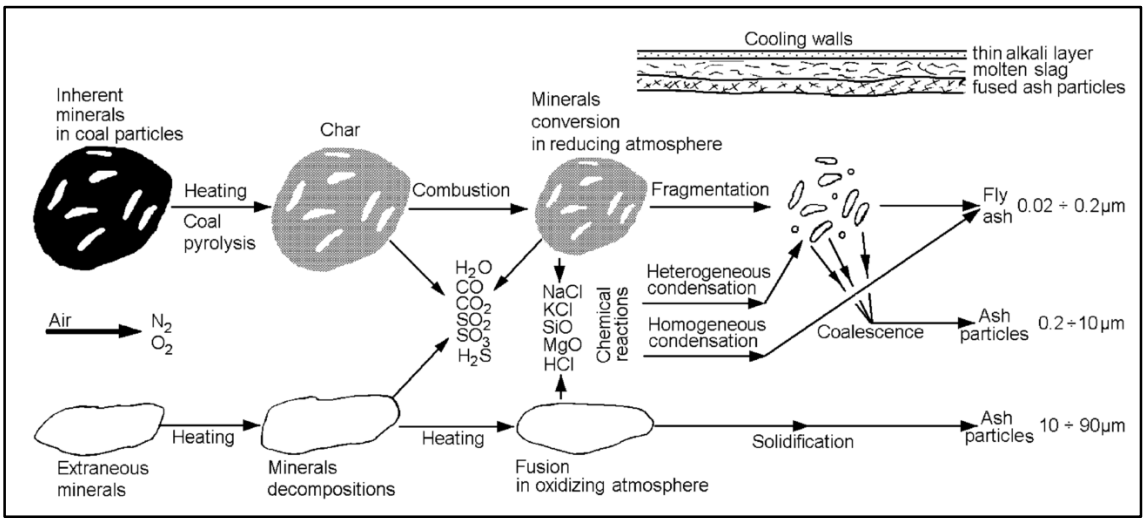

Figure 2.1. Mineral matter transformation mechanism during combustion of coal to produce fly ash (Tomeczec & Palugniok, 2002).

The first step of this transformation mechanism is the conversion of the coal to char which only burns out at much higher temperatures. The fine included minerals reduces progressively and are released from within the char as it fragments. It is at this stage that the minerals decompose, and volatilise and ultimately condense to form solid ash particles (Tomeczec & Palugniok, 2002). Homogeneous condensation results in ash particles between 0.02 and 0.2 µm and fragmentation of included mineral matter produces particles between 0.2 and 10 µm. The extraneous minerals undergo a series of transformations to form predominantly spherical particles in the size range 10-90 µm (Blissett & Rowson, 2012; Sarkar *et al.*, 2005).

The morphology of CFA particles is controlled predominantly by the coal combustion temperature and subsequent rate of cooling, which results in fly ash consisting of solid spheres, hollow spheres (cenospheres), spheres that contain smaller spheres within (plerosopheres) and irregular unburnt carbon (Blissett & Rowson, 2012). The general bulk chemical composition of fly ash contain a variety of metal oxides (SiO_2 , Al_2O_3, Fe_2O_3, CaO, MgO, K_2O, Na_2O, TiO_2), with the primary components being silica and alumina, with varying amounts of ferrous oxide, calcium oxide (as lime or gypsum), carbon, magnesium, sulfur (sulfides or sulfates), and other elements. There are significant differences in fly ash composition between regions (Blissett & Rowson, 2012; Iyer & Scott, 2001) as a result of variable coal chemistry and coal combustion plant efficiency.

2.2.2. Fly ash classification according to EN 450 / SANS 50450

The European standards body devised a classification system designed to distinguish types of fly ash that will be suitable for utilisation in cement replacement (Blissett & Rowson, 2012). This standard has also been adopted in South Africa as SANS 50450-1:2014, Fly ash for concrete - Part 1: Definition, specifications and conformity criteria (SABS, 2013b). It defines fly ash as follows: *"fine powder of mainly spherical, glassy particles, derived from burning of pulverised coal, with or without combustion materials, which has pozzolanic properties and consists essentially of SiO_2 and Al_2O_3 and which:*

- *is obtained by electrostatic or mechanical precipitation of dust-like particles from the flue gases of the power stations; and*

- *may be processed, for example by classification, selection, sieving, drying, blending, grinding or carbon reduction, or by combination of these processes, in adequate production plants, in which case it may consist of fly ashes from different sources, each conforming to the definition given in this clause.*

The chemical requirements for the use of fly ash in concrete, as stipulated in the abovementioned standard, are listed in Table 2.1. No consideration is given to variation in mineralogies between different types of coal fly ash (Blissett & Rowson, 2012).

Table 2.1. Classification system of the European (and RSA) standards bodies for fly ash used in concrete according to EN 450 and SANS 50450.

	Category A	Category B	Category C
LOI (%)	< 5	< 7	< 9
Chloride (%)	< 0,1	-	-
SO_3 (%)	< 3,0	-	-
Free CaO (%)	<1,5	-	-
Reactive CaO (%/m)	< 10	-	-
Reactive SiO_2 (%/m)	> 25	-	-
$SiO_2 + Al_2O_3 + Fe_2O_3$ (%/m)	> 70	-	-

2.2.3. Global perspective of fly ash production and utilization

The International Energy Agency (IEA) reported in their 2015 Coal Information report that coal continues to be primarily utilised for the generation of electricity and commercial heat, with 68% of coal being used for this purpose in 2013 (IEA, 2015). Coal ash accounts for 5-20% of the feed coal in electricity production, and typically consists of 5-15% bottom ash and 85-95% fly ash. This means that a minimum of approximately 85% of coal ash produced globally is fly ash (Heidrich *et al.*, 2013) (Yao *et al.*, 2015).

It is well known that the current principal use of fly ash is within the construction industry, typically as supplementary cementitious material. However, its utilisation remains less than 30% of the total fly ash produced worldwide, estimated to be approximately 700 million tons per year (Wee, 2013). In the United States alone, at least 150 million tons of fly ash is generated annually of which only 27% is reused, while the remaining is landfilled or surface impounded (Wee, 2013). The latest available coal combustion and fly ash production statistics, as well as fly ash utilisation statistics from the respective ash association websites for America (American Coal Ash Association) (ACAA, 2014), Australia (Ash Development Association of Australia) (ADAA, 2014) and the United Kingdom (UK Quality Association) (UKQAA, 2014) are presented in Figure 2.2. America produces and utilises by far the largest amount of fly ash.

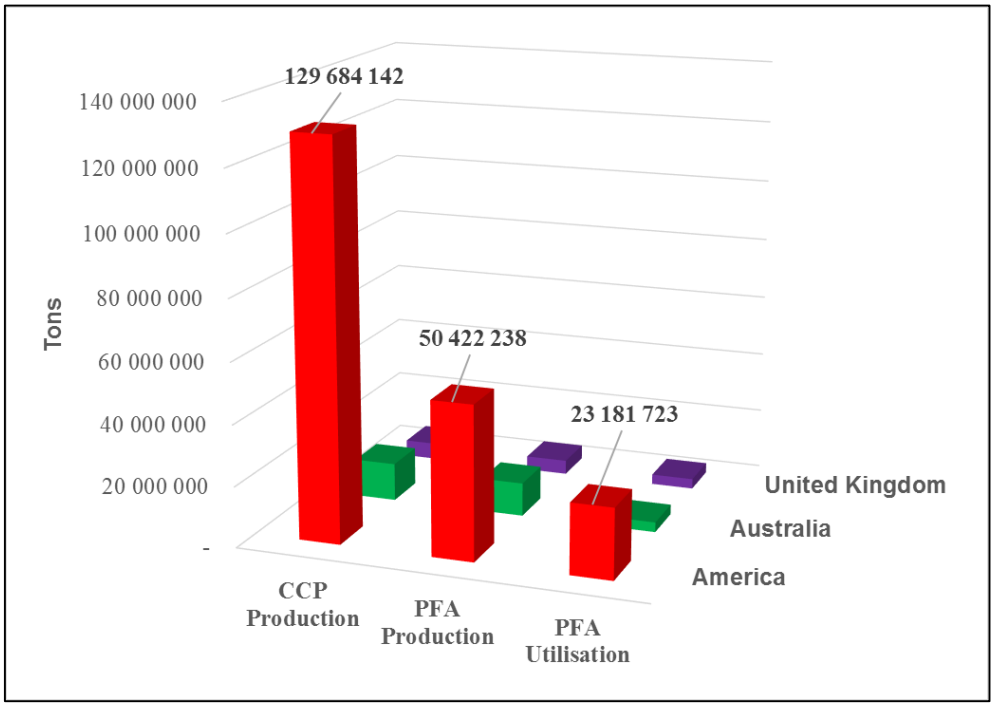

Figure 2.2. Coal combustion products (CCP) and pulverised fly ash (PFA) production statistics for America, UK and Australia for the year 2014.

2.2.4. South African perspective on fly ash production and utilization

During the late 1970's and early 1980's, South Africa experienced rapid industrial growth which resulted in a sudden rise in electricity demand, and with the vast coal reserves available, large (3000-3600 MW) pulverised coal-fired power stations were constructed (Kruger & Krueger, 2005). The availability of inexpensive land at the time enabled low-cost disposal of the coal ash which meant that South Africa's fly ash industry was born with a connotation of huge mountains of waste of little or no value. Governmental research agencies realised their responsibility towards reducing the environmental impact of ash dumping, and launched a nationally coordinated programme under the auspices of the Cooperative Scientific Programmes, the forerunner of the National Research Foundation (NRF) (Kruger & Krueger, 2005).

Initial characterisation of fly ash obtained from all South African ash sources established that the ash was high in silica and alumina, with moderate amounts of calcium and iron, and small amounts of alkali. Power stations like Matla, Kendal and Lethabo were found to produce fly ash with remarkable pozzolanic properties. The combustion technology utilised at these stations required mindful control in order to maximise energy recovery from the low-grade high-ash (30 - 40%) coal supplied by the mines. The result was a consistent fly ash with a low carbon content and significant amount of amorphous glassy phase – a typical pozzolan (Kruger & Krueger, 2005).

In the 2014/15 financial year, Eskom consumed 119.2 million tons of coal and produced 34.4 million tons of total coal ash from their coal-fired stations (Reynolds-Clausen & Singh, 2017).

By 1988, research had proved that the market for fly ash in concrete was economically viable, resulting in the production of blended cement in South Africa as the main conduit for supplying fly ash to the building and construction industry, occupying approximately 72% of the fly ash market (2011) in the country (Kruger, 2013). Today, Eskom coal-fired power stations consume approximately 119 million tons of coal per annum, producing about 34 million tons of ash to supply the bulk of South Africa's. Approximately 7% of this ash is sold to the construction industry for inclusion in cement and bricks (Reynolds-Clausen & Singh, 2017).

2.3. Fly ash as a component in the production of blended cement

2.3.1. The restrictions of fly ash-containing cements in the cement market (locally and globally) according to EN 197-1:2011 Edition 2

When considering fly ash reactivity in cementitious systems, it is important to take cognisance of the content of activated silica and aluminates in fly ash that is available for reaction with lime and soluble alkalis at ambient temperatures. During the production of blended cement, the maximum fly ash content is constrained due to insufficient early strength and slow strength development ascribed to the rate of the pozzolanic reaction between cement and fly ash (Blanco *et al.,* 2006; Heinz *et al.,* 2010). It is also well known that the degree of hydration and early age compressive strength tends to decrease with an increase in level of fly ash (Al-Zahrani *et al.*, 2006). As a result a maximum of 55 % fly ash (see Table 2.2) is specified for a CEM IV/B Pozzolanic cement in the European Standard on composition, specifications and conformity criteria for common cements (EN 197-1:2011 Edition 2) (CEN, 2011), also adopted by South Africa. These standards list 27 products in the family of common cements and dictates the products allowed in the cement market.

Table 2.2. The 27 products in the family of common cements as published in EN 197 / SANS 50197 (CEN, 2011).

Main types	Notation of the 27 products (types of common cement)		Composition (percentage by mass[a])										
			Main constituents										Minor additional constituents
			Clinker	Blast-furnace slag	Silica fume	Pozzolana		Fly ash		Burnt shale	Limestone		
						natural	natural calcined	siliceous	calca-reous				
			K	S	D[b]	P	Q	V	W	T	L	LL	
CEM I	Portland cement	CEM I	95-100	–	–	–	–	–	–	–	–	–	0-5
CEM II	Portland-slag cement	CEM II/A-S	80-94	6-20	–	–	–	–	–	–	–	–	0-5
		CEM II/B-S	65-79	21-35	–	–	–	–	–	–	–	–	0-5
	Portland-silica fume cement	CEM II/A-D	90-94	–	6-10	–	–	–	–	–	–	–	0-5
	Portland-pozzolana cement	CEM II/A-P	80-94	–	–	6-20	–	–	–	–	–	–	0-5
		CEM II/B-P	65-79	–	–	21-35	–	–	–	–	–	–	0-5
		CEM II/A-Q	80-94	–	–	–	6-20	–	–	–	–	–	0-5
		CEM II/B-Q	65-79	–	–	–	21-35	–	–	–	–	–	0-5
	Portland-fly ash cement	CEM II/A-V	80-94	–	–	–	–	6-20	–	–	–	–	0-5
		CEM II/B-V	65-79	–	–	–	–	21-35	–	–	–	–	0-5
		CEM II/A-W	80-94	–	–	–	–	–	6-20	–	–	–	0-5
		CEM II/B-W	65-79	–	–	–	–	–	21-35	–	–	–	0-5
	Portland-burnt shale cement	CEM II/A-T	80-94	–	–	–	–	–	–	6-20	–	–	0-5
		CEM II/B-T	65-79	–	–	–	–	–	–	21-35	–	–	0-5
	Portland-limestone cement	CEM II/A-L	80-94	–	–	–	–	–	–	–	6-20	–	0-5
		CEM II/B-L	65-79	–	–	–	–	–	–	–	21-35	–	0-5
		CEM II/A-LL	80-94	–	–	–	–	–	–	–	–	6-20	0-5
		CEM II/B-LL	65-79	–	–	–	–	–	–	–	–	21-35	0-5
	Portland-composite cement[c]	CEM II/A-M	80-88	<---------- 12-20 ---------->									0-5
		CEM II/B-M	65-79	<---------- 21-35 ---------->									
CEM III	Blast furnace cement	CEM III/A	35-64	36-65	–	–	–	–	–	–	–	–	0-5
		CEM III/B	20-34	66-80	–	–	–	–	–	–	–	–	0-5
		CEM III/C	5-19	81-95	–	–	–	–	–	–	–	–	0-5
CEM IV	Pozzolanic cement[c]	CEM IV/A	65-89	–	<---------- 11-35 ---------->					–	–	–	0-5
		CEM IV/B	45-64	–	<---------- 36-55 ---------->					–	–	–	0-5
CEM V	Composite cement[c]	CEM V/A	40-64	18-30	–	<----- 18-30 ----->			–	–	–	–	0-5
		CEM V/B	20-38	31-49	–	<----- 31-49 ----->			–	–	–	–	0-5

[a] The values in the table refer to the sum of the main and minor additional constituents.

[b] The proportion of silica fume is limited to 10 %.

[c] In Portland-composite cements CEM II/A-M and CEM II/B-M, in pozzolanic cements CEM IV/A and CEM IV/B and in composite cements CEM V/A and CEM V/B the main constituents other than clinker shall be declared by designation of the cement (for examples, see Clause 8).

2.3.2. A short review on the hydration chemistry of ordinary Portland cement

Ordinary Portland cement consists mainly of four main clinker phases i.e. alite (C_3S), belite (C_2S), aluminate (C_3A) and ferrite (C_4AF) as well as some clinker alkali sulfates and gypsum, from which cement hydration products are formed (Winter, 2009).

The main products produced from hydration of these four phases are (Winter, 2009):

- Calcium silicate hydrate, C-S-H
- Ettringite (AFt phase),
- Monosulfate (AFm phase),
- Calcium hydroxide, $Ca(OH)_2$
- Calcium carbonate, $CaCO_3$

Tricalcium silicate ($3CaO{\cdot}SiO_2$, abbreviated as C_3S) is the main and most important constituent of Portland cement, which to a great extent controls its setting and hardening. Tricalcium silicate found in Portland clinkers is also called 'alite'. Its exact composition and reactivity may vary between different cements. The hydration of alite is rather complex and is still not fully understood. An amorphous calcium silicate hydrate phase with a CaO/SiO_2 molar ratio of less than 3.0, called the 'C-S-H phase', and calcium hydroxide ($Ca(OH)_2$, abbreviated as CH, are known to form as hydration products from alite at ambient temperature (Hewlett, 2004). Typically, about 70% of the C_3S reacts within 28 days and virtually all in 1 year (Taylor, 1997).

The term 'C-S-H phase' is used to denote amorphous or nearly amorphous calcium silicate hydrate products of the general formula $CaO_x{\cdot}SiO_2{\cdot}H_2O_y$, where both x and y may vary over a wide range (Hewlett, 2004). C-S-H is also a generic name for any amorphous or poorly crystalline calcium silicate hydrate (Taylor, 1997).

Belite (C_2S), shows hydration behaviour similar to alite, with notable differences being a lower amount of $Ca(OH)_2$ being formed and a decrease in the reaction rate. The reactive polymorph which is of value to cement chemists and industries is the ß-C_2S polymorph. About 30% of the belite reacts within 28 days and 90% in 1 year (Taylor, 1997).

Aft (Al_2O_3-Fe_2O_3-tri) phases have the general constitutional formula $[Ca_3(Al,Fe)(OH)_6{\cdot}12H_2O]_2{\cdot}X_3{\cdot}xH_2O$, where x is normally at least ≤ 2 and X represents one formula unit of a doubly charged, or, two formula units with a singly charged anion. The most important Aft phase is ettringite. Ettringite is the mineral name for calcium sulfoaluminate, $3CaO{\cdot}Al_2O_3{\cdot}3CaSO_4{\cdot}32H_2O$, ($C_3A{\cdot}3CaSO_4{\cdot}32H_2O$ in cement chemistry notation) which is normally found in hydrated Portland cement and concretes (PCA, 2001). It forms through the reaction of available calcium and alumina in cementitious matrices, with sulfate either

inherently present in the cement paste or introduced into the system through an external source (Chrysochoou & Dermatas, 2006; Taylor, 1997). Ettringite formation mainly depends on the presence of C_3A (calcium aluminate hydrate), which in the presence of sufficient sulfate, will produce ettringite as hydration product (Taylor, 1997; Winter, 2009). The reaction of C_3A with water takes place in two stages. The first stage happens within 30 minutes and indicates the formation of ettringite. During the second stage of hydration (within 24-48 hours) the ettringite reacts further and AFm phases are formed. These reactions occurs to an extent that depends on the ratio of gypsum to C_3A.

AFm (Al_2O_3-Fe_2O_3-mono) phases are formed when the ions they contain are brought together in appropriate concentrations in aqueous systems at room temperature. They are among the hydration products of ordinary Portland cements. Under favourable conditions they form plate-like, hexagonal crystals with excellent cleavage (0001), however, they can also be poorly crystalline and intermixed with C-S-H. AFm phases have the general formula $[Ca_2(Al,Fe)(OH)_6]\cdot X\cdot xH_2O$, where X denotes one formula unit of a singly charged anion, or half a formula unit of a doubly charged anion e.g. CaX_2 in another way of writing the formula, and *x* denotes the amount of crystal water present (Taylor, 1997).

2.3.3. A short review on the hydration chemistry of typical fly-ash (pozzolana) containing cement

The term 'pozzolana' is defined or explained as follows: *"It includes all inorganic materials, either natural or artificial, which harden in water when mixed with calcium hydroxide (lime) or with materials that can release calcium hydroxide (Portland cement clinker)"* (Hewlett, 2004).

The reaction products resulting from the hydration of pozzolanic cements are the same as those occurring in Portland cement pastes. The differences solely involve the ratios of the various compounds and their morphology (Hewlett, 2004).

The composition of fly ash obtained from different sources may differ considerably, but its chemical nature is generally dominated by an amorphous aluminosilicate glass phase (Kruger, 1997; Van Der Merwe *et al.*, 2014). During hydration of cement, it is this glass phase of the fly ash that reacts with the portlandite produced from the cement hydration to form calcium

silicate hydrate (C-S-H) and ettringite; a process which is also referred to as the so-called pozzolanic reaction. This reaction only starts after 7 days, and the delay could be explained by the pH of the pore water not being sufficiently high to break down the glassy phase of the fly ash and make it available for reaction (Baert *et al.*, 2008; Hewlett, 2004).Thus, the pozzolanic reaction between fly ash and cement becomes apparent as soon as 70-80% of the alite contained in the cement clinker has reacted. The rate of the pozzolanic reaction depends on the properties of the fly ash (e.g. amount of reactive glass phase, unreactive quartz and unburnt carbon), the composition of the cementitious blend, as well as on the temperatures applied during hydration or curing of the fly ash-cement blend.

Hence, during the hydration of cement clinker, $Ca(OH)_2$ is released and activates the release of silica from fly ash due to dissolution of the glass phase at increased pH, where the silica can be absorbed or consumed and produce C-S-H with a reduced Ca/Si ratio (Baert *et al.*, 2008; Deschner *et al.*, 2012). This reaction (pozzolanic reaction) manifests slowly due to the reaction rate between the pozzolan (fly ash) and the portlandite, whereby the glass phase of fly ash only gets activated once portlandite from cement hydration is formed and made available to raise the system pH (Blanco *et al.*, 2006; Heinz *et al.*, 2010). It is therefore common practice to measure the consumption of portlandite to serve as indication of the onset of the pozzolanic reaction (Baert *et al.*, 2008; Deschner *et al.*, 2012).

Ettringite can form rapidly in cements containing fly ash (5h up to 28 days), and can even disappear again after 3 days due to its transformation into monosulfate. This conversion depends on the amount of SO_3 available and the CO_2 content of the cement paste, and has been observed in low-SO_3 but not in high-SO_3 fly ashes. Carbon dioxide can react with excess calcium aluminate hydrate and give rise to carboaluminate, thus preventing it from reacting with ettringite to form monosulfate. This is the reason why ettringite is often found with carboaluminate hydrate (Hewlett, 2004). Monocarboaluminate has been observed to be prevalent in seven-day product (Garcia-Lodeiro *et al.*, 2016b; García-Lodeiro *et al.*, 2013a).

2.4. Hybrid cement

Ordinary Portland cement has been studied for many years and its properties and behaviour is quite well understood. However, the global construction industry (and current research trends) is embarking on a movement toward more environmentally friendly construction products by partial or total replacement of ordinary cement. This results in the need for research to investigate and understand the production, behaviour and sustainability of alternative cements i.e. hybrid cement in order to assist with a much needed mind switch within the construction industry, and even within society towards more environmentally responsible materials.

2.4.1. What is hybrid cement?

A formal definition for the term "hybrid cement" is not available in literature, however, in an effort to distinguish this type of binder from geopolymers and alkali activated fly ash cements; literature explains this type of binder as being midway between pozzolanic fly ash cements and alkali activated fly ash cements (Donatello *et al.*, 2014a). It may also be termed as blended or hybrid alkaline cement, and usually have initial CaO, SiO_2 and Al_2O_3 contents of around 20% (Inés García-Lodeiro, 2012). Figure 2.3 graphically presents the position of hybrid fly ash cements relative to pozzolanic fly ash cements on the pure Portland cement (PC)-pure alkali activation of fly ash (AAFA) spectrum.

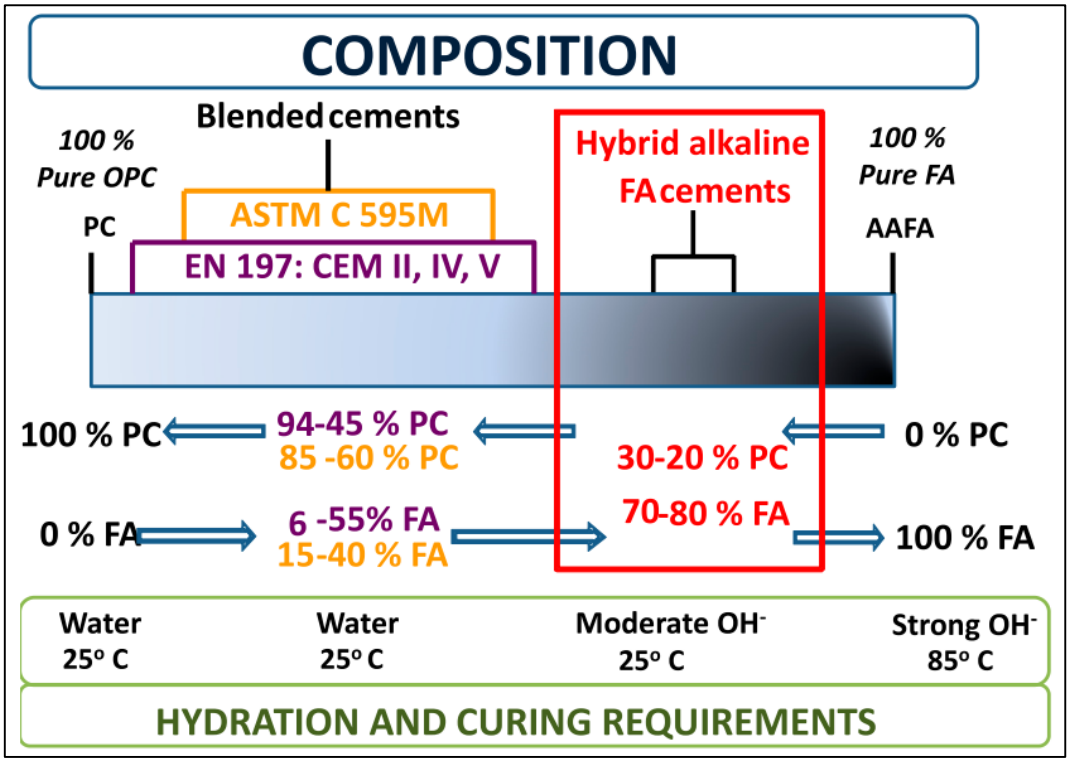

Figure 2.3 The position of hybrid fly ash cements relative to pozzolanic fly ash cements on the pure Portland cement (PC)-pure alkali activation of fly ash (AAFA) spectrum (Garcia-Lodeiro *et al.*, 2016b).

One may find that literature does not always make clear distinction between geopolymers, alkaline activated fly ash cement and hybrid alkaline cement. This observation may be attributed to the fact that all three of these binders undergo an alkaline activation step during some point in their reaction mechanism. Hybrid alkaline cements are complex cementitious blends and available information regarding these binders are quite limited (Donatello *et al.*, 2014a).

Palomo *et al*. (2014) grouped hybrid materials into two groups. Group A consists of materials that contain a low Portland cement clinker content and high mineral addition (70% and above), while Group B comprises of blends that contain no Portland cement but a combination of blast furnace slag + fly ash, phosphorous slag + blast furnace slag + fly ash, and other similar mixtures.

Hybrid cementitious systems most frequently studied include (Inés García-Lodeiro, 2012):

- Portland cement – blast furnace slag blends
- Portland cement – phosphorous slag blends
- Portland cement – fly ash blends
- Portland cement – steel mill and blast furnace slag blends
- Portland cement – fly ash – blast furnace slag blends
- Multi-constituent cement blends.

An important advantage of hybrid alkaline cement when compared to pure alkali activated fly ash cements, is the fact that they do not require the addition of highly alkaline chemicals, but rather use a safe source of *in situ* formed alkali to promote dissolution of fly ash glassy phases. Furthermore, hydration of hybrid alkaline cements occur at ambient temperature instead of energy intensive curing procedures often applied in the production of geopolymers (Donatello *et al.*, 2013; Donatello *et al.*, 2014b). The cementitious gels posed to form during hydration of hybrid alkaline cements are very complex and are proposed to be mixed, (C,N)-A-S-H or N-(C)-A-S-H-type gels (Fernández-Jiménez *et al.*, 2011; Inés García-Lodeiro, 2012).

Literature defines typical fly ash hybrid cements to contain no less than 70% fly ash by mass (Palomo *et al.*, 2014). This definition ultimately leaves hybrid cements outside of the scope of current standards (CEN, 2011), hence the need for relevant research in order to promote the use and specification of hybrid cements within the construction industry as well as certification bodies.

2.4.2. Activation and production of high fly ash-containing hybrid cements

Fly ash reactivity can be improved by either chemical or mechanical activation or a combination of these two techniques (Donatello *et al.*, 2013; Donatello *et al.*, 2014b; Fernández-Jiménez *et al.*, 2011; Garcia-Lodeiro *et al.*, 2016c; Kumar *et al.*, 2007; Kumar & Kumar, 2011; Qian *et al.*, 2001; Qiao *et al.*, 2006; Temuujin *et al.*, 2009; Velandia *et al.*, 2016). For this thesis, a combination of chemical (Na_2SO_4) and mechanical (milling) activation was investigated. Hence, the literature that follows include studies where either one or both of these activation methods were applied to fly ash-containing hybrids cements.

Upon finding research on the production and investigation of hybrid cements specifically, a handful of authors' names come up repeatedly i.e. Inés García-Lodeiro, Ángel Palomo, Ana Fernández-Jiménez and Shane Donatello, irrespective of the activation method and raw materials used (Donatello *et al.*, 2014b; Garcia-Lodeiro *et al.*, 2016a; García-Lodeiro *et al.*, 2013a, 2013b; Inés García-Lodeiro, 2012).

Lee *et al.* (2003) investigated fly ash cement blends (40% fly ash and 60% cement clinker) using three different chemical activators, one of which was sodium sulfate at various levels of addition. The authors concluded that while all three activators accelerated the strength development at an early age, sodium sulfate was the most effective in accelerating the consumption of calcium hydroxide and also produced more ettringite than the other two activators. These results explain the improved early compressive strength of mortars when sodium sulfate was used (Lee *et al.*, 2003; Velandia *et al.*, 2016).

Shi and Day (1995) explored the acceleration of the reactivity of fly ash in a fly ash – lime system by means of different chemical activators like sodium sulfate (Na_2SO_4) amongst others (Shi & Day, 1995). Although the high fly ash – lime specimens were cured at elevated temperature (50°C), they concluded that chemical activators can significantly improve the rate of strength gain, especially the early rate of strength gain, which is generally associated with fly ash reactivity. They found that for pastes with high calcium ash, Na_2SO_4 was the more efficient activator.

The efficacy of using sodium sulfate as an activator was studied by measuring its influence on the early-age hydration of very high volume fly ash cement (80% fly ash activated with 4% sodium sulfate) (Donatello *et al.*, 2013). The compressive strength at 2 days was predicted by extrapolation of data after 45 hours of curing. A comparison of the reference paste with gypsum instead of sodium sulfate revealed that Na_2SO_4 reduced setting times, shortened the induction period related to cement hydration, and increased early alite hydration and compressive strength (2 days) development, but also restricted ettringite formation. Subsequently, efficiency of sodium sulfate as an activator for hybrid cement containing a high content of coal bottom ash was investigated (Donatello *et al.*, 2014b). Although no strength results were reported, the team concluded that both the cement clinker phases and the ash glassy phases are highly reactive during the first three days of hydration. *In situ* formed reaction products portlandite and gypsum were shown to be metastable and disappeared within 3 days of hydration. Ettringite stability was limited in the hybrid system, but unlike gypsum and portlandite, remained

detectable after the first 3 days of hydration. SEM-EDX and FTIR spectroscopy evidence suggested the development of three gel bond environments, tentatively attributed to C-(A)-S-H, C-A-S-H and (N,C)-A-S-H) type gels.

The benefit of mechanical activation of fly ash has been reported by several authors as a viable method of achieving ambient temperature curing of both alkali activated and blended cements (Fanghui *et al.*, 2015; Kumar *et al.*, 2007; Kumar & Kumar, 2011; Temuujin *et al.*, 2009; Zhao *et al.*, 2015). The research indicated that mechanical activation improves both bulk and surface reactivity. It also offers the possibility of changing the reactivity of solids without altering their overall chemical composition. It was shown that the reactivity of fly ash varies with the median particle size and increases rapidly when the size is reduced to less than 5-7 μm (Kumar *et al.*, 2007; Kumar & Kumar, 2011). Results indicate that mechanical activation of fly ash can be used to produce blended cements containing higher proportions of fly ash without degrading performance characteristics (Kumar *et al.*, 2007).

The effect of mechanical activation of the fine fraction of fly ash was investigated by using milled fly ash. The results indicate that mechanical activation only had a slight effect on 28 day compressive strength, but was very effective in improving the strength at 90 days (Qiao *et al.*, 2006). As part of this study, a specimen of the mechanically activated fly ash was prepared with sodium sulfate added to the mix, thus effectively combining chemical and mechanical activation into the same fly ash-lime blend. It was concluded that the combination of sodium sulfate together with the milled ash produced results which significantly improved the strength characteristics compared to the control sample (only mechanical activation) at both curing ages. Another fly ash-lime system, containing 80% fly ash (mechanically and chemically activated with sodium sulfate) and 20% lime (no cement clinker), was investigated by Qian *et al.* (2001). After mechanical activation of the fly ash, the lime-fly ash mortars hardly had any strength at 3 days, but achieved about 1 MPa at 7 days and 2.3 MPa at 28 days. When 3% sodium sulfate was added to the ground fly ash, the mortars achieved 2.5 MPa at 3 days, 5.5 MPa at 7 days and approximately 12.5 MPa at 28 days. The investigation focussed on the compressive strength behaviour of mortar specimens, up to a maximum curing age of 28 days, and concluded that the combination of grinding along with the addition of sodium sulfate resulted in higher compressive strengths than either grinding or sodium sulfate addition individually (Qian *et al.*, 2001).

It is evident that either sodium sulfate (chemical activation) or milling of fly ash (mechanical activation), or a combination of the two thereof, are effective activation methods for high fly ash – containing cement/lime systems.

2.4.3. Hydration chemistry of high fly ash-containing hybrid cements

Literature on the proposed reaction chemistry whereby high fly ash-containing hybrid cement systems are activated specifically with Na_2SO_4 is limited. The most comprehensive hypothesis for this specific reaction was researched and published by Donatello and his co-authors (Donatello *et al.*, 2013).

The early age hydration process of hybrid cement produced with 80% coal fly ash (dry mass) which was activated with Na_2SO_4 was hypothesized in 2013 by Donatello *et al*. The following reaction scheme was proposed (Donatello *et al.*, 2013; Donatello *et al.*, 2014b):

$$Na_2SO_{4(s)} + H_2O_{(l)} \rightarrow 2Na^+_{(aq)} + SO_4^{2-}{}_{(aq)} \quad \textbf{(2. 1)}$$

$$C_3S_{(s)} + H_2O_{(l)} \rightarrow C\text{-}S\text{-}H_{(s)} + CH_{(s)} \text{ (accelerated in presence of } SO_4^{2-}{}_{(aq)}) \quad \textbf{(2. 2)}$$

$$CH_{(aq)} + 2Na^+_{(aq)} + SO_4^{2-} \rightarrow C\underline{S}_{(s)} + NaOH_{(aq)} \quad \textbf{(2. 3)}$$

$$CH_{(aq)} + NaOH_{(aq)} + FA_{(s)} \rightarrow \text{(N,C)-A-S-H gel} \quad \textbf{(2. 4)}$$

$$C\underline{S}_{(aq)} + C_3A_{(s)} \rightarrow \text{ettringite}_{(s)} \quad \textbf{(2. 5)}$$

The authors who posed the above reaction equations provided the following explanations based on their research (Donatello *et al.*, 2013):

- Initially, the Na_2SO_4 dissolves whereby SO_4^{2-} ions most likely retard the initial hydration of the small quantity of C_3A present, producing a limited quantity of poorly ordered ettringite. It is evident that the presence of soluble SO_4^{2-} greatly enhances early

alite hydration, and in turn produces soluble Ca^{2+}, OH^- and silicate anions promoting the precipitation of C-S-H and CH nuclei, and subsequently, paste setting.

- Formation of NaOH (eqn 2.3) results in an increased system pH which inhibits the formation of ettringite. However, the alkali dissolution of fly ash glassy phases (eqn 2.4), effectively reduces the system pH to some extent that is sufficient to favour a limited degree of ettringite formation, and is considered to result in the formation of an additional gel phase that contributes significantly to early compressive strength.
- An important consideration which was taken into account was the competition in the complex hybrid system for Ca^{2+}, *in situ* formed gypsum and SO_4^{2-}. Any dissolved $Ca^{2+}$and thus portlandite, will react to produce either *in situ* gypsum-type phases or be incorporated into secondary gels formed by alkali activation of fly ashes. Any gypsum produced will likely react with C_3A phases and dissolved Al^{3+}/ SO_4^{2-} to form ettringite.

Garcia-Lodeiro *et al.*(2016) published a comprehensive review on the hydration models for hybrid alkaline cement containing a very large proportion of alkaline cement in collaboration with Donatello and other known researchers in the field (Garcia-Lodeiro *et al.*, 2016b). In this publication, the reaction chemistry model for the use of an inorganic salt (Na_2SO_4) as activator for fly ash hybrid cement remained in agreement with Donatello's 2013 publication as discussed above. It was also noted that monocarboaluminate formed and was prevalent in the 7-day materials, and that no ettringite was detected. The conclusion drawn was that the type of activator used within these fly ash hybrid systems has a direct impact on the secondary products precipitating and on reaction kinetics (essentially through increased pH being generated in the medium), accelerating or retarding the precipitation of the main reaction products (cementitious gels).

Despite the statement made above with regard to different activators influencing the secondary product e.g. ettringite formation, as well as the hypothesized hydration reactions, different authors have found variances in the results obtained for characterisation of the secondary products formed when making use of only Na_2SO_4 as chemical activator on high fly ash-containing hybrid cements.

In two publications where Donatello and his peers investigated the reaction mechanisms of hybrid fly ash (or bottom ash) cement with the addition of Na_2SO_4 as a chemical activator, it was concluded that ettringite formation and stability became inhibited as alkalinity increased

at early ages (the maximum hydration period studied was 3 days) (Donatello *et al.*, 2013; Donatello *et al.*, 2014b). The authors also found that in situ formation of gypsum could not be confirmed with XRD. Two possible explanations for the latter were posed (Donatello *et al.*, 2013):

1. The in situ formed gypsum was a metastable phase which was consumed as quickly as it was formed; or
2. the gypsum precipitating was impure and did not give regular diffraction patterns.

This verdict on the undetected gypsum was also supported and published by Garcia-Lodeiro *et al.*(2016) and Fernández-Jiménez *et al.* (2011) in studies completed with the same activators (Na_2SO_4) on high fly ash-conatining hybrid cements (Fernández-Jiménez *et al.*, 2011) (Garcia-Lodeiro *et al.*, 2016c)

Velandia *et al*. (2016) also investigated the hydration products produced from high fly ash-containing hybrid cements (50% fly ash), adding Na_2SO_4 as a chemical activator. These authors found results contradicting that of the formerly mentioned authors, in that they found mixes which contained Na_2SO_4 had the highest ettringite content. A noteworthy conclusion from the work done by Velandia *et al.* is that the Na_2SO_4 activation did not have the same effect on ettringite formation when fly ashes with higher Fe_2O_3 (~ 9-11%) was used compared to fly ashes with lower Fe_2O_3 content (~ 4-5%). The latter proved to enhance both ettringite formation and portlandite consumption (Velandia *et al.*, 2016).

2.5. Conclusion

Globally, cement companies are producing nearly two billion tons of CO_2 per annum, approximately 6-7% of the planet's total CO_2 emissions. Should this trend continue, the cement industry will be emitting CO_2 at a rate of 3.5 billion tons/annum by the year 2025 (Shi *et al.*, 2011). Immediate global replacement of Portland cement by any of the possible alkaline cements (or any other binder) is currently not possible due to technical concerns around paste, mortar and concrete rheology or the supply of universally available, standardised quality prime cementitious raw materials. However, partial replacement i.e. hybrid cements, are deemed to be technologically viable materials for contemporary construction (Shi *et al.*, 2011).

Literature discussed in this chapter proved that factors like the type of alkaline activator used to produce alkaline fly ash-cement hybrid binders, the degree of the pozzolanic reaction, curing temperature, and presence of soluble silica all have an impact on the reaction kinetics, the formation of secondary reaction products (carbonates, ettringite, AFm phases, etc.) and the proportion and structure of the main reaction products or gels ((N,C)-A-S-H/C-A-S-H) present. All these parameters may be different when using South African fly ash, making it necessary to investigate the hydration chemistry resulting from utilising local raw materials.

"The main advantages of these hybrid alkaline binders over pure alkali activated fly ash cements are that they use a safe source of in situ formed alkali, that mixing is carried out on a "just add water" basis and that they hydrate normally at ambient temperatures." (Donatello et al., 2014b).

~ Chapter 3 ~

Experimental program

3.1. Introduction

This chapter contains information on the materials and methods used to produce and characterise the activated hybrid fly ash cement specimens, which make out the core theme of this thesis.

In this study three different, commercially available fly ashes were utilised along with Portland cement. The fly ashes, sourced from a single South African producer, included an ultra-fine air-classified ash (d_{50} about 5 µm), an unclassified ash (d_{50} about 60 µm), and the mechanically activated (milled) residue (d_{50} about 7 µm) of the unclassified ash. These three fly ashes will forthwith be identified using the following descriptors:

- FCFA : **F**ine **C**lassified **F**ly **A**sh
- UFA : **U**nclassified **F**ly **A**sh
- MUFA : **M**echanically Activated **U**nclassified **F**ly **A**sh

The Portland cement (MC), produced by milling clinker along with approximately 10% limestone and 5% gypsum in a vertical roller mill, until a mean particle size of approximately 13 µm is achieved, had a density of 3.14 g/cm^3 and was also sourced from a South African supplier.

Commercially available (99%, Merck) sodium sulfate (Na_2SO_4, anhydrous) was used in all the chemically activated mixes, and was directly added in powder form to each mix being prepared for the hybrid cements (except in the sulfate optimisation study discussed under heading Figure 3.4 where two different methods were compared).

The experimental work started off with an assessment of the effect of an alkaline environment on the reactivity of fly ash (FCFA, UFA or MUFA), without addition of cement (MC), by exposing it to a saturated calcium hydroxide (portlandite) solution. Seeing that cement hydration chemistry is a complex study on its own, this decision was made to simplify the

system under investigation in order to avoid possible side-effects and reactions due to the presence of heterogeneous cement. The system was therefore set up to attain a clear understanding of the reactions taking place between fly ash (FCFA, UFA or MUFA), $Ca(OH)_2$ and Na_2SO_4. Field emission scanning electron microscopy (FESEM) and X-ray powder diffraction (XRD) were used to develop a better understanding of the reactivity of the fly ash particles after their exposure to calcium hydroxide and sodium sulfate.

In order to determine the working range for the percentage Na_2SO_4 addition for the work that follows, a sulfate optimisation study was completed. For this experiment a hybrid fly ash cement mortar blend, consisting of 75% standard reference silica sand (CEN, 2016) and 25% hybrid cement (containing 70% unclassified fly ash (UFA) and 30% cement (MC)) by mass was produced at a water:binder mass ratio of 0.5. The outcome of the experiment was based on setting time (minutes) and mortar compressive strength (MPa) results measured after 1 day, 2, 7, and 28 days of water curing.

It was anticipated that the combined findings from the latter two experiments should prove the definite advantages of chemical activation (Na_2SO_4), mechanical activation and a combination of activation approaches.

Characterisation of all cementitious materials (FCFA, UFA, MUFA and MC) was performed using an extensive range of analytical techniques. These techniques included X-ray fluorescence (XRF), X-ray powder diffraction (XRD), Particle size distribution (PSD) analysis, Field emission scanning electron microscopy (FESEM), Thermogravimetric analysis (TGA) and Fourier transform infrared spectroscopy (FTIR).

Hybrid fly ash cement pastes (without any aggregates) were prepared by mixing 70% of dry UFA, or MUFA respectively with 30% cement (MC) by mass, keeping the water:binder ratio constant at 0.5. It is common practice to exclude any aggregates when studying cement hydration as to not dilute hydration products with unreactive materials. This methodology simplifies the characterisation process of newly formed hydration products.

The hybrid fly ash cement pastes were not just used for characterisation of hydration products. Leading up to the characterisation work, three tests were done (i.e. setting time, heat evolution and expansion) on the same hybrid cement compositions as mentioned above. Setting times and heat evolution tests were performed on pastes made from all three fly ash specimens

(FCFA, UFA and MUFA). Expansion studies were only performed on the MUFA5 hybrid which is the specimen of concern because of the high amount of additional sulfates added to it.

To investigate the hydration chemistry of the hybrid fly ash cement pastes, FCFA was excluded from the chemical characterisation study, and sulfate addition was limited to the minimum and maximum (extreme) scenarios, thus 0% and 5% Na_2SO_4. This decision was made due to limited availability of expensive, advanced analytical equipment and resources, and the selected parameters being sufficient for the aim of this thesis. The hybrid fly ash cement pastes were cast in expanded polystyrene (EPS) moulds and removed from water at ambient temperature after curing for different durations, up to a period of 1 year. Relevant characterisation techniques applied to the hydrated pastes included XRD, TGA, FTIR and FESEM as a supplementary technique. The reason for the utilisation of these specific techniques are provided and discussed in more detail in the remainder of this chapter.

Hybrid fly ash cement mortar blends were prepared by mixing 70% of dry UFA, FCFC, or MUFA respectively with 30% cement and standard reference sand (CEN, 2016). The sand:cement mass ratio was kept constant at 75:25 and the water:binder ratio at 0.5. The aim of preparing the mortar blends was to compare standard compressive strengths. All three fly ashes were included in this section of the work, since the resources for the mixing of the mortars, curing and relevant test work were readily available. Different percentages of Na_2SO_4 had been manually added to the fly ash-mortar blends. All hybrid mortar specimens were cured for up to 1 year in water at ambient conditions before determining the mortar compressive strength (MPa).

Seeing that most types of cement ultimately ends up being used to produce concrete and concrete structures, hybrid fly ash cement blends were prepared by mixing 70% of dry UFA, FCFC, or MUFA respectively with 30% cement (MC) which made up the cementitious part of the concrete. Aggregate (Andesite sand and stone) was mixed with the cementitious materials to produce concrete. Both the water and the binder contents of the concrete mixes were kept constant at 200 l/m^3 and 300 kg/m^3 respectively. Once again all three fly ashes were included in the concrete test work for the same reason as was mentioned above for the mortar tests, and the Na_2SO_4 additions were performed in a similar manner. The test work included workability (slump retention / mm) and concrete compressive strength (MPa). The concrete mixes were prepared and specimens were cured in water for up to 1 year.

3.2. Chemical characterisation techniques

3.2.1 X-ray fluorescence (XRF)

Wilhelm Conrad Roentgen discovered X-rays in 1895, and the first industrial X-ray spectrometer was available about 60 years later. An unprecedented series of discoveries, all within a couple of decades after that of Roentgen, paved the way towards commercialized analysis using X-rays.

Current X-ray spectrometers are compact and capable of analysing dozens of elements in minutes, although analysis of eight elements (Si, Al, Fe, Ca, Mg, S, Na, K) is normally sufficient for Portland cement characterisation. The materials routinely analysed at a cement plant are the raw materials used to produce cement clinker, corrective materials, alternative cementitious materials, clinkers and cements. An accurate chemical analysis of materials used in cement manufacturing is required in order to design a proper cement raw mix, determine target clinker composition and produce cement meeting desired specifications (PCA, 2004).

The chemical composition of the raw materials used in this study was determined by X-ray fluorescence (XRF) fused bead analysis (PANalytical Axios). The glass beads were prepared by mixing 1 g of the sample with 5 g of fluxing agent (XRF Analytical, 100% $Li_2B_4O_7$) and fusing the mixture at 1000 °C. The fine powdered samples required no additional milling prior to the analysis. The loss-on-ignition (LOI) was determined by roasting the sample at 1050 °C for 1 hour until a constant weight was achieved.

3.2.2 X-ray powder diffraction (XRD)

X-ray powder diffraction (XRD) analysis is one of the most prominent analytical techniques used for the characterisation of crystalline, fine-grained materials, such as cements. The power of XRD is in the rapid and, if carried out appropriately, reliable delivery of quantitative mineralogical data compared to traditional quantitative phase analysis methods such as Bogue calculations and optical microscopy (Snellings, 2016; Snellings *et al.*, 2014). In cements the technique is mostly used for qualitative, i.e. phase identification, and quantitative phase analysis, but other potential uses may include the determination of polymorphic modification and state of crystallinity (Snellings, 2016; Taylor, 1997).

In this study, XRD was especially valuable in identifying and trending the production and consumption of secondary hydration products like portlandite and ettringite. Unfortunately, the type of gel products expected to form during hydration are amorphous to X-rays and need to be characterised by alternative analytical techniques such as Fourier-transform infrared spectroscopy (FTIR).

X-ray powder diffraction (XRD) measurements were carried out using a PANalytical X'Pert Pro powder Diffractometer an X'Celerator detector and variable divergence- and fixed receiving slits, with Fe filtered Co-Kα radiation (λ=1.789Å). The phases were identified using X'Pert Highscore plus software. The relative phase amounts (weight %) were estimated using the Rietveld method (Autoquan Program).

Twenty percent silicon (Aldrich, 99% pure) was also added to each sample for the determination of amorphous content. The samples were then micronized in a McCrone micronizing mill, and prepared for XRD analysis using a back loading preparation method. XRD analysis of the fly ash specimens cured in calcium hydroxide did not include the addition of silicon, since only the crystalline phases were identified for the purpose of the study.

3.2.3 Particle size distribution (PSD)

Almost all powders exhibit a variety of particles distributed over a range of sizes, and the width, shape and position of this size distribution will influence many aspects of their processing. Knowledge of particle size and the distribution of sizes are therefore essential for tight process control, maintenance for quality and minimisation of costs (Mingard *et al.*, 2009).

The particle size distribution (PSD) of the raw cementitious materials were obtained by laser diffraction using a Malvern Mastersizer 2000 fitted with a Scirocco 2000 sample handling unit. Scattered light data was recorded for 25 seconds. A refractive index of 1.68 and absorption of 1 was chosen. Size data collection was performed within the recommended 10-20% obscuration range.

3.2.4 Field emission scanning electron microscopy (FESEM)

More often than not, microscopy data is used for the physical study of morphologies of solid products, either as a principal analytical technique or as a supporting characterisation technique.

The morphology of the solid samples was studied using a Zeiss Ultra SS (Germany) field emission scanning electron microscope (FESEM), operated at an acceleration voltage of 1 kV under high-vacuum conditions. Specimens were dried and then procured by dipping carbon stubs into the powders. Excess powder was removed by gentle blowing with compressed nitrogen. The samples were sputter-coated with carbon (Emitech K550X Ashford, England) and placed in the microscope for examination.

3.2.5 Thermogravimetric analysis (TGA)

Thermogravimetric analysis (TGA) and the derivative curve of thermogravimetric analysis (DTG) are commonly employed in material science to determine thermal characteristics of materials, rate of degradation, absorbed moisture content and kinetics of a reaction based on weight changes (Dilnesa). TGA and DTG curves of cement paste can be divided into three major parts (Dilnesa):

- < 300 °C : removal of water from hydrated products which are likely to include most cement phases e.g. C-S-H. Several other minor dehydration steps attributed to removal of pore water, interlayer water and adsorbed water are also likely to take place.
- 400 °C – 500 °C : removal of water via dehydroxylation of mostly portlandite
- 600 °C : removal of carbon dioxide via decarbonation of mostly calcite

The following reaction equations explain how the above information is applied to identify the presence of certain hydration products in cementitious materials from analysing their TGA and DTG curves (Lothenbach *et al.*, 2016).

The initial loss of water (< 100 °C) from a cement sample is associated with the loss of surface moisture if the sample was not properly dried. Between 100 and 200 °C, numerous dehydration reactions of phases present in ordinary Portland cement take place. The most prominent

dehydration, dehydroxylation temperature regions for cement and hydrated cement, summarised in order of ascending temperature, are presented in Table 3.1.

Table 3.1. The most prominent dehydration, dehydroxylation and decarbonation temperature regions for cement and hydrated cement.

	Cement phase	Chemical formula	Temperature range (°C)
Dehydration < 300 °C	C-S-H (Calsium silicate hydrates)	-	100 - 200
	Gypsum	$CaSO_4 \cdot 2H_2O$	100 - 120
	Ettringite	$3CaO \cdot Al_2O_3 \cdot 3CaSO_4 \cdot 32H_2O$	100 - 120
	Hemihydrate	$CaSO_4 \cdot 0.5H_2O$	120 - 130
	Monocarboaluminate	$4CaO \cdot Al_2O_3 \cdot CO_3 \cdot 11H_2O$	150 - 170
Dehydroxylation 400 °C – 500 °C	Portlandite	$Ca(OH)_2$	400 - 500
Decarbonation > 600 °C	Calcium Carbonate	$CaCO_3$	600 - 800

Clearly most of the dehydration reactions overlap in some way on the thermogram. This renders it difficult to quantify any of the phases by making use of the dehydration reactions in this temperature region.

Once a temperature between 400 to 500 °C is reached, dehydration of portlandite is evident. This temperature range of this reaction does not overlap with that of the other major dehydration reactions, which means that TGA is a commonly used method to measure the portlandite content in a cement sample.

Decarbonation (i.e. decomposition) of carbonates (mostly calcite) occurs between 600 and 900 °C.

An example of the TGA and DTG for typical hydrating Portland cement is provided in Figure 3.1.

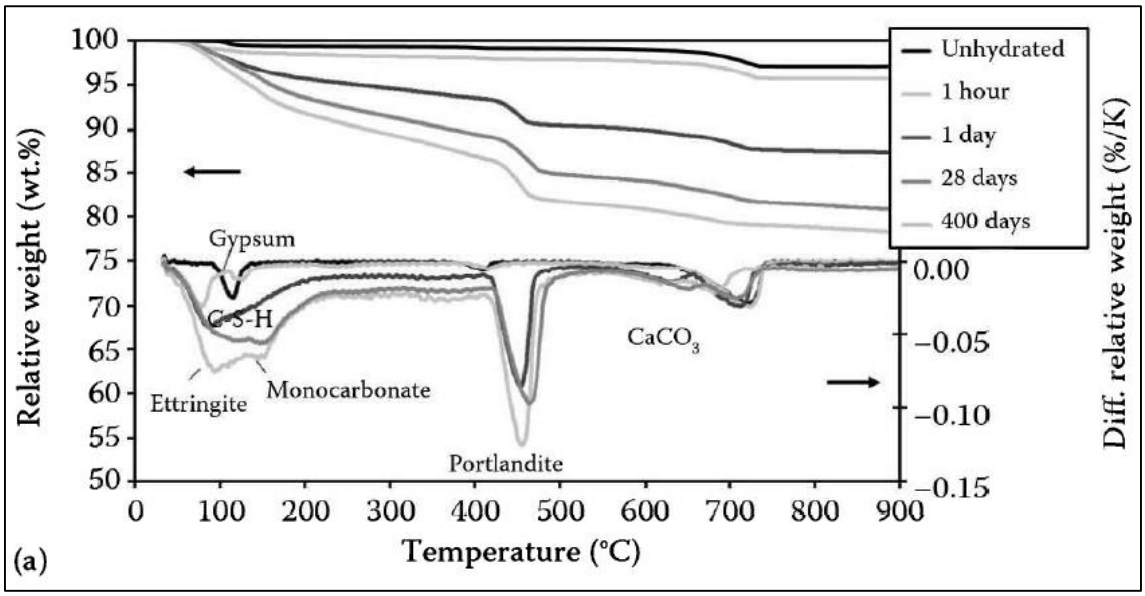

Figure 3.1. TGA and DTG of a hydrating Portland cement at different curing ages, illustrating typical decomposition processes of solids occurring in cementitious systems (Lothenbach *et al.*, 2016).

Figure 3.1 visibly shows the overlap dehydration processes of many cement hydration products between approximately 100 and 200 °C, whereas the mass loss associated with dehydroxylation of portlandite and decarbonation of calcium carbonate do not overlap with any other mass loss events in the cement sample.

Thermal analysis for this study was performed on a TGA/DSC 1 STARe system from METTLER TOLEDO. Data evaluation was performed on version 9.10 of the STARe Excellence software. Samples were heated in uncovered 70 µl alumina oxide crucibles from 40 °C to 1000 °C at a dynamic heating rate of 10 °C/min. Nitrogen gas, purged at a flow rate of 20 mL/min, was used as the measurement atmosphere.

3.2.6 Fourier transform infrared spectroscopy (FTIR)

Unlike XRD, Fourier transform infrared spectroscopy (FTIR) is able to provide information about chemical bond environments regardless of their degree of crystallinity (Donatello *et al.*, 2014b). The benefit of the latter statement means that the typical amorphous or poorly crystalline C-S-H-type gels in hydrated cement may be identified and studied with FTIR, which is not possible with techniques such as XRD. Moreover, FTIR analysis gives rapid results after a few minutes while other methods need at least a few hours to study one sample (Horgnies *et al.*, 2013). Typical characteristic transmission bands for ordinary unhydrated cement clinker minerals, as well as the expected band positions for hydrated cement is presented in Table 3.2.

Table 3.2. Typical FTIR characteristic transmission bands for species occurring in cement and hydrated cement (cm^{-1}).

Mineral	Unassigned fundamentals		Overtones	O-H Stretch	O-H Bend	References
Clinker phases						
C_3S, Alite	Si-O	935, 521	2000-1600			(Choudhary *et al.*, 2015; Donatello *et al.*, 2014b; Hughes *et al.*, 1995; Mejía *et al.*, 2015; Mollah *et al.*, 2000; Palomo *et al.*, 2007; Ylmén *et al.*, 2009)
C_2S, Belite	Si-O	991, 879, 847, 509	2060-1600			
C_3A	Al-O	889, 860, 812, 785, 762,621, 586, 518, 506				
C_4AF	Fe-O	700-500				

	Fundamentals			Overtones	O-H Stretch	O-H Bend	References
	υ_1	υ_3	υ_4				
Sulfates							
Gypsum	1005	1142, 1114	669, 604	2500-1900	3553, 3399	1686, 1618	(Hughes *et al.*, 1995) (Donatello *et al.*, 2014b; Ylmén *et al.*, 2009)
Syngenite	1001	1192, 1130,1113	658, 644, 604	2500-1900	3309	1678	
Anhydrite	1015	1163	677,615, 600	2500-1900			
Carbonates and Hydroxides							
Calcium carbonate	876, 849	1458	714	2980-2500, 1794			(Hughes *et al.*, 1995) (Donatello *et al.*, 2014b; Hughes *et al.*, 1995; Kontoleontos *et al.*, 2013; Mollah *et al.*, 2000; Ylmén *et al.*, 2009)
Calcium hydroxide					3641-3642		
Hydration phases							
Ettringite		1114					(Kontoleontos *et al.*, 2013) (Donatello *et al.*, 2014b)
C-S-H		970-980					

Typical characteristic transmission bands for fly ash include a strong peak in the area between 900 and 1200 cm^{-1}. The presence of this band is attributed to Si-O-Si asymmetric stretching vibrations with contributions of quartz, mullite and glass. The band at approximately 900 cm^{-1} originates from Al-O symmetric stretching vibrations from mullite, and the characteristic doublet of quartz is evident at around 772 – 797 cm^{-1} (Criado *et al.*, 2007; Van Der Merwe *et al.*, 2014).

The FTIR measurements in this thesis were recorded with a Bruker Tensor Fourier transform infrared (FTIR) spectrometer by placing the finely ground samples in a diamond ATR (attenuated total reflection) cell. Data was collected from 400 cm^{-1} to 4000 cm^{-1} and data analysis was performed using OPUS 7.2 software. Thirty two scans were signal-averaged in each interferogram.

Unfortunately, due to the poor sensitivity of the instrument below 500 cm^{-1} and the small amount of cement present in the hybrid fly ash cement studied, anhydrous minerals associated with cement (e.g. tricalcium aluminate (C_3A)) could not be characterised in this study.

3.3. Characteristics of the fly ash surface reactivity exposed to a calcium hydroxide environment

In order to assess the effect of an alkaline environment on the reactivity of fly ash, it was exposed to a saturated calcium hydroxide solution. Cement as a source of calcium hydroxide was excluded due to all the possible effects that the heterogeneous cement can contribute to the hydration investigation.

Five gram of each of the three fly ash products, FCFA, UFA and MUFA, were placed in 1 L glass containers to which 200 ml of the calcium hydroxide solution (2 g/L) was added to serve as the curing medium.

In addition to this, chemical activation by addition of sodium sulfate was investigated (5%, calculated as a mass percentage of the total fly ash content). The glass containers were sealed and placed in a shaking water bath at 25 °C and shaking speed of 150 min^{-1}. At specified curing ages (1, 7, 28 and 56 days), a small amount of the sample was removed, filtered and washed

with deionised water followed by isopropanol, and dried at 40 °C for 24 hours after which XRD and FESEM analyses were performed.

3.4. Sulfate optimisation of a hybrid cement produced from unclassified fly ash (UFA) and cement (MC)

3.4.1 Introduction

The maximum fly ash content is constrained due to extended setting times, insufficient early strength and slow strength development ascribed to the rate of the pozzolanic reaction between cement and fly ash (Blanco *et al.*, 2006; Heinz *et al.*, 2010). It is also well known that the degree of hydration and early age compressive strength tends to decrease with an increase in level of fly ash (Al-Zahrani *et al.*, 2006). In order to meet the standard physical and mechanical requirements as indicated in Table 3.3, a hybrid cement containing as much as 70% of fly ash will require activation.

In this part of the study initial tests were conducted to determine whether the setting time and early age strength development of the fly ash based hybrid cement could be enhanced through chemical activation with sodium sulfate. To ensure financial viability of the hybrid cement it is necessary to optimize the sulfate content by adding just enough sulfate to ensure that the required properties can be obtained. In order to attain a general working range (0% - 5%) that would be considered in this study for the addition of sodium sulfate, at a level that would still be cost effective, it was not deemed necessary to complete this study on all 3 fly ashes, but only on one, i.e. UFA.

Table 3.3. Mechanical and physical requirements from EN 197 given as characteristic values (CEN, 2011).

Strength class	Compressive strength MPa				Initial setting time	Sound-ness (expan-sion)
	Early strength		Standard strength			
	2 days	7 days	28 days		min	mm
32,5 L[a]	-	≥ 12,0	≥ 32,5	≤ 52,5	≥ 75	≤ 10
32,5 N	-	≥ 16,0				
32,5 R	≥ 10,0	-				
42,5 L[a]	-	≥16,0	≥ 42,5	≤ 62,5	≥ 60	
42,5 N	≥ 10,0	-				
42,5 R	≥ 20,0	-				
52,5 L[a]	≥ 10,0	-	≥ 52,5	-	≥ 45	
52,5 N	≥ 20,0	-				
52,5 R	≥ 30,0	-				
a Strength class only defined for CEM III cements.						

3.4.2 Setting time

The progress of the stiffening and hardening of a cement paste may be recorded by the change in resistance of a test specimen, made up of a cement/water paste of standard consistency, to penetration of loaded needles of specified cross-sectional area (Alexander *et al.*, 1986).

Setting time tests were performed as per SANS 50196-3: Determination of setting times and soundness (SABS, 2006c). For this test 500 g of cementitious materials was weighed, and the amount of water added was based on the result of the standard consistence test as set out in SANS 50196-3. Specimens were cast in plastic, cylindrical moulds with a depth of 40 ± 0.2 mm and internal diameter of 70 ± 1 mm.

3.4.3 Early age strength development

The aim of this investigation was to determine the minimum amount of sulfate that needs to be added to a hybrid cement containing 70% fly ash and 30% cement to ensure that the early age

strength development of the hybrid cement meets strength requirements as specified in compulsory cement standards. This aspect of the work focussed solely on chemical activation (Na_2SO_4) of unclassified fly ash/cement blends prepared at a 70/30 mass ratio in a five litre countertop cement mixer. The standard mixture containing 75% standard reference sand (with a relative density of 2.63 g/m^3) and 25% hybrid cement. The sand used to produce mortars for compressive strength testing, complied with the specifications of EN 196-1/ SANS 50196-1 (CEN, 2016). The sand originated from France. It is a natural sand and has a silica content of 98.06%. The grading analysis for the sand is supplied in Table 3.4

Table 3.4. Grading analysis of CEN sand complying with EN 196 / SANS 50196.

Sieve size	Minimum value	Maximum value
mm	Cumulative percentage retained (%)	
2.000	0	0
1.600	6.3	6.7
1.000	31.6	33.7
0.500	66	69
0.160	87.7	88.8
0.080	99.7	99

Different amounts of Na_2SO_4 (0 – 5 wt.% of the total cementitious content) were added to the fly ash-cement blends in 1% increments. Two methods of addition were used; in the first, the sulfate was mixed in as a dry powder, while in the second it was dissolved in 225 ml of the mixing water before being added to the blend. A water-to-binder ratio of 0.5 was maintained for all of the blends prepared for compressive strength testing.

Curing and strength testing were done according to SANS 50196-3. Sets of three 40 mm x 40 mm x 160 mm mortar prisms were cast in steel moulds and demoulded 24 hours after casting (SABS, 2006c). The mortar prisms were then placed in curing baths at 23±1 °C where they remained up to the day of testing. Compressive strength was determined 1, 2, 7 and 28 days after casting. Compressive strength testing of all blends were done as per SANS 50196-1: Methods of testing cement Part 1: Determination of strength (SABS, 2013a). At each curing

age, both ends of the mortar prisms were crushed between two 40 mm x 40 mm plates and the maximum loads recorded was used to calculate the compressive strength. Values reported in this thesis are the average of six compressive strength tests (three mortar prisms). Figure 3.2 provides images of the steel moulds in which the mortar prisms are cast, as well as the compressive strength testing equipment.

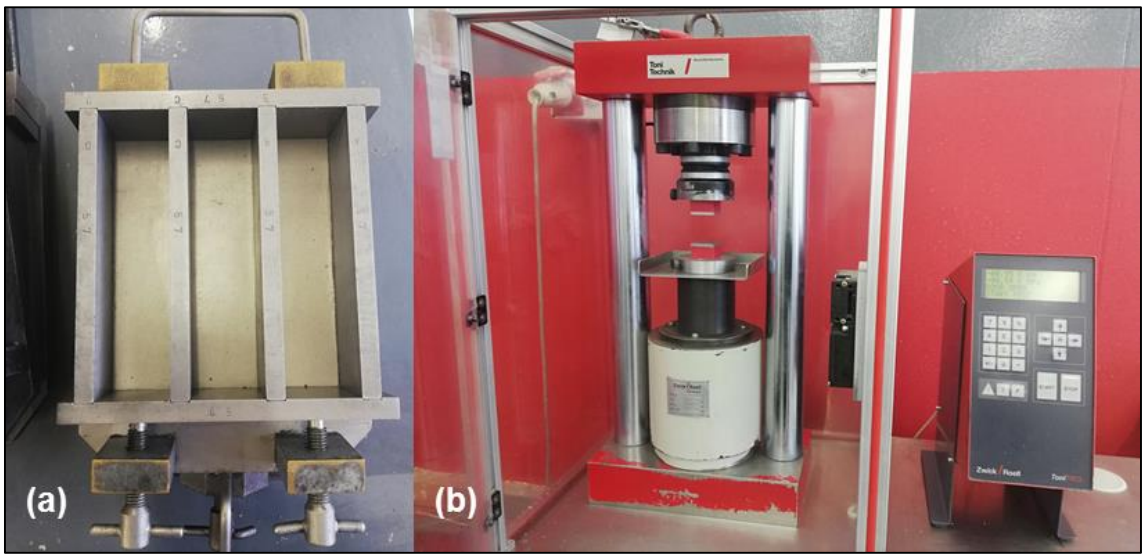

Figure 3.2. (a) The steel moulds in which mortar prims are cast and (b) the compressive strength testing equipment for mortar prisms.

3.5. Hybrid fly ash cement paste

3.5.1 Characterisation techniques

Cement pastes (without any aggregates) were prepared by mixing 70% of dry UFA or MUFA respectively with 30% cement (MC) by mass and a constant water:binder ratio of 0.5. It is common practice in cement hydration research to exclude any aggregates so as to not dilute hydration products and render characterisation of hydration products a lot more challenging.

Sulfate addition for the characterisation work was limited to the minimum and maximum (extreme) scenario, thus 0% and 5% Na_2SO_4, to investigate the hydration chemistry. This

decision was made due to limited availability of expensive, advanced analytical equipment and resources.

Neat paste specimens for the purpose of the investigation and characterisation of hydration products by means of analytical techniques, were prepared with a 0.5 water:binder ratio, using the mixing equipment as specified in SANS 50196-1: Methods of testing cement Part 1: Determination of strength. However, due to the fact that no sand or aggregates were added (resulting in a smaller volume of paste), and smaller amounts of sample were needed for analyses, the standard steel moulds were replaced with expanded polystyrene (EPS) moulds. Each EPS mould consisted of 6 cavities (55 x 52 x 45 mm), and duplicate specimens were cast for each curing age (see Figure 3.3).

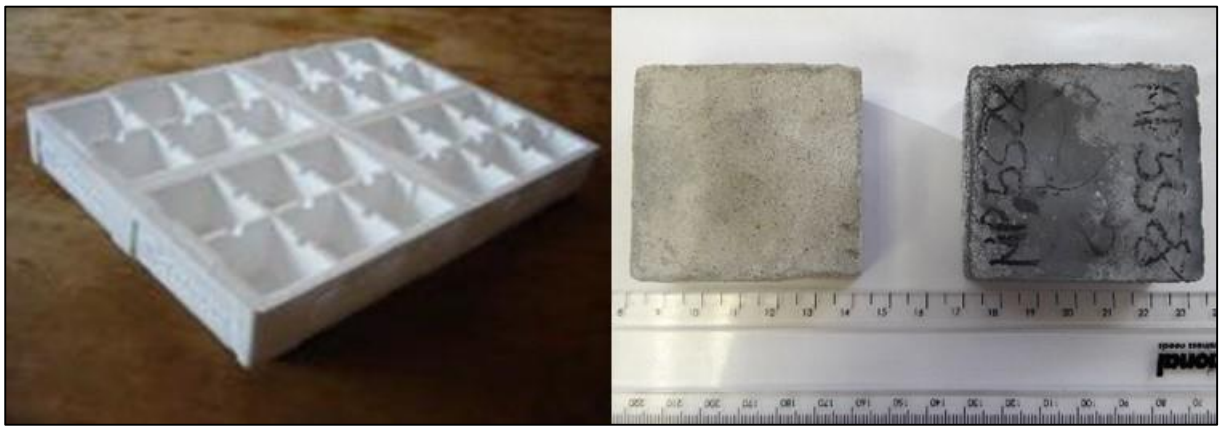

Figure 3.3. Example of the EPS moulds used (left) and neat pastes cast in the EPS moulds (right) for analytical characterisation.

The specimens were prepared for the following curing ages: 1, 7, 28, 90, 180 and 365 days. After casting, the pastes were cured in temperature controlled water tanks at 23±1 °C.

Upon demoulding of the specimens at the specified curing ages, they were immediately crushed into small fractured pieces and immersed into sealed isopropanol containers for 7 days (Kocaba, 2009), where after they were dried at 40 °C to drive off any remaining isopropanol

and stored in desiccators under vacuum in order to arrest hydration until the appropriate analyses could be performed.

Hydration products of the hybrid fly ash cement pastes were characterised using the following techniques: X-ray powder diffraction (XRD), thermogravimetric analysis (TGA), Fourier transform infrared spectroscopy (FTIR) and Field emission scanning electron microscopy (FESEM) as a supplementary technique.

3.5.2 Setting time

Setting time tests were conducted in an effort to link changes in early age chemical characteristics to setting times. These tests were executed in exactly the same manner as previously discussed (see section 3.4.2 for detail) as per SANS 50196-3: Determination of setting times and soundness (SABS, 2006c).

3.5.3 Heat of hydration

Calorimetry was used to measure the rate of heat production. It is a generic way of studying processes (physical, chemical and biological), seeing that all processes are generally related to an enthalpy change. One of the oldest and most common applications of calorimetry is the study of hydration of cement (Wadso *et al.*, 2016). Hydration of cementitious materials in a mortar and concrete mixture results in a number of exothermic chemical reactions that liberate heat. The heat evolution process is strongly influenced by the chemical and physical properties of Portland cement, water-to-cement ratio (w/c), mineral and chemical admixtures, mortar and concrete mix proportions and curing conditions, to only name a few (Hu *et al.*, 2014).

Isothermal calorimetry tests, often used in studying the kinetics of cement hydration, are conducted at a constant temperature. Each specimen's rate of heat evolution is directly measured by monitoring the heat flow released (reaction rate). The total heat flow can be readily determined from the integration of the measured heat flow rate over time (Hu *et al.*, 2014).

The rate of heat evolution of a typical ordinary Portland cement paste, determined by isothermal calorimetry, is illustrated in Figure 3.4.

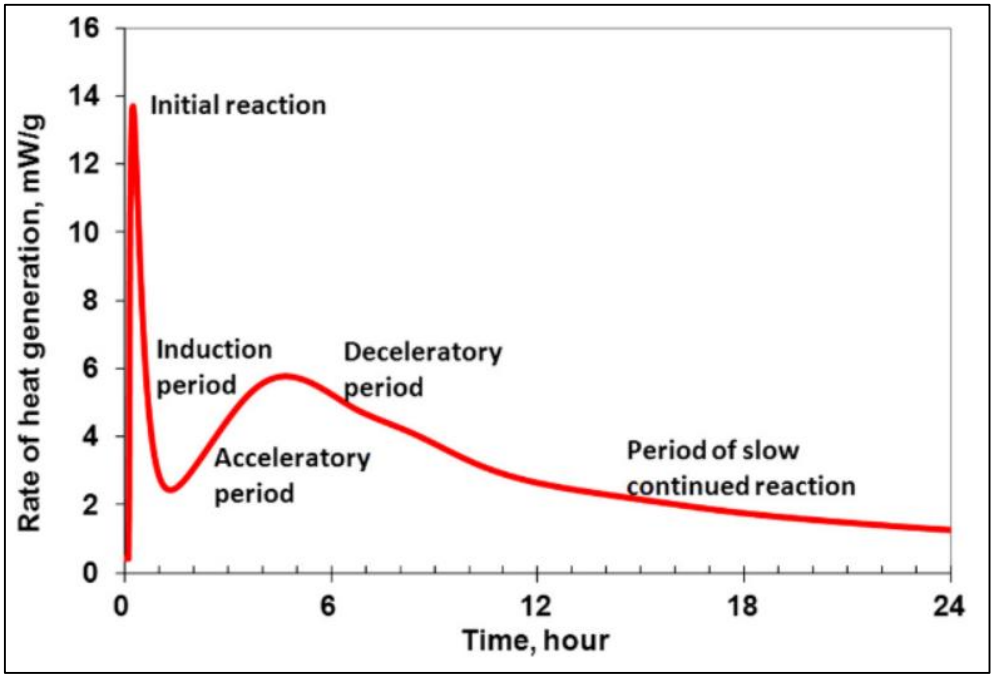

Figure 3.4. Example of a heat of hydration curve, presenting the typical five stages of heat evolution for ordinary Portland cement (Hu *et al.*, 2014).

The curve clearly shows the five typical stages of cement hydration reactions as described in literature (Taylor, 1997). These are the initial reaction (initial maximum rate of heat evolution, the induction period (so called minimum rate of heat evolution), the acceleratory period, the deceleratory period and the period of slow continued reaction (Figure 3.3).

The initial reaction is attributed to a combination of exothermal hydration and the early-stage reactions which produce gelatinous coating, and rods of the AFt phase (usually ettringite). Rehydration of hemihydrate to produce gypsum may also contribute (Taylor, 1997). It is generally accepted that setting takes place in the acceleratory period. During this period, the silicates begin to hydrate rapidly, producing the main hydration products (C-S-H) and portlandite, and the hydration reaction reaches a maximum rate of heat generation (Hu *et al.*, 2014).

After 24 hours, there is a gradual rate loss of heat evolution, corresponding to the continuous slow reactions of the late stage, producing once again C-S-H and portlandite. Heat of hydration curves of many cement specimens indicate a shoulder or more definite peak at about 16 hours during the deceleratory period, which has often been erroneously associated with the replacement of AFt by an AFm phase. However, this phenomenon is better described to represent renewed formation of ettringite (Taylor, 1997).

During their study on very high volume fly ash cements at early age hydration, using Na_2SO_4 as an activator, Donatello *et al*. (2013) provided the following explanation regarding heat evolution (see Figure 3.5). The considered sample which is similar to the scenario in this thesis (labelled FAN4) is a fly ash hybrid cement consisting of 78% fly ash, 18% clinker and 4% Na_2SO_4.

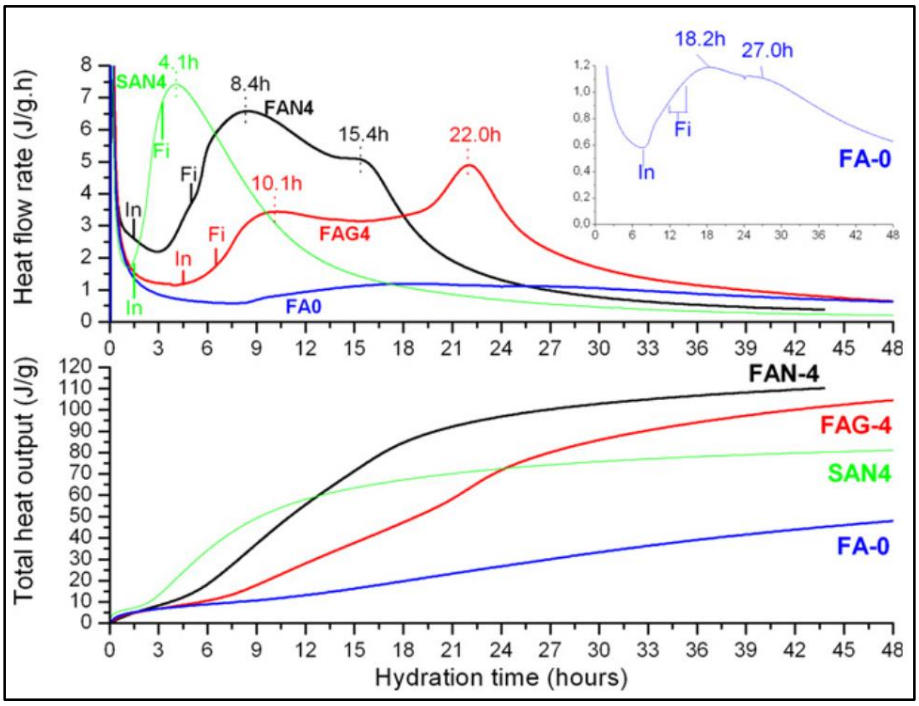

Figure 3.5. Early age calorimetric data. Initial (In.) and final (Fi) setting times are indicated on the graphs. FAN4 is the considered scenario. (Donatello et al., 2013).

A reasonable assumption was made that heat output in all of the pastes was dominated by alite hydration, and that the presence of SO_4^{2-} greatly accelerates the rate of early alite hydration.

The greater early heat release of FAN4 compared to the other specimens, was ascribed to SO_4^{2-} ions accelerating the rate of early hydration of alite, along with the Na^+ cations from the dissolved Na_2SO_4, increasing the solution pH and the precipitation of alite hydration products such as C-S-H gel (Donatello *et al.*, 2013).

In this study heat evolution during cement hydration was measured using a TAM Air microcalorimeter at 25 °C and a water:binder ratio of 0.5. Dry hybrid cement blends were weighed into the ampules, water was added to the dry blend via syringes and then mixed to produce neat pastes (see Figure 3.6). Heat evolution data was collected up to 21 days. Data evaluation was performed using TAM Assistant software version 0.9.

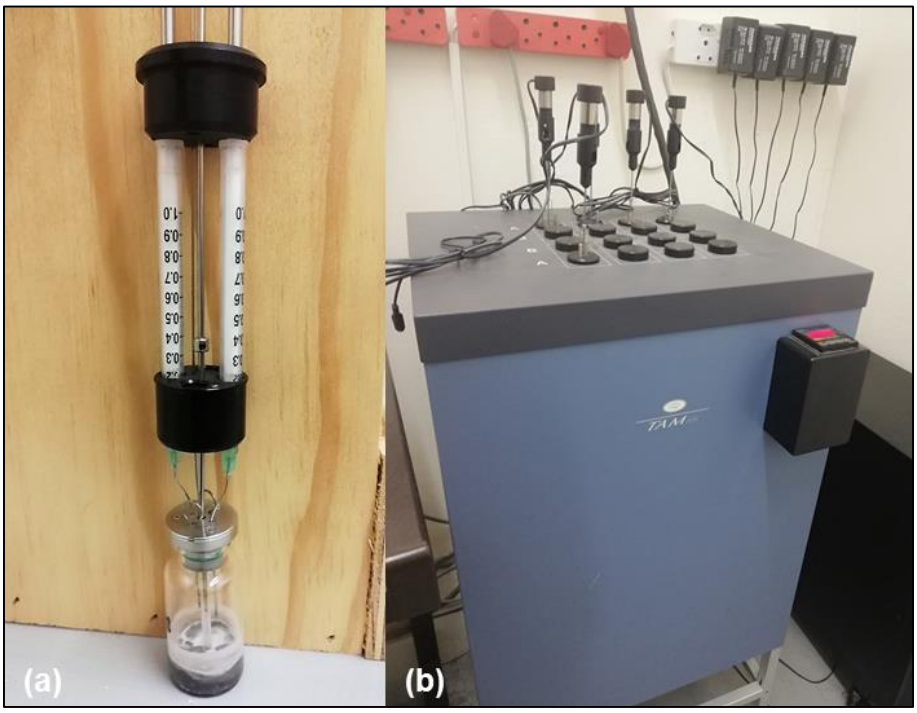

Figure 3.6. Example of an (a) ampule and syringes and (b) the TAM Air microcalorimeter.

3.5.4 Expansion (soundness)

Early age expansion measurements provide an indication of any unwanted swelling occurring in the cement once hydration takes place. For this study there may be a concern that excess

expansion (caused by delayed ettringite formation) can take place due to the addition of sulfates (Na_2SO_4) as a chemical activator.

Expansion testing was done according to per SANS 50196-3: Determinaion of setting times and soundness (SABS, 2006c) for the specimen of concern, thus the chemically and mechanically activated MUFA5 hybrid cement.

A cement paste of standard consistency was prepared. The same paste composition that was prepared for setting time purposes was used for this test. A lightly oiled *Le Chatelier* mould was placed on a lightly oiled base-plate and filled to the top. The mould was covered with a lightly oiled cover plate, and then immediately placed in curing tanks maintained at 20 ± 1 °C for 24 hours ± 30 minutes. When the 24 hours ± 30 minutes period has passed, the distance between the indicator points was measured to the nearest 0.5 mm (A). Then, the mould was gradually heated in a water bath to boiling for a period of 30 ± 5 minutes. Boiling temperature was maintained for 3 hours ± 5 minutes. The mould was removed from the heat and allowed to cool to laboratory temperature. The distance, C, between the indicator points, was measured to the nearest 0.5 mm. The difference between A and C (C - A) was calculated to the nearest millimetre and reported as the expansion value.

3.6. Hybrid fly ash mortar tests

Hybrid fly ash cement mortar blends were prepared by mixing 70% of dry UFA, FCFC, or MUFA respectively with 30% cement (MC) as binder and adding standard sand (in compliance with EN 196-1) to this mix in a binder:sand mass ratio of 1:3 to form a mortar with a water:binder mass ratio of 0.5. The aim of preparing the mortar blends was to compare standard compressive strengths; hence, all blends were mixed, cured and tested in accordance with EN 196 / SANS 50196 (CEN, 2016) which is the standard practice in the South African cement industry. Different percentages of Na_2SO_4 at 0%, 1%, 3% and 5% wt%, relative to the cementitious content, had been manually added to the fly ash-mortar blends.

Preparation, mixing and compressive strength testing of all blends were done as per EN 196-1: Methods of testing cement Part 1: Determination of strength (CEN, 2016). The temperature of the curing room and water inside the curing tanks were maintained at 23±1 °C

and the humidity in the room was above 90%. At predetermined curing ages (1 day, 2-, 7-, 28-, 90-, 180 days and 1 year); samples were removed from the curing tanks and their compressive strength determined. Strength tests were conducted on the ends of 40 mm x 40 mm x 160 mm mortar prisms. Compressive strength testing of all blends were done as per EN 196-1: Methods of testing cement Part 1: Determination of strength (CEN, 2016). Compressive strengths reported are the arithmetic mean of 6 measurements (n = 6).

3.7. Hybrid fly ash concrete testing

3.7.1 Mix composition

Since the majority of all cement end up being used in concrete applications, hybrid fly ash cement for use in concrete were prepared by mixing 70% of dry UFA, FCFC, or MUFA respectively with 30% cement (MC). Different percentages of Na_2SO_4 at 0%, 1%, 3% and 5% Na_2SO_4, were manually added to the fly ash cement blends while mixing the concrete. Andesite (crusher sand and 22.4 mm stone) made up the aggregates for each concrete mix. The chemical composition (XRF, wt %) of the two aggregates used in the production of the concrete mixes, i.e. an andesite 22.4 mm stone and andesite crusher sand, is shown in Table 3.5, and the grading analysis in Table 3.6.

Table 3.5. Chemical composition (XRF, wt %) of the aggregates used in the concrete mixes.

	22.4 mm Stone	Crusher sand
SiO_2	55.49	
Al_2O_3	14.80	14.42
CaO	6.90	8.09
Fe_2O_3	11.92	11.97
MgO	4.52	4.31
K_2O	1.24	1.09
Na_2O	3.89	2.94
TiO	0.93	0.89
Mn_2O_3	0.16	0.17
P_2O_5	0.14	0.14
LOI	1.72	2.88

Table 3.6. Grading analysis of the 22.4 mm stone and crusher sand used in the concrete mixes.

Sieve size	22.4 mm Stone	Sieve size	Crusher sand
mm	Cumulative % retained	mm	Cumulative % retained
37.5	0.0	9.5	0.0
26.5	0.3	6.7	0.0
22.4	5.9	4.75	2.8
19.0	28.4	2.36	33.3
13.20	92.0	1.18	56.2
9.50	99.2	0.600	70.1
6.700	99.6	0.300	75.8
4.75	99.7	0.150	84.6
0.075	99.7	0.075	-

The mix design for all of the hybrid fly ash concrete mixes are provided in Table 3.7 from which it can be seen that the water and binder contents of the mixes remained constant at 200 l/m^3 and 300 kg/m^3 respectively resulting in concrete with a water:binder ratio of 0.67.

Table 3.7. Target mix design for hybrid fly ash concrete mixes.

Material	Target content (kg/m^3)	Relative density (kg/L)
Cement (MC)	90	3.14
Fly ash (FCFA, UFA or MUFA)	210	2.16
Water	200	1.00
Andesite crusher sand	903	2.87
Andesite 22.4 mm stone	1050	2.92

3.7.2 Workability (Slump retention)

Workability (slump retention) is generally accepted to refer to the ease of transporting, placing and compacting concrete in such a way that there is no segregation or separation of the individual constituents. The slump test, which serves as one of the tests that can supply an indication of workability of a concrete mix, is by far the most widely used, and has been adopted by American Society for Testing and Materials (ASTM); the British Standards Institution (BS) and the South African Bureau of Standards (SABS) (Alexander *et al.*, 1986). It is important to keep in mind that apart from some drawbacks like the sensitivity to small changes in water content and the fact that the test is heavily operator dependent, there also exists differences in practice with its use in different countries (see Figure 3.7) (Domone, 2003).

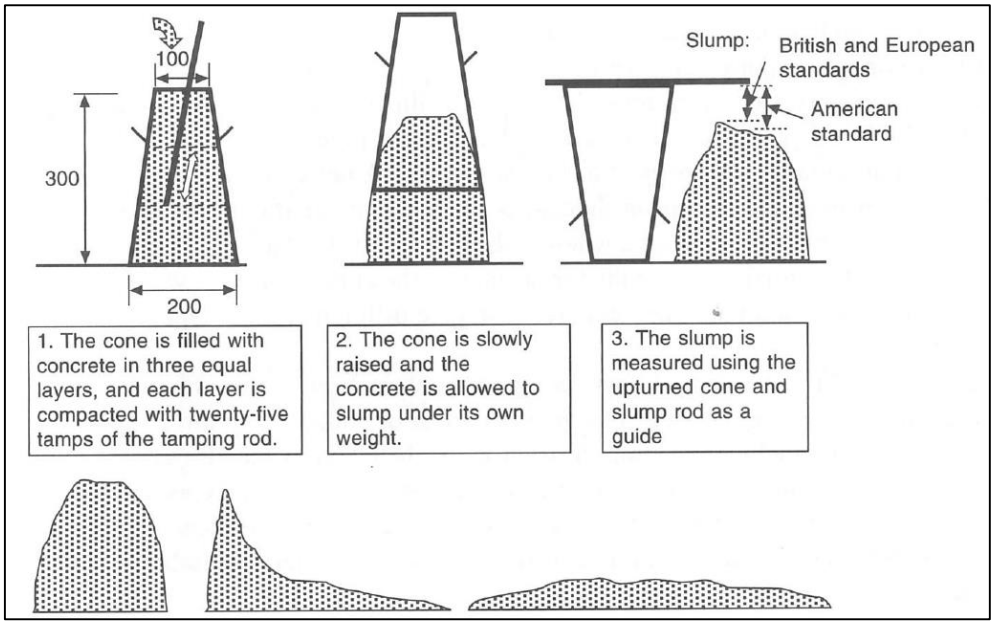

Figure 3.7. The slump test, also illustrating the difference between the different practices (Domone, 2003).

For South African conditions, Table 3.8 shows the slumps recommended for various types of construction (SABS, 1982). It is important to note the large tolerances that are accepted in the specification.

Table 3.8. Slump limits according to SABS 1200 G 1982 and accepted in South Africa (SABS, 1982).

1	2	3	4	5
Type of construction	Hand-placed		Vibrated	
	Max.	Min.	Max.	Min.
Paving and precast units ...	70	50	50	30
Heavy mass construction	70	30	50	20
Reinforced foundation walls and footings	120	50	80	30
Slabs, beams, columns, and reinforced walls	120	50	80	30
Slabs and industrial floors on ground	120	70	80	50
Plain footings, caissons, and substructure walls	100	30	60	20
Heavy duty industrial floors	-	-	80	50

Consistency for this study was determined according to SANS 5862-1: Consistence of freshly mixed concrete – slump test (SABS, 2006b).

3.7.3 Strength behaviour

Compressive strength testing of all concrete blends were done as per SANS 5863: Concrete tests - Compressive strength of hardened concrete (SABS, 2006a). Sets of two 100 mm cubes were cast for each curing age after the slump test was applied to each mix. The cast specimens were placed in a temperature and humidity controlled curing room for 24 hours, after which specimens were tested for 24 hour strength gain. The remainder of the specimens were placed in temperature controlled (23±1 °C) curing tanks inside the curing room, for testing after 1, 7, 28, 90, 180 and 365 days of curing.

3.8. Overview of experimental program

An overview of the different experiments, cementitious blends, sodium sulfate additions and applied test methods, as described in Chapter 3, is provided in Figure 3.8.

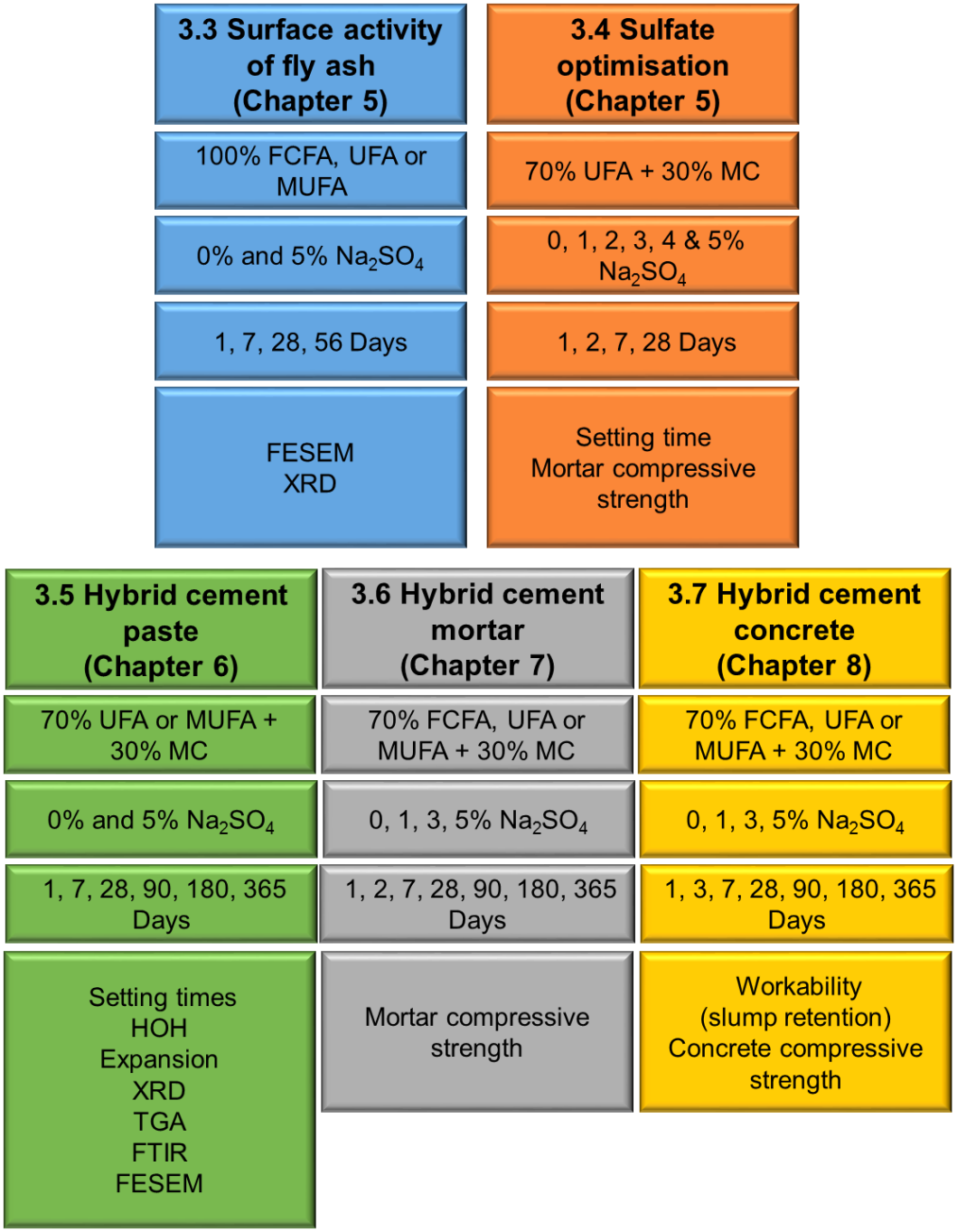

Figure 3.8. Diagram providing an overview of the experimental program.

~ Chapter 4 ~

Characterisation of raw cementitious materials

4.1 Introduction

In this chapter, the results on characterisation of the raw cementitious materials (FCFA, UFA, MUFA and MC) is presented and discussed. These materials were identified with the following descriptors:

- FCFA : **F**ine **C**lassified **F**ly **A**sh
- UFA : **U**nclassified **F**ly **A**sh
- MUFA : **M**echanically Activated **U**nclassified **F**ly **A**sh
- MC : Portland cement (**M**illed **C**linker)

The characterisation techniques applied include XRF, XRD, PSD, FESEM, TGA and FTIR.

4.2 X-ray fluorescence (XRF)

The mass percentages of the major elements in the cementitious starting materials were determined using XRF. Table 4.1 provides the chemical composition of the raw cementitious materials (cement and fly ash).

Table 4.1. Chemical composition (XRF, wt. %) of the starting materials.

	FCFA	UFA	MUFA	Cement (MC)
SiO_2	50.09	54.83	54.87	20.36
Al_2O_3	34.35	30.86	31.11	4.73
CaO	4.54	4.84	5.06	65.08
Fe_2O_3	3.09	3.62	3.83	2.80
MgO	1.28	1.17	1.19	1.78
K_2O	0.73	0.63	0.63	0.46
Na_2O	0.25	0.16	0.17	0.07
TiO	1.73	1.57	1.55	0.45
Mn_2O_3	0.03	0.03	0.03	0.10
P_2O_5	1.10	0.63	0.63	0.07
SO_3	0.28	0.40	0.31	2.73
LOI	0.79	1.19	1.64	5.67
Total	98.26	99.93	101.02	104.30

The two major constituents of all the fly ash samples were SiO_2 (approx. 50-55%), Al_2O_3 (approx. 30 -35%) and to a lesser extent CaO, Fe_2O_3, MgO, TiO and P_2O_5. The remainder of the elements were present in weight percentages less than 1%. All three fly ash samples had LOI values less than 5% and a (SiO2 + Al2O3 + Fe2O3) mass % content exceeding 70%. According to the requirements of EN 450/SANS 50450 for LOI and the total (SiO_2 + Al_2O_3 + Fe_2O_3) mass % content, FUFA, UFA and MUFA all comply with a Class A fly ash (refer to Table 2.1).

The two major constituents for the cement (MC) sample are CaO (65.08%) and SiO_2 (20.36%), and to a lesser extent Al_2O_3, Fe_2O_3, and MgO. The remainder of the elements were present in weight percentages less than 1%.

4.3 X-ray powder diffraction (XRD)

XRD analysis was used for mineral identification and quantification of the crystalline phases and amorphous content of the raw cementitious materials. The mineralogical composition (wt. % normalised) of the cementitious materials are presented in Table 4.2.

Table 4.2. Mineralogical composition (XRD, wt. % normalised) of the starting materials.

	FCFA	UFA	MUFA	Cement (MC)
Anhydrite	-	-	-	1.3
Belite	-	-	-	7.7
Alite	-	-	-	43.2
Brownmillerite	-	-	-	12.9
Tricalcium aluminate	-	-	-	3.4
Calcite	-	-	-	9.9
Gypsum	-	-	-	1.3
Hematite	0.3	1.0	0.8	-
Mullite	28.9	31.5	27.5	-
Quartz	3.7	12.2	10.3	0.8
Amorphous	67.1	55.3	61.5	19.3

Although there are no major differences in chemical composition (XRF results, Table 4.1) the mineralogy of the fly ashes differ, particularly as far as amorphous and quartz content is concerned. The fly ash samples consist predominantly of an amorphous alumina silicate phase, which is higher in FCFA than in either UFA or MUFA. The mineralogy of the fly ashes differ particularly as far as their amorphous and quartz content is concerned. Mullite, the most abundant crystalline phase, occur in comparable amounts. The hematite and quartz content of FCFA is however substantially lower than that of the other two ashes. The effect of milling UFA to produce MUFA decreased the mullite and quartz content slightly, accompanied by a concomitant increase of approximately 6% in the amorphous content. Based on mineralogical data composition, FCFA should, by virtue of its higher amorphous content be a more reactive and effective pozzolan (Kaur *et al.*, 2017).

The composition of the Portland cement (MC) sample is typical of that produced in South Africa.

4.4 Particle size distribution (PSD)

The particle size distribution (PSD) of the cementitious starting materials (FUFA, UFA, MUFA and MC) are presented in Table 4.3 and Figure 4.1.

Table 4.3. The particle size distribution (µm) of the raw materials at 10%, 50% and 90% of the respective sample size.

	d_{10}	d_{50}	d_{90}
FCFA	0.53	3.07	6.67
UFA	4.44	52.46	224.2
MUFA	0.55	4.79	19.00
MC	1.29	12.69	31.63

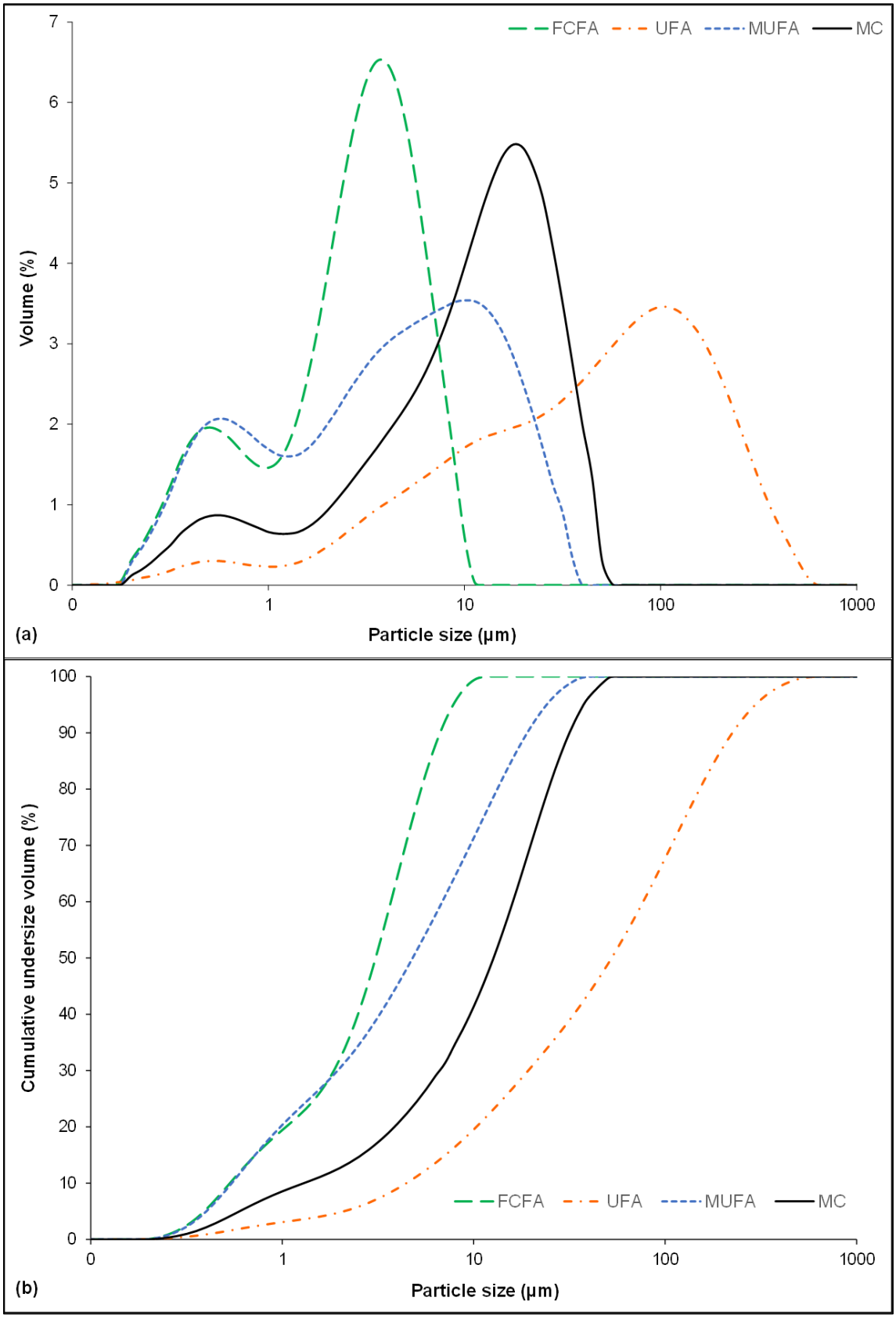

Figure 4.1. Particle size distribution of the three FA samples: (a) volume % and (b) cumulative undersize volume

It is evident that with its complete range of particles being below 10 µm, FCFA is finer than MUFA, whereas UFA is significantly coarser than both of these. Although the particle size distribution of MUFA indicates a somewhat coarser material than FCFA, their mean particle size (d_{50}) of 8 and 5 µm, respectively, are almost identical. Owing to the greater abundance of smaller particles, FCFA will have the larger surface area and is therefore expected to be more reactive and achieve higher compressive strengths than either UFA or MUFA when used in cementitious binders. The larger number of smaller spherical particles in FCFA should in theory also provide more nucleation sites for reaction, improve particle packing density and by implication the physical properties like strength gain of blended cement (Tangpagasit et al., 2005).

MC has a very similar bimodal particle distribution compared to FCFA, however, the portion of coarser particles is more than for FCFA and MUFA, but less than for UFA.

4.5 Field emission scanning electron microscopy (FESEM)

Field emission scanning electron microscopy (FESEM) was applied to study the morphology of the cementitious starting materials (see Figure 4.2 and Figure 4.3).

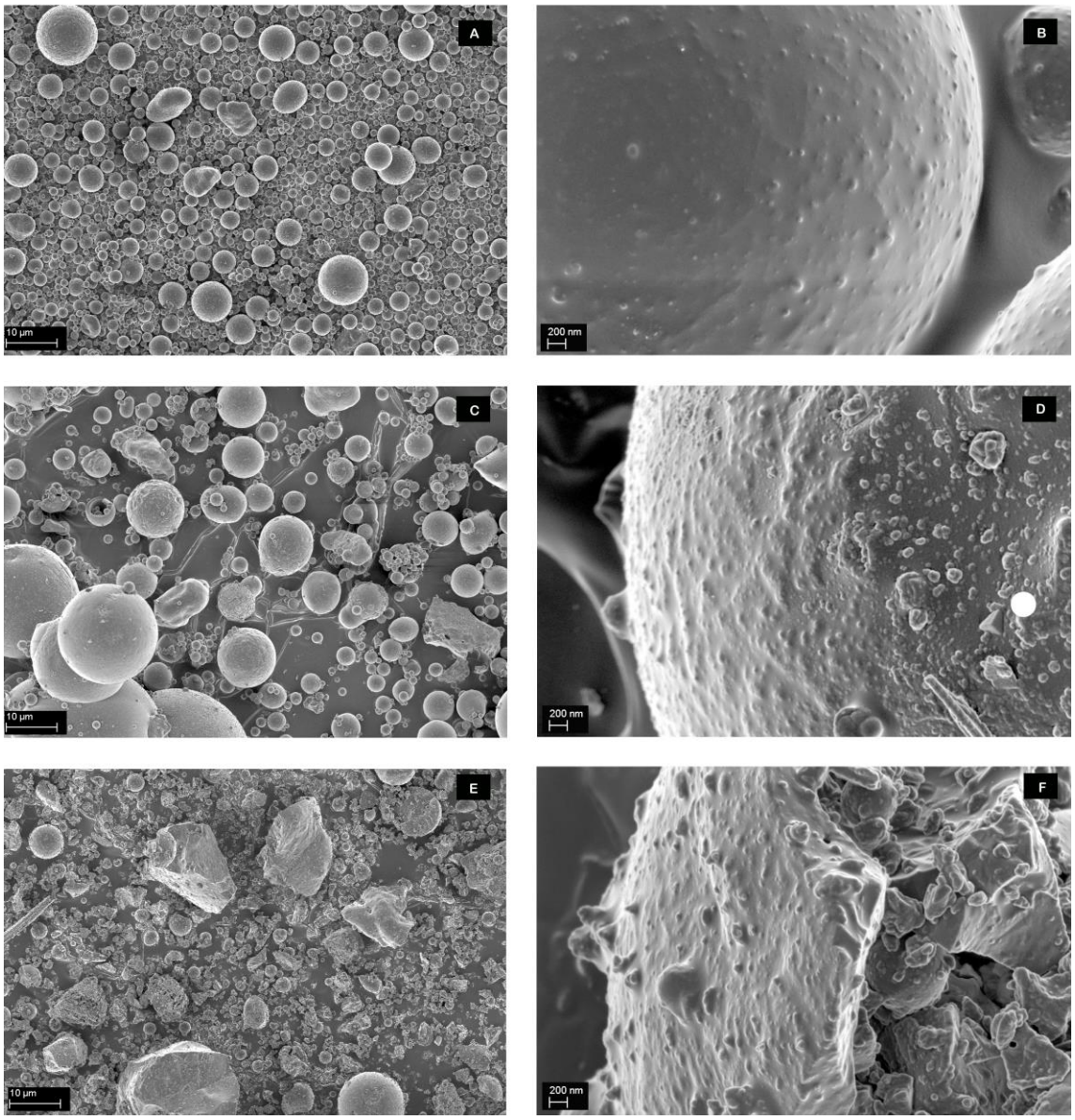

Figure 4.2. Scanning electron micrographs representing the morphology of untreated (a-b) FCFA, (c-d) UFA and (e-f) MUFA at 3000x and 50000x magnification respectively.

The morphology of the three fly ashes (Figure 4.2) indicates that spherical particles which are known to improve particle packing density in mortar and (Kearsley & Wainwright, 2003), are more predominant in FCFA than in either UFA or MUFA. Each of the specimens contained irregularly shaped particles, many of which are associated with mullite and quartz. The mechanically activated sample, MUFA has a plethora of broken spheres as well as spherical particles seemingly unaffected by the milling process. Consequently, the remnants of the broken spheres may reduce the physical advantages associated with spherical morphology i.e.

improved particle packing and lower water demand. This once again reiterates that of the three, FCFA is expected to be the superior fly ash with regards to strength development. The validity of these statements relating to their contribution of these fly ashes towards compressive strength development is investigated in this study.

Figure 4.3 presents the morphology of the Portland cement sample (MC) used as starting material to produce the fly hybrid-cement blends in this study.

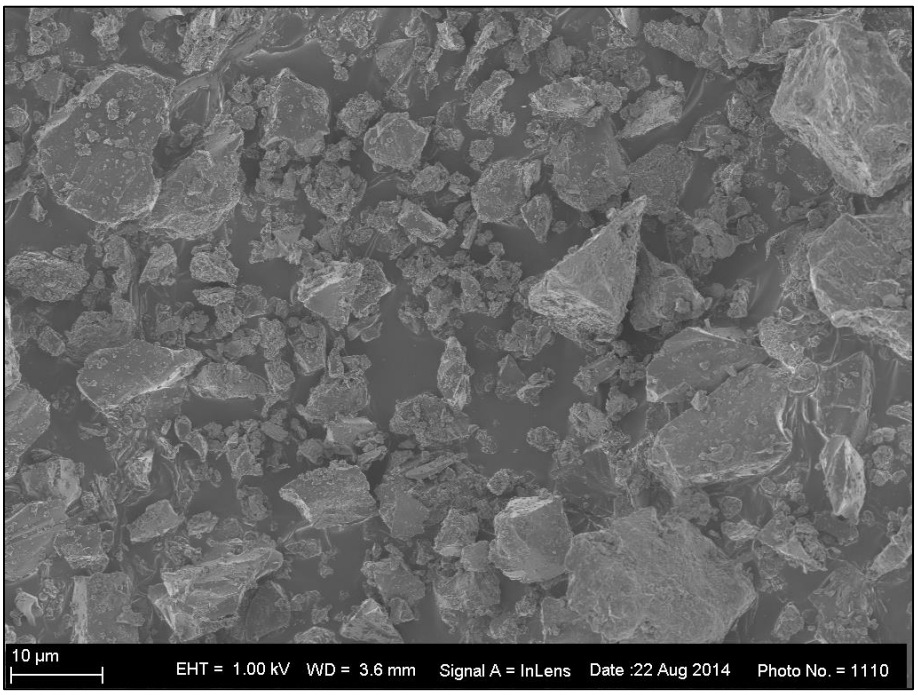

Figure 4.3. Scanning electron micrographs representing the morphology of the unhydrated Portland cement sample (MC).

From this micrograph it is clear that the Portland cement sample (milled clinker) and the milled fly ash particles which constitutes MUFA (Figure 4.2 e) have similar morphologies. The implication of this observation is that these samples may be mistaken for one another, should they be blended and viewed under the microscope. This contributed to the decision made during the experimental development of the study on the surface reactivity to study 100% fly ash specimens (i.e. no cement) exposed to a calcium hydroxide environment (as per section 5.2).

4.6 Thermogravimetric analysis (TGA)

The thermal behaviour of the starting materials used to produce the hybrid cement blends was investigated using TGA analysis. The TGA data of the starting materials UFA, MUFA and MC are presented in Figure 4.4.

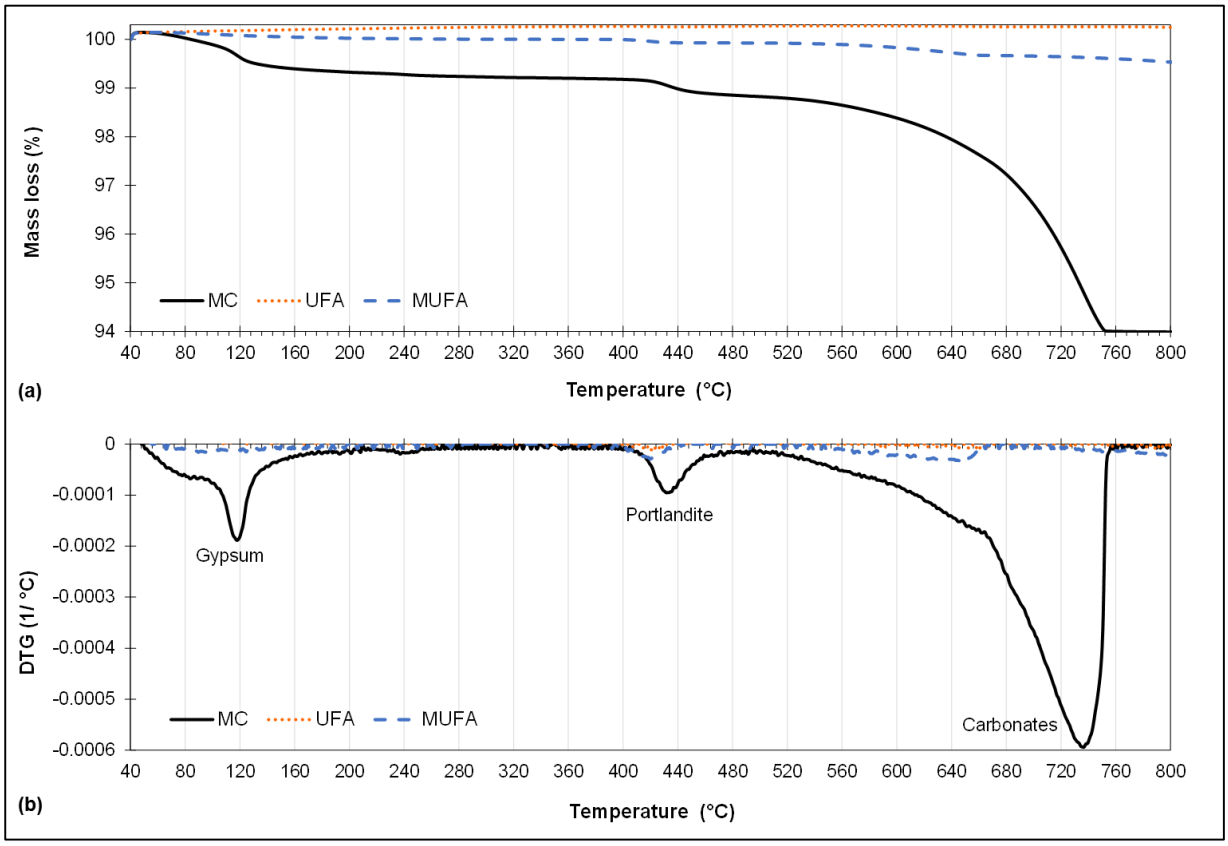

Figure 4.4. TGA (a) and DTG (b) data for the unhydrated, raw cementitious materials MC, UFA and MUFA.

XRD analysis was used to determine the mineralogical analysis of the Portland cement sample (MC) used as starting material (refer to Table 4.2). TGA analysis of this sample confirmed the presence of gypsum (dehydration between 100-140 °C), portlandite (400-500 °C) and calcite (700-800 °C).

The TGA results confirm the low LOI observed for fly ash during XRF measurements. The phases identified during XRD measurements will not contribute to mass loss.

4.7 Fourier transform infrared spectroscopy (FTIR)

The FTIR transmittance spectra for MC, UFA and MUFA are presented in Figure 4.5.

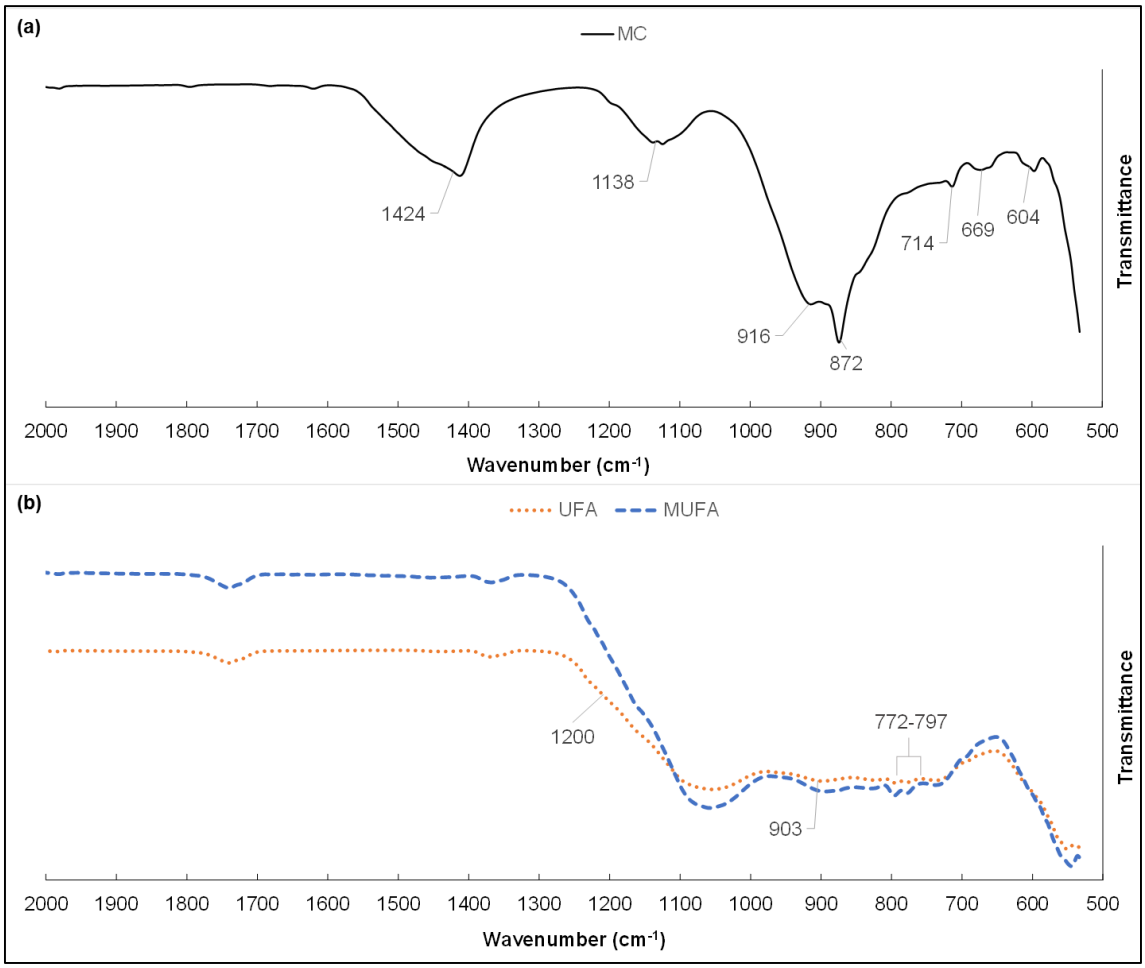

Figure 4.5. FTIR transmission spectra of the cementitious materials used as starting material: (a) MC, (b) UFA and MUFA.

The major vibrational bands identified in the anhydrous cement (MC) used in this study occur within the 500 – 2000 cm^{-1} wavenumber range. The characteristic bands for gypsum due to

S-O stretching appear at 1138 cm^{-1}, while weak bands at 669 and 604 cm^{-1} due are associated to bending vibrations of SO_4^{2-}.

The carbonate bands, specifically assigned to calcite, show characteristic peaks at 714, 872 and 1424 – 1430 cm^{-1} (v_2 and v_3 band). These are attributed to the C-O bond out-of-plane and in-plane bending and stretching vibrations of the calcite polymorph. The presence of calcium carbonate may be ascribed to the limestone that was interground with the clinker to produce the cement sample, but also to carbonation of other calcium species once they are hydrated.

A silica band appears at 916 cm^{-1} from Si-O asymmetric stretching vibrations of calcium silicate mineral phases within the cement clinker. There are bands attributed to Al-O and Al-OH around 841 cm^{-1}. The positions of these vibrational bands are well supported by literature (see Table 3.2).

The FTIR spectrum of UFA (Figure 4.5 b) indicates a strong band in the area between 900 and 1200 cm^{-1}. The presence of this band is attributed to Si-O-Si asymmetric stretching vibrations with contributions of quartz, mullite and glass. The band at 903 cm^{-1} originates from Al-O symmetric stretching vibrations from mullite, and the characteristic doublet of quartz is evident at around 772 – 797 cm^{-1} (Criado *et al.*, 2007; Van Der Merwe *et al.*, 2014).

Figure 4.5 b shows that mechanical activation of the fly ash did not result in significant changes in the relative intensity or positions of the FTIR peaks associated to the Si-O-Si asymmetric stretching vibrations or the Al-O symmetric stretching, as discussed for UFA. However, it appears as though the doublet of quartz at 772 – 797 cm^{-1} may be slightly more intense after milling, indicating possible subtle structural rearrangement of the fly ash after mechanical activation (Kumar *et al.*, 2007; Kumar & Kumar, 2011).

4.8 Conclusion

Considering the favourable particle shape, size distribution and mineralogy of FCFA, it can be presumed that a hybrid cement produced from the inclusion of FCFA should theoretically provide the most reactive and best physically performing cement and concrete. The latter is discussed comprehensively in the upcoming chapter.

~ Chapter 5 ~

Investigation into the effect of chemical and mechanical activation

5.1 Introduction

This chapter provides a discussion of the results obtained for the preliminary test work and experiments performed as part of an effort to better plan for, and understand the main test program and the results thereof. Two experiments are discussed as mentioned in Chapter 3 i.e. characteristics of the fly ash surfaces exposed to a calcium hydroxide environment and sulfate optimisation study of a hybrid cement produced from unclassified fly ash (UFA).

5.2 Characteristics of the fly ash surface reactivity exposed to a calcium hydroxide environment

It is important to bear in mind that within each fly ash sample examined there are countless individual particles, not one of which is identical in size, chemical composition and therefore ultimate reactivity to any of the others (Van Der Merwe *et al.*, 2014). Hence, the discussion and conclusions made in this aspect of the study only takes into account the general trend observed during the FESEM imaging of a particular fly ash, and only relates to the overall predicted reactivity of the fly ash as manifested by changes in the topography.

The morphologies of FCFA, UFA and MUFA after exposure to a saturated solution of calcium hydroxide, with and without 5% sodium sulphate addition, is shown in Figure 5.1 to Figure 5.3.

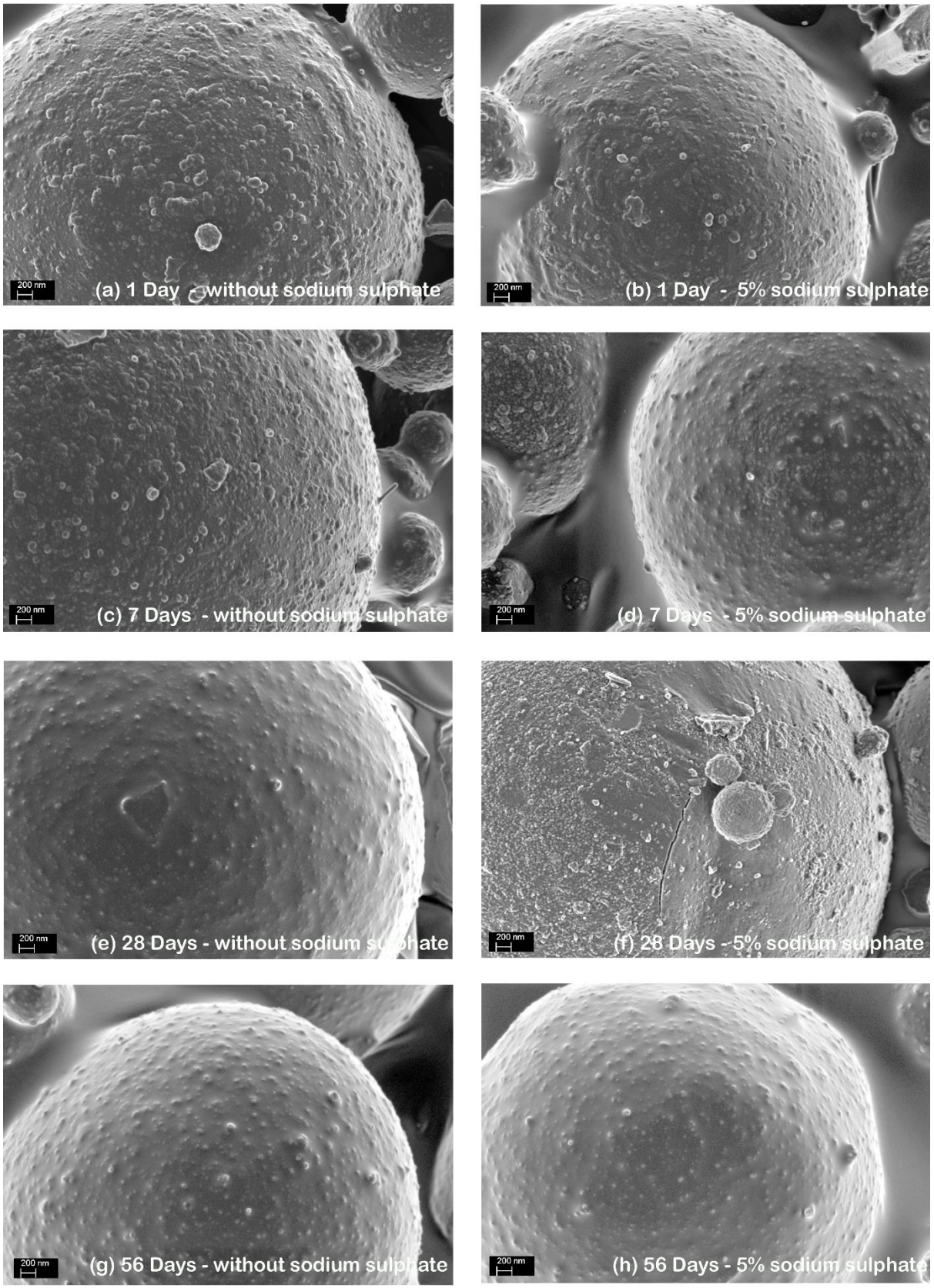

Figure 5.1. Morphology of FCFA after exposure (1 to 56 days) to a saturated solution of calcium hydroxide, with and without 5% sodium sulfate addition (50000x).

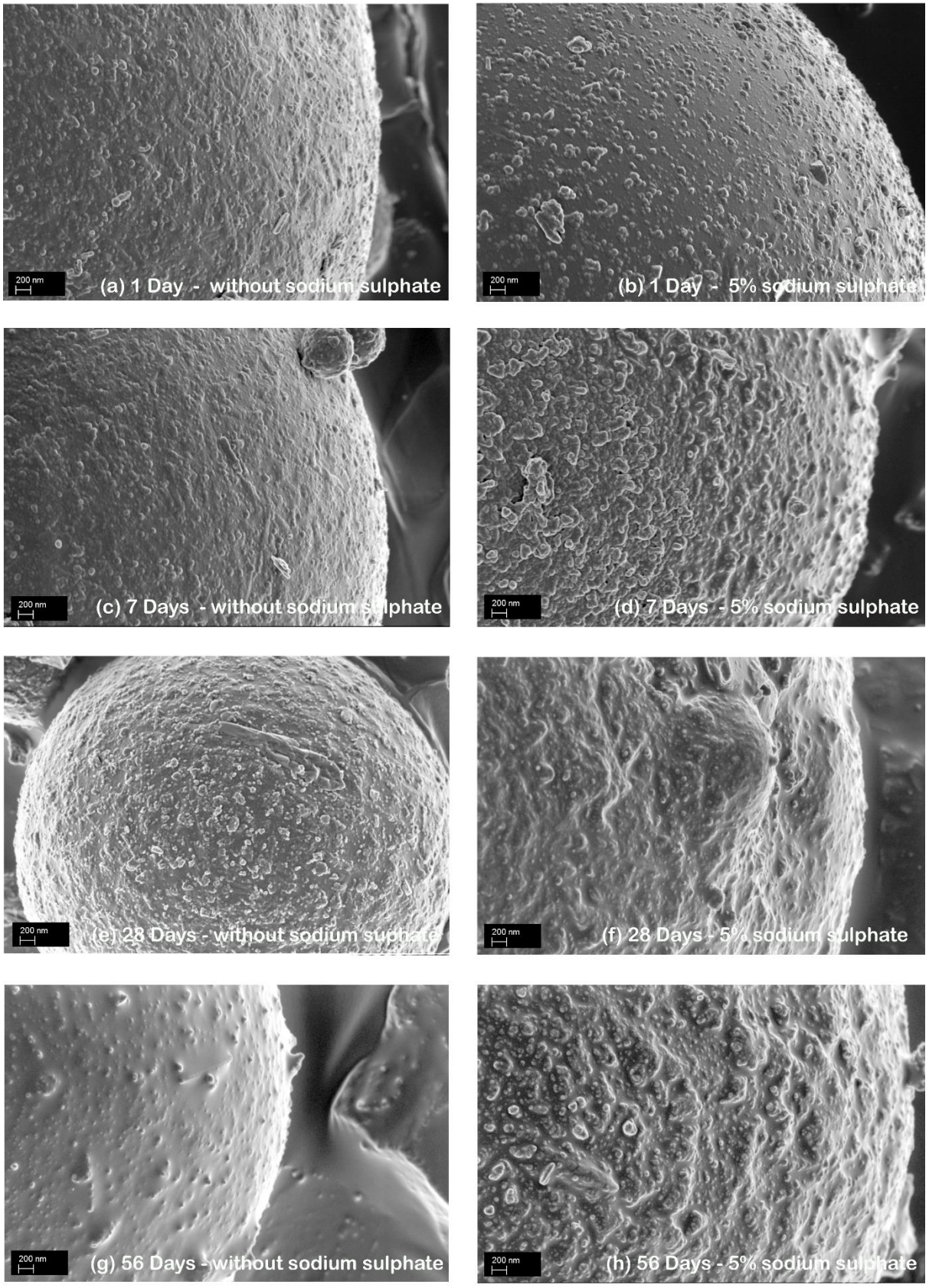

Figure 5.2. Morphology of UFA after exposure (1 to 56 days) to a saturated solution of calcium hydroxide, with and without 5% sodium sulfate addition (50000x).

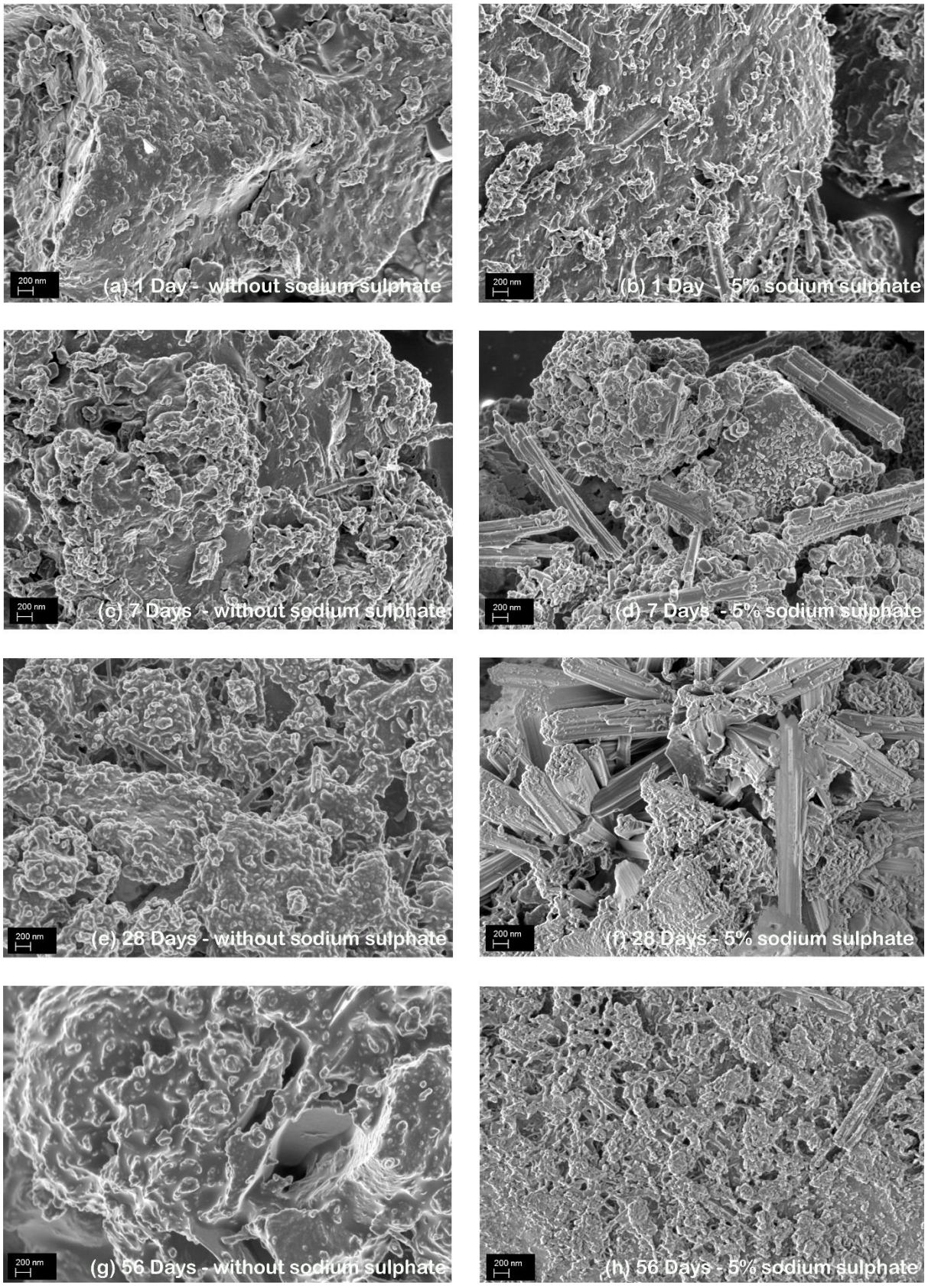

Figure 5.3. Morphology of MUFA after exposure (1 to 56 days) to a saturated solution of calcium hydroxide, with and without 5% sodium sulfate addition (50000x).

It is postulated that the degree of alteration in the appearance and surface topography of fly ash spheres provides an indication of reactivity. Based on this assumption it is evident that, of the three fly ashes exposed to the saturated calcium hydroxide solution, the surface of fly ash FCFA exhibited the least change Figure 5.1). Even with the addition of chemical activation (Figure 5.3 b, d, f, h), FCFA particles appear to be rather dormant. This suggests that it is relatively inert towards sulfate activation as well. Any compressive strength benefits that are realised from its utilisation in blended cement will most probably be ascribed to its contribution to improved physical properties as mentioned previously.

The appearance and surface topography of UFA (Figure 5.2), seems to suggest it is more susceptible to etching and therefore possibly more reactive. The etching to be seen on the surface after 7 days exposure to a saturated solution of calcium hydroxide containing 5% sodium sulfate could be an indication of its reactivity (Figure 5.2 d). The reference sample, in which the specimen is exposed only to saturated calcium hydroxide, appears to be non-reactive, with very little, if any, surface activity visible even after curing for 56 days (Figure 5.2 a, c, e and g).

As can be seen in the micrographs (Figure 5.3), the situation changes quite significantly once the particles are mechanically activated by milling Figure 5.3 a, c, e, g), and even more so when chemically activated with the addition of 5% sodium sulfate Figure 5.3 b, d, f, h). Some surface activity is already visible after 1 day on the mechanically activated reference sample (Figure 5.3 a), and this continues throughout the curing process up to 56 days (Figure 5.3 g). This activity appears in the form of a gel-like substance with some needle shaped crystals on the surface of the particles.

Should the early age hydration reactions of a fly ash based hybrid cement, activated with sodium sulfate as hypothesized by Donatello *et al.* (2013) be applied, the following reactions may be possible within the fly ash – calcium hydroxide system. The reaction products will, however, be highly dependent on fly ash reactivity as well as calcium hydroxide and sodium sulfate concentration, in essence the availability of silica, aluminium, calcium and sodium in the system:

$$Na_2SO_{4(s)} + H_2O_{(l)} \rightarrow 2Na^+_{(aq)} + SO_4^{2-}{}_{(aq)} \qquad \textbf{5. 1}$$

$$CH_{(aq)} + 2Na^{+}_{(aq)} + SO_4^{2-} \rightarrow C\underline{S}_{(s)} + NaOH_{(aq)} \quad \textbf{5. 2}$$

$$CH_{(aq)} + NaOH_{(aq)} + FA_{(s)} \rightarrow (N,C)\text{-A-S-H gel} \quad \textbf{5. 3}$$

Even though there is no cement present in this specific experimental environment, any dissolved aluminium and sulfate may react to form ettringite (Donatello *et al.*, 2013):

$$CS_{(aq)} + C3A_{(s)} \rightarrow \text{ettringite}_{(s)} \quad \textbf{5. 4}$$

The XRD phase identification of the raw fly ash samples and 56 day fly ash specimens exposed to a calcium hydroxide environment, with and without 5% sodium sulfate addition is presented in Figure 5.4.

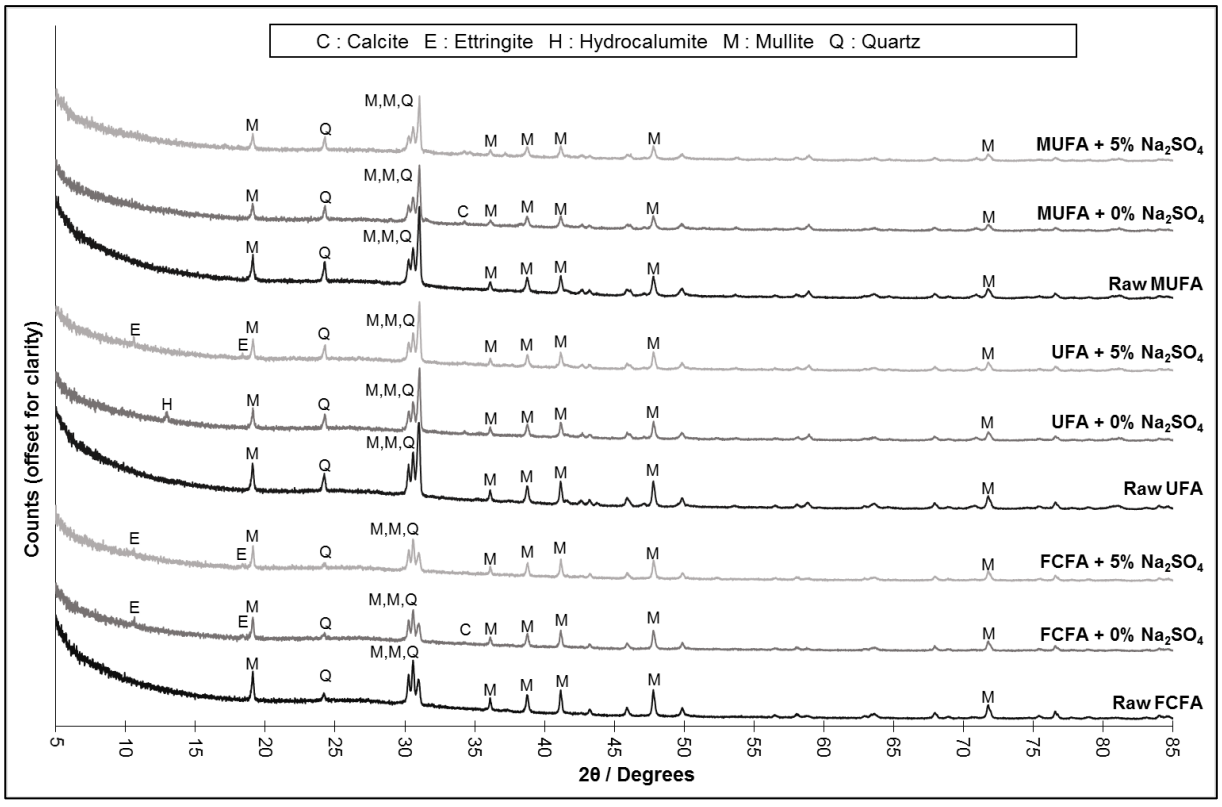

Figure 5.4. XRD phase identification of the untreated fly ash samples and 56 day fly ash specimens exposed to a calcium hydroxide environment, with and without 5% sodium sulfate addition.

In this work, the presence of ettringite was confirmed in some samples after being cured for 56 days (Figure 5.4). It was identified in FCFA specimens with and without the addition of sodium sulfate, as well as in UFA plus 5% sodium sulfate. However, the ettringite peaks are very small, indicating minor concentration. In the absence of any other source, it can be concluded that the required alumina was supplied by the fly ash.

The XRD pattern of the 56-day specimens also indicated the presence of mullite and quartz as major crystalline phases, as well as minor amount of calcite. Despite the presence of fractured needles in MUFA (Figure 5.3 d, f), no ettringite needles were identified with XRD. It is possible that more ettringite may have existed at earlier curing ages; however equation 2 could have resulted in an increase in pH which is known to inhibit the formation of stable, well crystallized ettringite. This may have resulted in ettringite not being detected by XRD (Donatello *et al.*, 2013). As was the case with UFA, the diffraction XRD patterns of the 56-days specimens also indicated the presence of mullite and quartz as the major crystalline phases, as well as a small amount of calcite as the minor crystalline phase.

Even though the mineralogical data of the fly ash products indicated that FCFA should be the most reactive due to it having the highest amount of amorphous alumina silica and the lowest amount of quartz, this is not evident from the etched surfaces observed in the FESEM images. In accordance with the results of the surface topography study, reactivity of the three fly ashes may be considered as follows: FCFA < UFA < MUFA. This result was unexpected and it was therefore necessary to carry out compressive strength tests on mortars at different curing ages to establish the validity of etching with calcium hydroxide as a means of predicting reactivity.

5.3 Sulfate optimisation study of a hybrid cement produced from unclassified fly ash (UFA) and cement

The major focus in cement research regarding sulfates has been on the interaction of the sulfates with the calcium aluminate (C_3A) phase in cement clinker and its role with regard to cement setting time. It is well understood that insufficient addition of sulfates to cement can result in flash setting as well as low early strengths, while an excess of sulfates may cause false set (Hewlett, 2004; Taylor, 1997). This results in the well-established practice of gypsum- or sulfate optimisation during the commercial production of cement, so that the benefit of sulfate

in cement reactivity is optimally realised. Substantial research has been published on the potential enhancement of alite (C_3S) hydration within cement clinker (Bentur, 1976; Donatello *et al.*, 2013; Zhang & Zhang, 2008), as well as fly ash activation by means of sulfate addition (Donatello *et al.*, 2013; Donatello *et al.*, 2014b; Qian *et al.*, 2001).

In this study, Na_2SO_4 was added as the chemical activator for the production of hybrid fly ash cements. This automatically adds additional SO_4^{2-} ions into the binder system besides those that are already available from the small amount of gypsum present in the Portland cement. It is therefore imperative that the sulfate content of the hybrid binder be optimised to avoid any anomalous setting behaviour and maximize strength development.

The method for the sulfate optimisation study was fully described in Chapter 3, which also indicated that all the blends were produced from 70% UFA, 30% cement and the respective amounts of Na_2SO_4. In order to abtain a general working range (0% - 5%) that would be considered in this study for the addition of sodium sulfate, at a level that would still be cost effective, it was not deemed necessary to complete this study on all 3 fly ashes, but only on one, i.e. UFA.

5.3.1. Setting time

The setting time behaviour for the unclassified fly ash (UFA) hybrid cement when chemical activation was applied in a dry powder form, is shown in Table 5.1.

Table 5.1. Setting time of the UFA hybrid cement when Na_2SO_4 is added in dry powder form (*n* = 1).

	Setting time (minutes)	
	Initial	Final
Control - 0 % Na_2SO_4	501	671
Dry – 1 % Na_2SO_4	400	566
Dry – 2 % Na_2SO_4	361	456
Dry – 3 % Na_2SO_4	365	440
Dry – 4 % Na_2SO_4	356	451
Dry – 5 % Na_2SO_4	370	440

In comparison to the control sample (0% Na_2SO_4) the setting time generally decreases with the addition of sulfate (see Table 5.1). The influence of the addition of Na_2SO_4 may be considered as have reached a maximum after addition of 2%. Furthermore there is an inconsequential difference in setting times once 2% or more sulfate is added, which is clearly evident from the graphical representation in Figure 5.5.

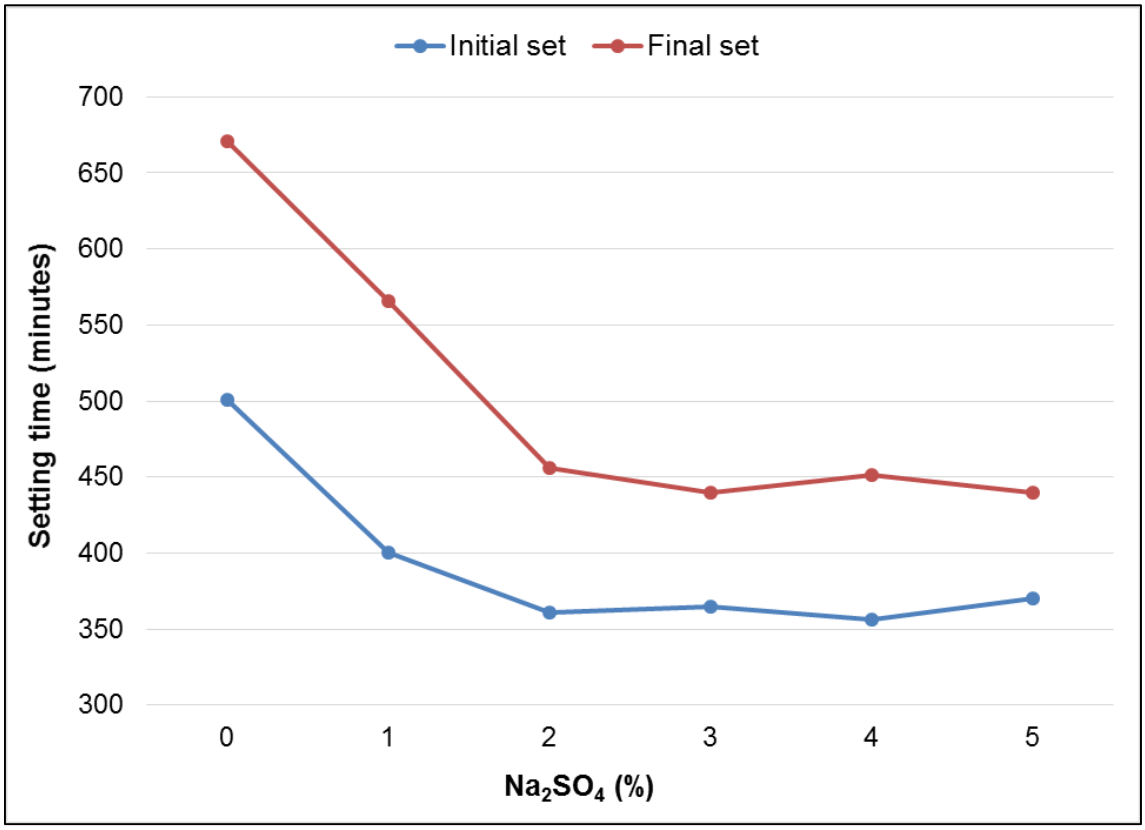

Figure 5.5. Initial and final time of the UFA hybrid cement when Na_2SO_4 is added in dry powder form (*n* = 1).

Figure 5.5 is demonstrating the existence of an optimal amount of Na_2SO_4 to be added to this hybrid blend. Adding more Na_2SO_4 will no longer serve as cost effective or more environmentally friendly, as it no longer provides significant activation.

5.3.2. Strength behaviour

Details of the different blends prepared, as well as their respective mortar compressive strength results are given in Table 5.2. The results are tabulated according to either dry addition of sulfate in the powder form, or where the sulfate was dissolved in water prior to addition

Table 5.2. Compressive strength (MPa) of the UFA hybrid cement when Na_2SO_4 is added in dry powder form compared to Na_2SO_4 added in dissolved form.

	1 Day	2 Days	7 Days	28 Days
Control - 0 % Na_2SO_4	2.2	4.2	8.5	14.8
Dry – 1 % Na_2SO_4	3.4	7.0	9.4	17.0
Dry – 2 % Na_2SO_4	3.8	6.3	10.9	20.0
Dry – 3 % Na_2SO_4	3.5	7.0	12.5	20.7
Dry – 4 % Na_2SO_4	3.7	6.8	14.0	22.2
Dry – 5 % Na_2SO_4	3.1	5.7	14.1	24.0
Dissolved – 1 % Na_2SO_4	3.1	5.9	10.6	17.5
Dissolved – 2 % Na_2SO_4	4.1	7.0	11.9	18.6
Dissolved – 3 % Na_2SO_4	3.7	7.3	12.3	21.0
Dissolved – 4 % Na_2SO_4	3.6	6.5	13.2	21.4
Dissolved – 5 % Na_2SO_4	2.9	5.6	13.6	23.0

The results indicate that, compared to the control sample without sulfate, chemical activation increases the compressive strength at all curing ages, irrespective of the manner in which it was added. Furthermore, it is also evident that to derive maximum benefit the sulfate concentration needs to be optimised (Bentur, 1976). This holds especially true for the early curing ages (1 day and 2 days), after which the strength indicates some degree of decline with increasing SO_4^{2-} concentration. This trend can be seen more clearly in the graphical depiction of the results (Figure 5.6 and Figure 5.7). These graphs also demonstrate the effect of the two methods of addition on mortar strength, as well as the increase of sulfate addition on the strength.

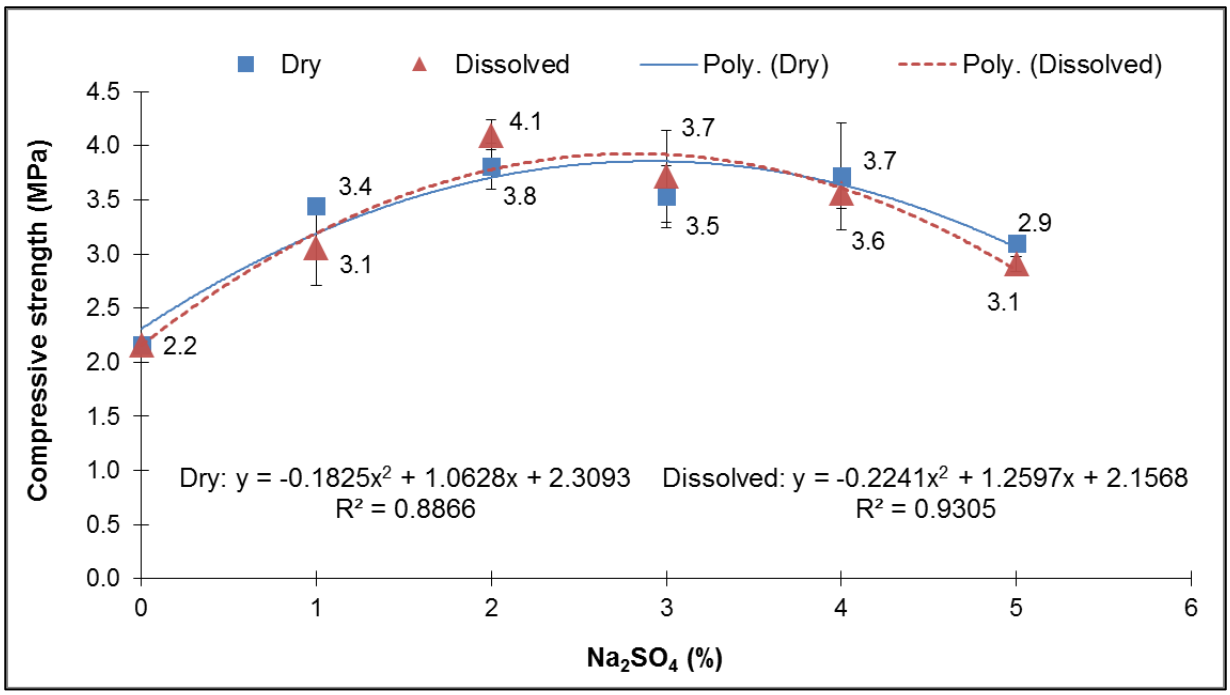

Figure 5.6. Sulfate optimisation - 1 day mortar compressive strengths.

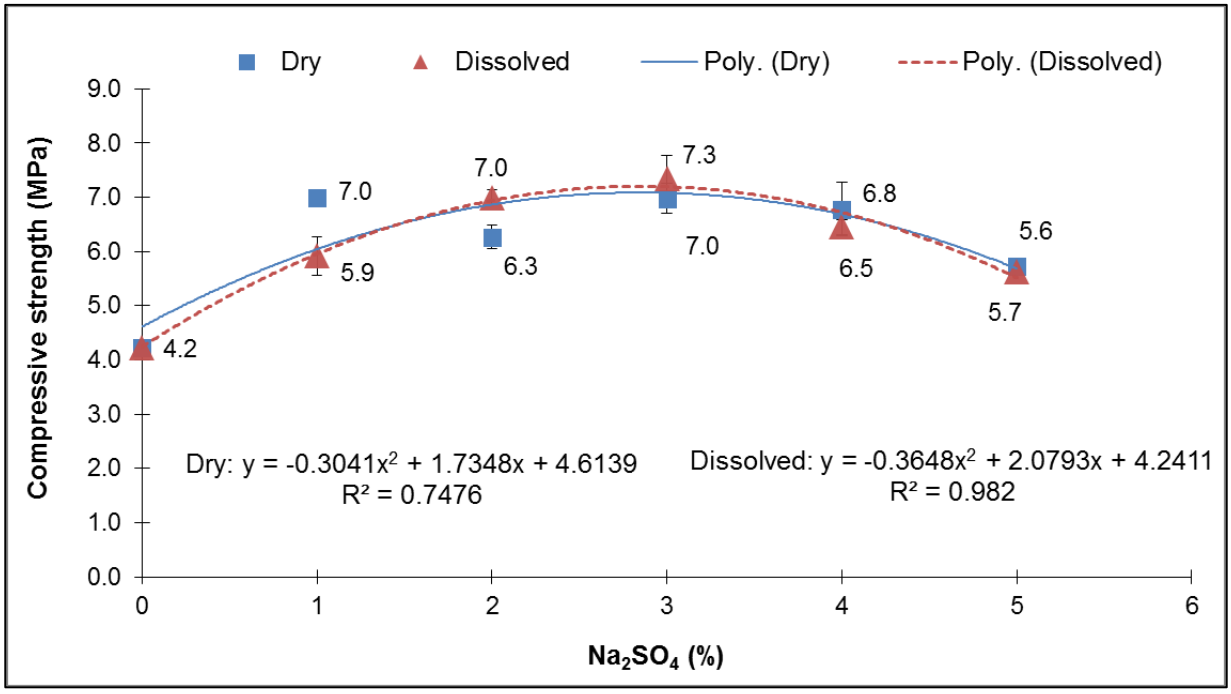

Figure 5.7. Sulfate optimisation - 2 days mortar compressive strengths.

Considering the early curing ages (1 day and 2 days) (Figure 5.6 and Figure 5.7), the data indicates a well-defined second order polynomial trend, which is more predominant for the wet Na_2SO_4 addition method than for the dry Na_2SO_4 addition method. However, when the first derivative of the polynomial fit is calculated to obtain the optimum points of both strength and % Na_2SO_4 for both of the sulfate addition methods, the optimum points obtained indicate no significant difference:

1 Day – dry addition of Na_2SO_4: $y = -0.1825x^2 + 1.0628x + 2.3093$ **(5. 5)**

$$x = \frac{-b}{2a} = \frac{-1.0628}{2(-0.1825)} = 2.9\%\ Na_2SO_4$$

$$y = 3.9\ MPa$$

$(2.9\%\ Na_2SO_4; 3.9\ MPa)$

1 Day – dissolved addition of Na_2SO_4: $y = -0.2241x^2 + 1.2597x + 2.1568$ **(5. 6)**

$$x = \frac{-b}{2a} = \frac{-1.2597}{2(-0.2241)} = 2.8\%\ Na_2SO_4$$

$$y = 3.9\ MPa$$

$(2.8\%\ Na_2SO_4; 3.9\ MPa)$

2 Days – dry addition of Na_2SO_4: $y = -0.3041x^2 + 1.7348x + 4.6139$ **(5. 7)**

$$x = \frac{-b}{2a} = \frac{-1.7348}{2(-0.3041)} = 2.9\%\ Na_2SO_4$$

$$y = 7.1\ MPa$$

$(2.9\%\ Na_2SO_4; 7.1\ MPa)$

2 Days – dissolved addition of Na_2SO_4: $y = -0.3648x^2 + 2.0793x + 4.2411$ **(5. 8)**

$$x = \frac{-b}{2a} = \frac{-2.0793}{2(-0.3648)} = 2.8\%\ Na_2SO_4$$

$$y = 7.2\ MPa$$

$(2.8\%\ Na_2SO_4\ ;\ 7.2\ MPa)$

The dry- and wet methods indicate an optimum of 2.9% Na_2SO_4 and 2.8% Na_2SO_4 respectively (3.9 MPa for both methods) after 1 day of hydration, and 2.9% Na_2SO_4 and 2.8% Na_2SO_4 (7.1 MPa and 7.2 MPa) respectively after 2 days of hydration. It is of interest to note that for both methods of Na_2SO_4 addition, nothing changed from 1 day to 2 days with regard to the optimum percentage addition of Na_2SO_4 after an additional 24 hours of curing. However, the optimum compressive strength increased by about 30% for both dry and wet addition of Na_2SO_4 between 1 day and 2 days of hydration.

The latter finding suggests that between 1 day and 2 days of hydration, the addition of more sulfates to the system is not the controlling factor for higher compressive strength in mortar specimens, indicating a saturation point for sulfates within the system at this specific stage of hydration. The increase in compressive strength might be attributed to additional hydration product forming between the two curing ages, without the aid of sulfates.

The 7 and 28 day compressive strength results for the optimisation study is presented in Figure 5.8 and Figure 5.9.

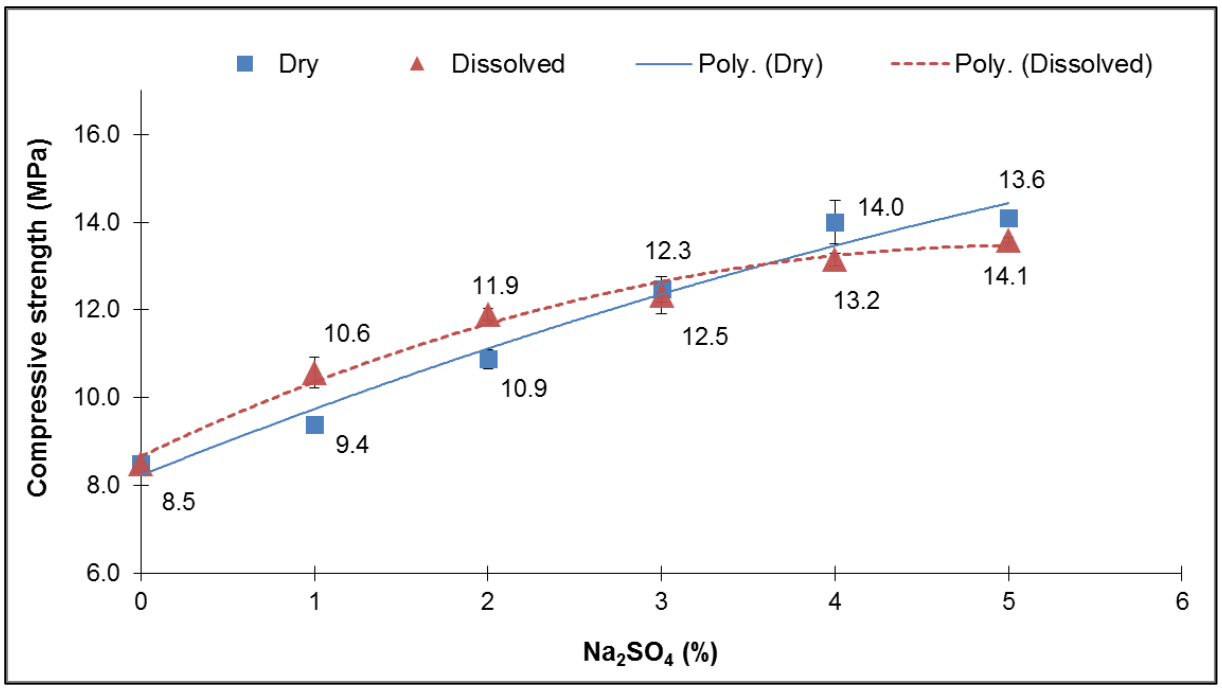

Figure 5.8. Sulfate optimisation - 7 days mortar compressive strengths.

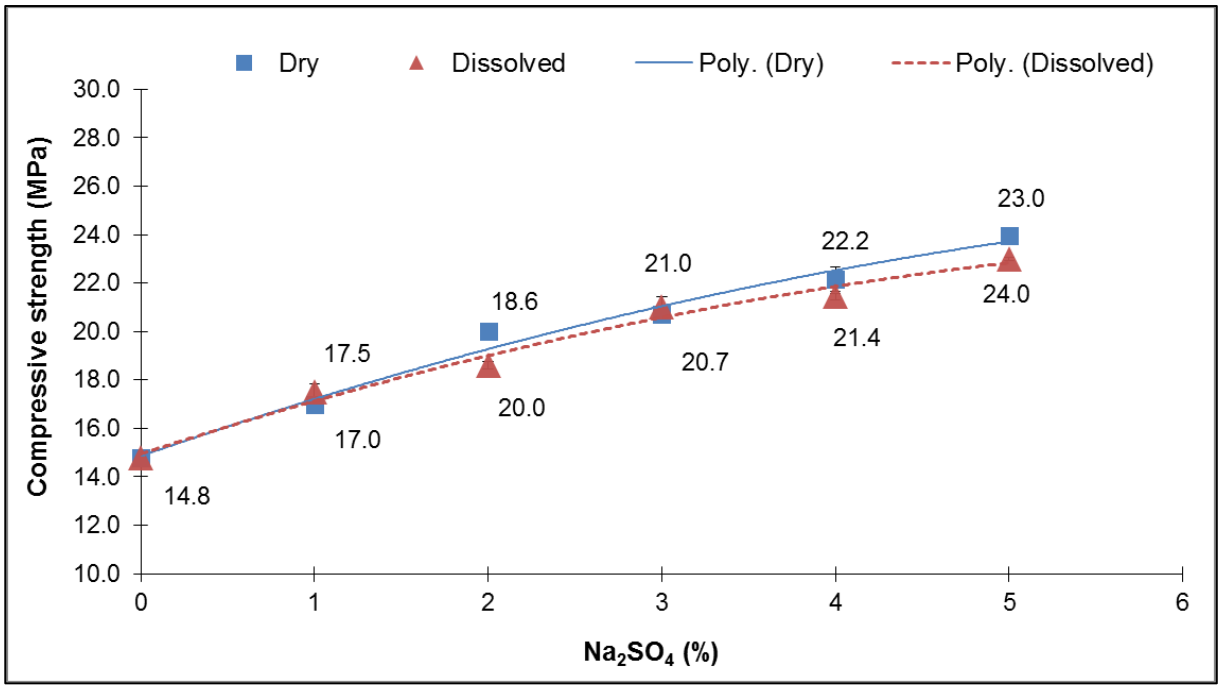

Figure 5.9. Sulfate optimisation - 28 days mortar compressive strengths.

A trend of optimum Na_2SO_4 addition and compressive strength is not that obvious for 7 and 28 days of hydration (Figure 5.8 and Figure 5.9). Compressive strength results seem to suggest a possible maximum or plateau between 4% and 5% Na_2SO_4 addition, 28 days of hydration suggest a continual growth in strength with increasing SO_4^{2-} addition. For these two curing ages, the optimal sulfate addition calculations are not reported since the strength trends are not clearly second order polynomials. If the polynomial formula is theoretically applied to these trends, the calculated percentage of Na_2SO_4 far exceeds the optimal amounts calculated and illustrated for the early stages of hydration, and will result in an undesirable effect on early strength gain as was discussed.

It is possible that the strength growth at 7 and 28 days could be related to other factors contributed by the use of fly ash rather than presence of additional sulfates, i.e. provision of additional nucleation sites, improved particle packing and also more effective water-solid ratio which promotes an increase in paste volume (Deschner *et al.*, 2012; Shi, 1996).

5.4 Conclusion

Surface activation

Curing fly ash in a saturated calcium hydroxide solution serves as a viable, easy and cost effective method to evaluate surface properties of fly ash.

Despite its favourable particle shape distribution and mineralogy, the fine classified fly ash (FCFA) proved not to be the most chemically reactive of the three fly ashes considered. Strength development in hybrid cement containing FCFA is likely attributed to physical and not chemical contributions.

The surface reactivity of the three fly ashes according to the presented results can be listed as follows: FCFA < UFA < MUFA, whereby the fine classified fly ash showed the least surface reactivity, and milled fly ash indicated the most surface reactivity.

The presence of increased amorphous phase within the fly ash specimens did not automatically result in superior surface reactivity upon activation for the respective fly ash products. The

combination of activation methods (mechanical and chemical) proved to be the most effective in increasing the surface reactivity of the fly ash.

Sulfate optimisation

Chemical activation via Na_2SO_4 addition is unquestionably effective in improving mortar compressive strength at all curing ages. The results indicate that the method of sulfate addition seems to be irrelevant under the conditions employed in this study.

Compressive strength data obtained for early curing age specimens (1 day and 2 days) indicate evidence of an optimum amount of sulfate addition. For these specimens, the compressive strength results indicate some degree of decline with increasing SO_4^{2-} content. The dry- and wet addition of sulfates produced maximum additions of 2.9% Na_2SO_4 and 2.8% Na_2SO_4 respectively after 1 day of hydration, and 2.9% Na_2SO_4 and 2.8 % Na_2SO_4 respectively after 2 days of hydration.

The results suggest that between 1 day and 2 days of hydration, the addition of more sulfate to the system is not necessarily the contributing factor to higher compressive strength in mortar specimens, indicating a possible saturation point for sulfate within the system at this stage of hydration. Results obtained for later curing ages indicate that the 7 day strength development seems to reach a plateau with increasing sulfate addition, whereas the 28 day mortar compressive strength continues to increase as the sulfate content increases.

Setting behaviour of both initial and final setting times proved a general decrease in setting time with the addition of sulfates in comparison to the control sample (0% Na_2SO_4). However, the differences between setting times observed for specimens containing Na_2SO_4 of more than 2% was insignificant.

Based on these results, the presence of a more favourable mineralogy within the fly ash specimens or a more favourable particle size distribution (as was the case with FCFA), did not necessarily result in superior surface reactivity upon chemical activation, and the combination of activation methods proved to be the most effective in increasing the chemical surface reactivity of the fly ash. The sulfate optimisation study proved that the chemical activation is effective in improving mortar compressive strength at all curing ages, and that an optimum

amount of sulfates exists especially for the early curing ages, where the addition of more sulfates to the system was not necessarily the contributing factor to higher compressive strength in mortar specimens, indicating a saturation point for sulfate within the system at this critical stage of hydration.

~ Chapter 6 ~

Characterisation of hydrating hybrid fly ash cement paste

6.1 Introduction

In this chapter the data that resulted from the application of analytical techniques used to identify the hydration products obtained for the fly ash hybrid cement pastes prepared, with and without chemical and mechanical activation is presented and discussed. The different characterisation techniques used (XRD, TGA, FTIR and FESEM) have different capabilities, each supplying unique information about the hydration products. The composition of the crystalline phases in the hydration products can be determined by XRD, but the technique cannot be used to characterise amorphous phases. For this reason, TGA and FTIR analysis were used as complementary techniques, as the results obtained using these techniques are not dependant on the degree of crystallinity of the product. Where applicable, FESEM was used to observe important changes in morphologies upon hydration of the starting materials. These results were interpreted in support of the findings from the other analytical techniques.

Leading up to the presentation and discussion of the results from characterisation techniques employed for the identification of the hydration products upon activation, the results for the setting time, heat evolution and expansion which were also measured for hybrid cement pastes, are discussed. The latter three tests were explained as per experimental program in Chapter 3.

The following sample abbreviations were used for the hydrated cements (hybrids) where applicable:

UFA hybrid	**No activation applied**
UFA5 hybrid	**Chemical activation applied (5% Na_2SO_4)**
MUFA hybrid	**Mechanical activation applied**
MUFA5 hybrid	**Combined activation applied (5% Na_2SO_4 + mechanical activation)**

6.2 Setting time

Setting time of cement paste serves as an indicator of the rates of the chemical reactions (i.e. hydration reactions) that take place within the first several hours of cement hydration. Table 6.1 lists the setting time of the three different fly ash hybrid mortars at the corresponding sulfate additions. The same information is presented graphically in Figure 6.1.

Table 6.1. Mortar hybrid setting times (minutes) at different Na_2SO_4 additions for FCFA, UFA and MUFA hybrids.

	0% Na_2SO_4	1% Na_2SO_4	3% Na_2SO_4	5% Na_2SO_4
FCFA	712	612	526	406
UFA	386	351	276	260
MUFA	351	316	218	230

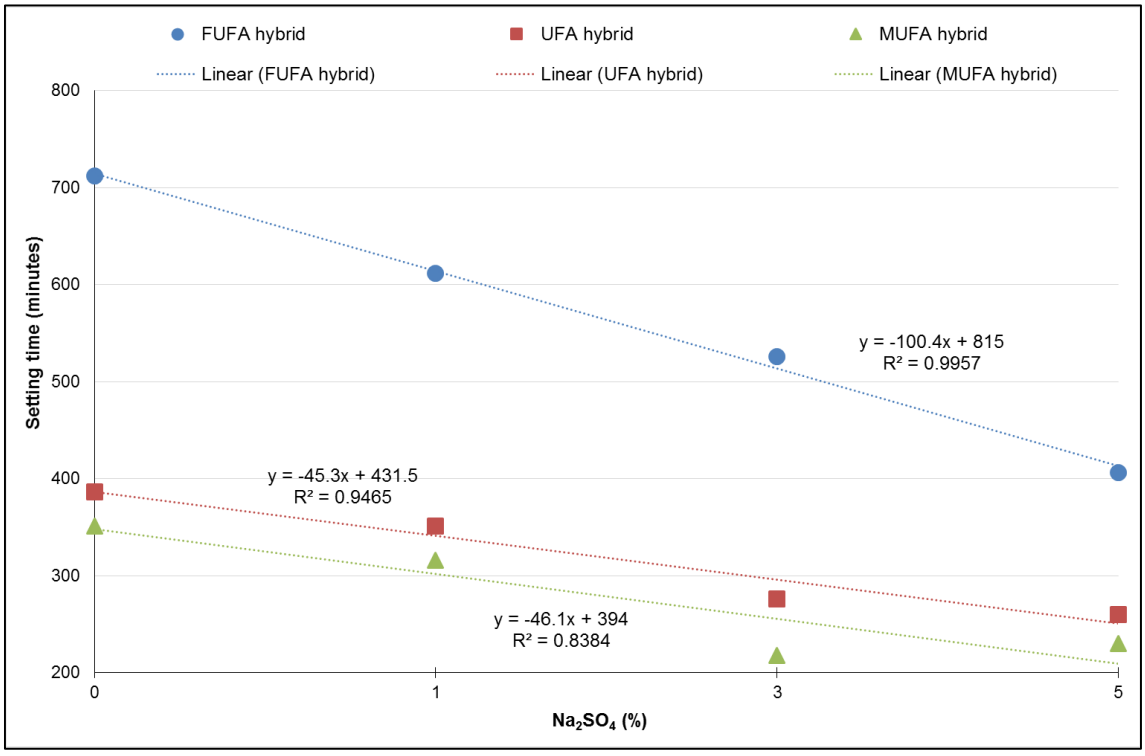

Figure 6.1. Graphical representation of the mortar hybrid setting times (minutes) at different Na_2SO_4 additions for FCFA, UFA and MUFA hybrids.

The setting time reduces with increasing sulfate addition for all three hybrids, however, this affect appears to reach a plateau for UFA and MUFA between 3% and 5% Na_2SO_4, whereas there is still a significant decrease in setting time evident for FUFA between these two sodium sulfate additions. The latter is clearly evident from the graphical representation of the setting times in Figure 6.1. The FCFA hybrid has significantly prolonged setting times compared to the UFA and MUFA hybrids. The MUFA hybrid had the shortest setting time at all levels of sulfate addition.

A decrease in setting time implies an increase in the rates of the hydration reactions. These results therefore suggest that the early age hydration reaction rate is slowest for the FCFA hybrid cement paste, regardless of the amount of Na_2SO_4 added to the system, and that the MUFA hybrid cement paste results in the fastest early age hydration reaction rate. If this is the case, it should also be evident in the heat evolution data discussed in the next section, and possibly follow the trend for the early age compressive strengths, which is discussed in Chapter 7 and Chapter 8.

6.3 Heat of hydration

Curves of the heat evolution over 48 hours and 7 days for all three fly ash – hybrid cement pastes with and without Na_2SO_4 are illustrated in Figure 6.2.

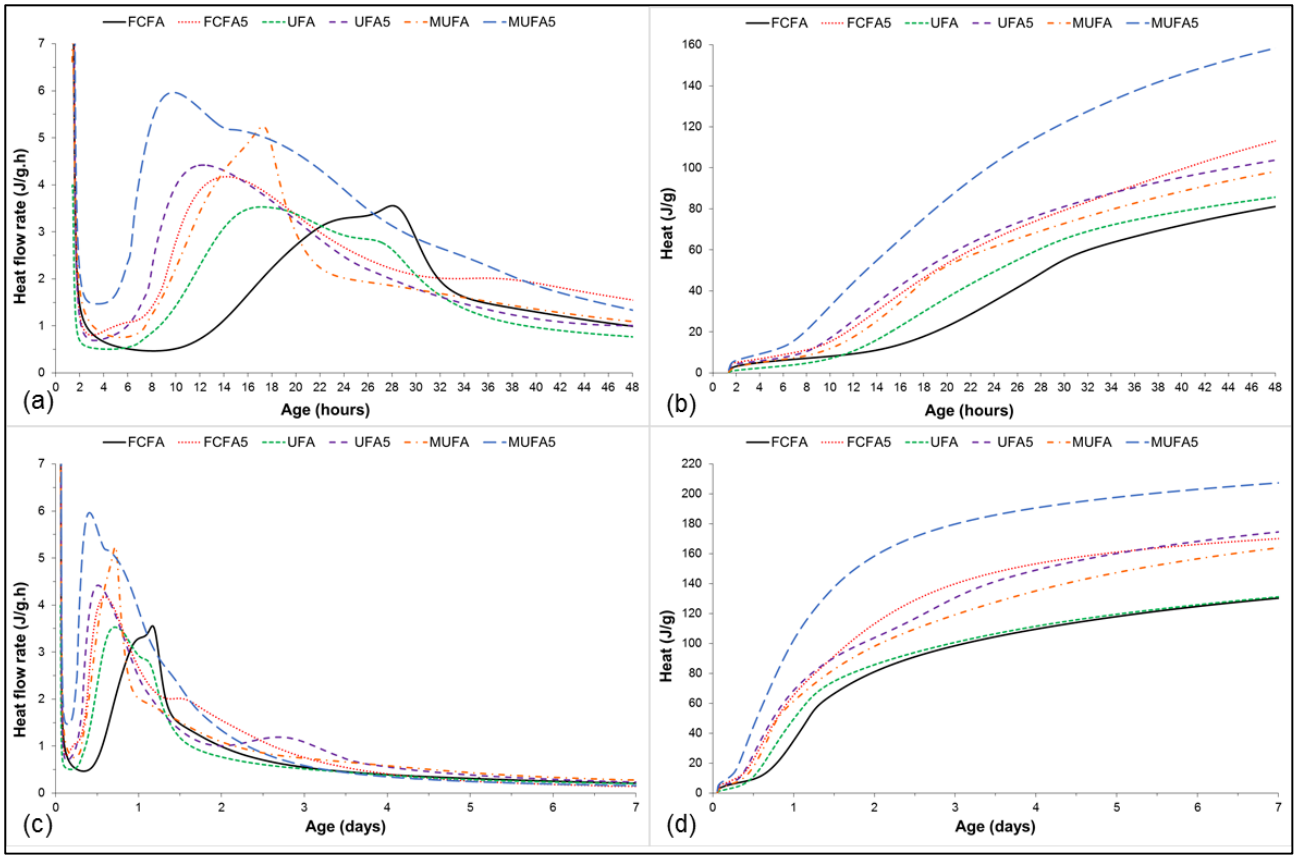

Figure 6.2. Heat evolution curves (heat flow rate (a,c) and cumulative heat (b,d)) for FCFA, UFA and MUFA at 0% and 5% Na_2SO_4, after 48 hours and 7 days.

The heat evolution curves (Figure 6.2 a-b) clearly indicate that the type of fly ash, mechanical activation of fly ash and addition of Na_2SO_4 (chemical activation) all affect the fly ash hybrid cement hydration at early ages (48 hours).

Focussing mainly on the induction (dormant), acceleration and deceleration periods of the heat flow rates (J/g.h) presented in Figure 6.2 (a), it is evident that the UFA hybrid is first to enter the induction period. However, the FCFA hybrid resides the longest in the induction period and also has the cumulative heat output before entering the acceleration period Figure 6.2 (b).

In comparison, the MUFA hybrid has the shortest induction period. The latter finding is in agreement with literature which states that milling of the ash (mechanical activation) already improves the reaction rate of the hybrids even without chemical activation (Kumar *et al.*, 2007; Kumar & Kumar, 2011; Kumar *et al.*, 2006).

A similarity occurs for the FCFA, UFA and MUFA hybrids during the deceleration period, namely a secondary peak occurring as a broad shoulder around 27-28 hours. For FCFA and UFA, this shoulder is more prominent than for MUFA, which shows a very broad, less significant secondary peak. Other authors associated the presence of these secondary peaks to the formation and precipitation of different reaction products e.g. recrystallization of ettringite (Fernández-Jiménez *et al.*, 2011; Taylor, 1997).

Once chemical activation (Na_2SO_4) is applied to the hybrids, the secondary peaks of the heat flow rate for FCFA5 and UFA5 appear at later hydration ages (between 2 and 3 days), and is also further separated from the main acceleration peak (see Figure 6.2 a and c). This is not the case for the MUFA5 hybrid after addition of Na_2SO_4. In this case, the shoulder on the descending arm of the acceleration period already appears at around 15 hours, and may be ascribed to an increase in the extent of ettringite crystallisation (Fernández-Jiménez *et al.*, 2011).

For all three types of hybrids, the addition of Na_2SO_4 accelerated the hydration reaction kinetics by effectively shortening the induction period and raising the maximum rate of heat release. This effectively causes the main acceleration peak to appear at earlier hydration ages. The resulting effect was most significant for MUFA and more for FCFA than for UFA.

The numerical data for the cumulative heat output for FCFA, UFA and MUFA, with and without the addition of chemical activation at 48 hours and 7 days, are provided in Table 6.2.

Table 6.2. Numerical data for the total heat output for FCFA, UFA and MUFA at 0% and 5% Na_2SO_4, after 48 hours and 7 days.

Hybrid sample	Total heat output at 48 hours (J / g)	Heat increase (%)	Total heat output at 7 days (J / g)	Heat increase (%)
FCFA	81.1	17	118.1	15
FCFA5	113.2		161.1	
UFA	85.8	10	119.5	15
UFA5	103.8		160.2	
MUFA	98.2	24	147.5	15
MUFA5	158.4		197.7	

From both the heat flow rate and cumulative heat output graphs (Figure 6.2 a-d), it is evident that the combination of chemical and mechanical activation (MUFA5), results not only in the fastest reaction rate, but also has the highest heat released during the first 48 hours, which continues for 7 days (Table 6.2). The FCFA hybrid was the least reactive hybrid with the slowest reaction rate (Figure 6.2 a and c) and the lowest cumulative heat over the 7 day period). This conclusion was also made from the setting time results discussed in the preceding section.

After 48 hours of hydration, the increase in total heat output once chemical activation has been applied, is approximately 17% for FCFA and 10% for UFA. Although FCFA has a higher increase than UFA, the combination of chemical and mechanical activation resulted in the highest percentage heat increase at approximately 24%. If the percentage heat increase at 7 days is considered, all three fly ashes presented the same increase in total heat output (approx. 15%) after application of chemical activation (refer to). This illustrates that chemical reactions were taking place within the first 48 hours of hydration, where the application of activation also had the biggest impact on reaction rate and total heat released for all three ashes. However, after 7 days, it is clear that when activation, whether chemical, mechanical or the combination of the two methods was applied to the ash, a constant rate of heat accumulation was acquired.

From this discussion on the heat evolution of the different specimens, it is expected that the combination of chemical and mechanical activation (MUFA5), will result in the highest early age mortar compressive strengths (1 day and 2 days) because of its superior reaction rate presented for early hydration ages. Mortar compressive strength results are presented and discussed in Chapter 7.

6.4 Chemical characterisation

6.4.1. X-ray powder diffraction (XRD) analysis

The mineralogical composition of the cementitious materials used as starting materials were discussed in Chapter 4.3. The diffractograms of the raw cementitious materials and the relevant hydrated specimens are presented in Figure 6.3 and Figure 6.4. In Figure 6.3, the combined diffraction patterns obtained for the UFA and UFA5 hybrid cement at all of the considered hydration ages are combined. Figure 6.4 combines the diffraction patterns obtained for the MUFA and MUFA5 hybrid cement at all of the considered hydration ages.

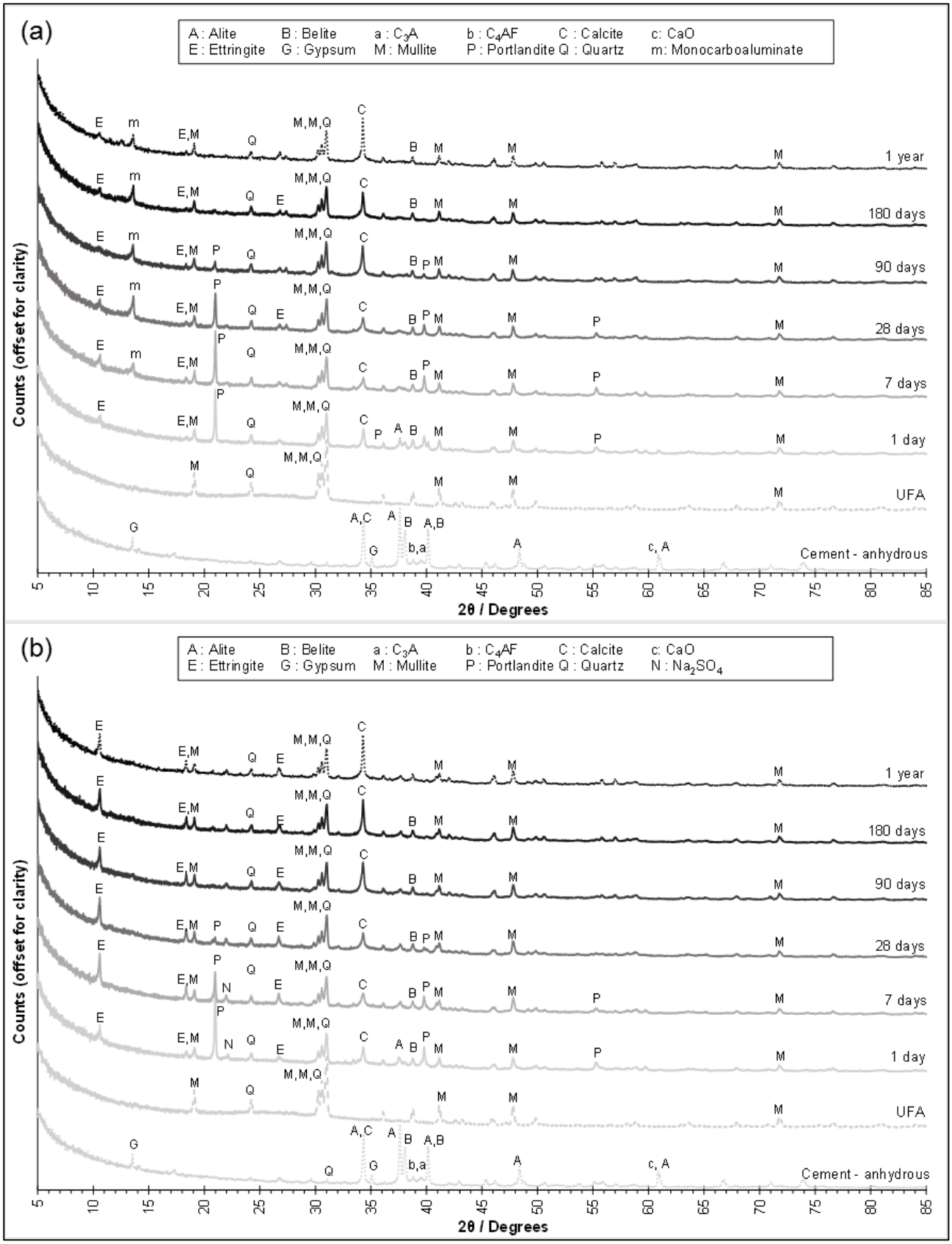

Figure 6.3. XRD diffractograms of anhydrous cement, UFA and hydrated (a) UFA and (b) UFA5 hybrid cement, at all curing ages tested.

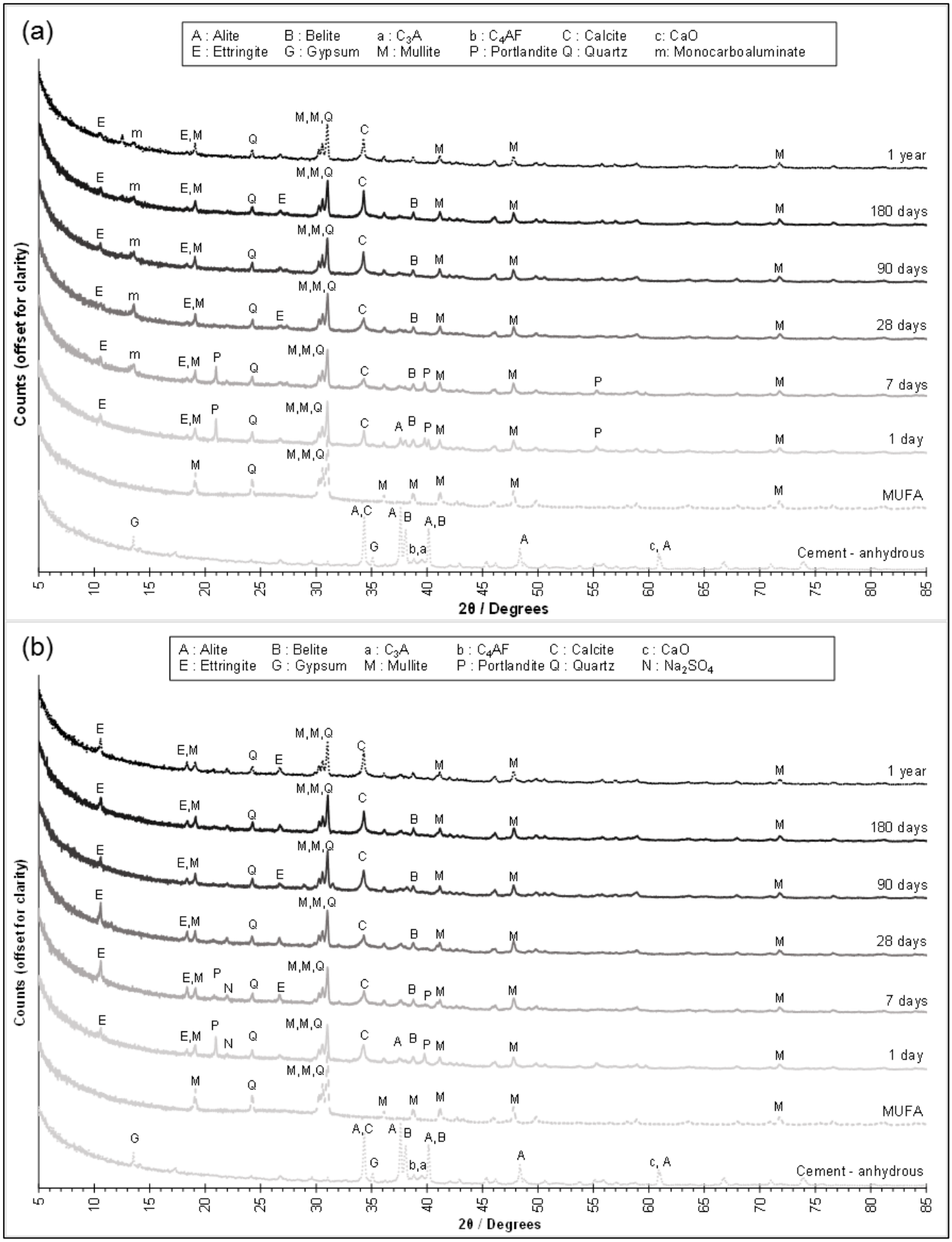

Figure 6.4. XRD diffractograms of anhydrous cement, MUFA and hydrated (a) MUFA and (b) MUFA5 hybrid cement, at all curing ages tested.

The diffractograms for the anhydrous cement (MC) show that the material is comprised of several common crystalline cement clinker phases of which alite (C_3S) is the main component. The cement component also contains crystalline phases such as belite (C_2S), tricalcium aluminate (C_3A), brownmillerite (C_4AF), calcite ($CaCO_3$) and a small amount of gypsum ($CaSO_4.2H_2O$). The same anhydrous cement specimen is presented for all four hybrid cement scenarios.

The anhydrous fly ash specimens (UFA and MUFA) exhibit the characteristic hump between the 20° and 40° 2Θ angles, attributed to the amorphous glass phase of fly ash (Criado *et al.*, 2010; Fernández-Jiménez & Palomo, 2003), as well as diffraction lines attributed to quartz and mullite.

After 1 day of hydration, the UFA hybrid (Figure 6.3 a) produced diffraction patterns consisting primarily of a combination of the characteristic lines identified for the raw materials, along with new hydration peaks associated with portlandite ($Ca(OH)_2$) and ettringite ($(3CaO)\cdot(Al_2O_3)\cdot 3CaSO_4\cdot 32H_2O$), and from 7 days onwards monocarboaluminate ($4CaO\cdot Al_2O_3\cdot CO_3\cdot 11H_2O$) is also present.

The latter three phases are typical secondary reaction products in ordinary Portland cement hydration as well as in high fly ash containing cements. The peaks associated with ettringite were identified at all of the presented curing ages. A sharp peak identified as portlandite appears after 1 day of hydration, and stays prominent up to 28 days of hydration. At 90 days of curing, this peak's intensity reduces significantly and it is no longer evident at 180 days.

After 28 days of hydration, most of the anhydrous cement phases have presumably been converted to a C-S-H-type gel as per normal cement hydration. This phase is unfortunately amorphous to X-rays but its existence is evident by the less intense peaks associated with anhydrous cement i.e. C_3S, C_2S, C_3A and C_4AF (García-Lodeiro *et al.*, 2013a, 2013b; Palomo *et al.*, 2007).

Once Na_2SO_4 have been added to the UFA hybrid (Figure 6.3 b), it is clearly evident that the intensity of the diffraction peaks of ettringite relative to the intensity of the main diffraction peak of quartz (which is regarded as mostly unreactive) increased throughout all curing ages. Also, the previously intense portlandite peaks evident up to 28 days of curing, and to some extent 90 days in the control UFA hybrid, now appears significantly less intense at 28 days of

curing and is non-existent at 90 days. The presence of monocarboaluminate is also no longer evident at any of the curing ages.

In comparison to the chemically unactivated UFA hybrid (Figure 6.3 a), the MUFA hybrid (Figure 6.4 a) also produces peaks identified as ettringite, portlandite and monocarboaluminate. Similarly to the UFA hybrid, the gypsum peak quickly disappears. Portlandite is identified after 1 day of hydration, although it is not as intense as for the UFA hybrid cement and is consumed before 28 days of hydration.

The MUFA5 hybrid (Figure 6.4 b) generally displayed similar diffraction patterns to the UFA5 hybrid after chemical activation. Portlandite was consumed at an even quicker rate compared to the UFA5 hybrid, and is completely consumed after only 7 days of hydration.

These results prove that chemical activation by means of Na_2SO_4 addition increases the degree of ettringite formation which may lead to denser hybrid specimens with increased strength. It is also evident that the extent of the pozzolanic reaction is increased via both chemical and mechanical activation, but more so by a combination of activation methods.

6.4.2. Thermogravimetric analysis (TGA)

The thermal analysis of the four different hybrid cement pastes (UFA, UFA5, MUFA and MUFA5) at different curing ages, are presented in Figure 6.5 to Figure 6.8. The raw cementitious materials (UFA, MUFA and MC) are also shown in each graph for comparative purposes. For a complete discussion of the TGA analysis for the raw cementitious materials, refer to Chapter 4.6.

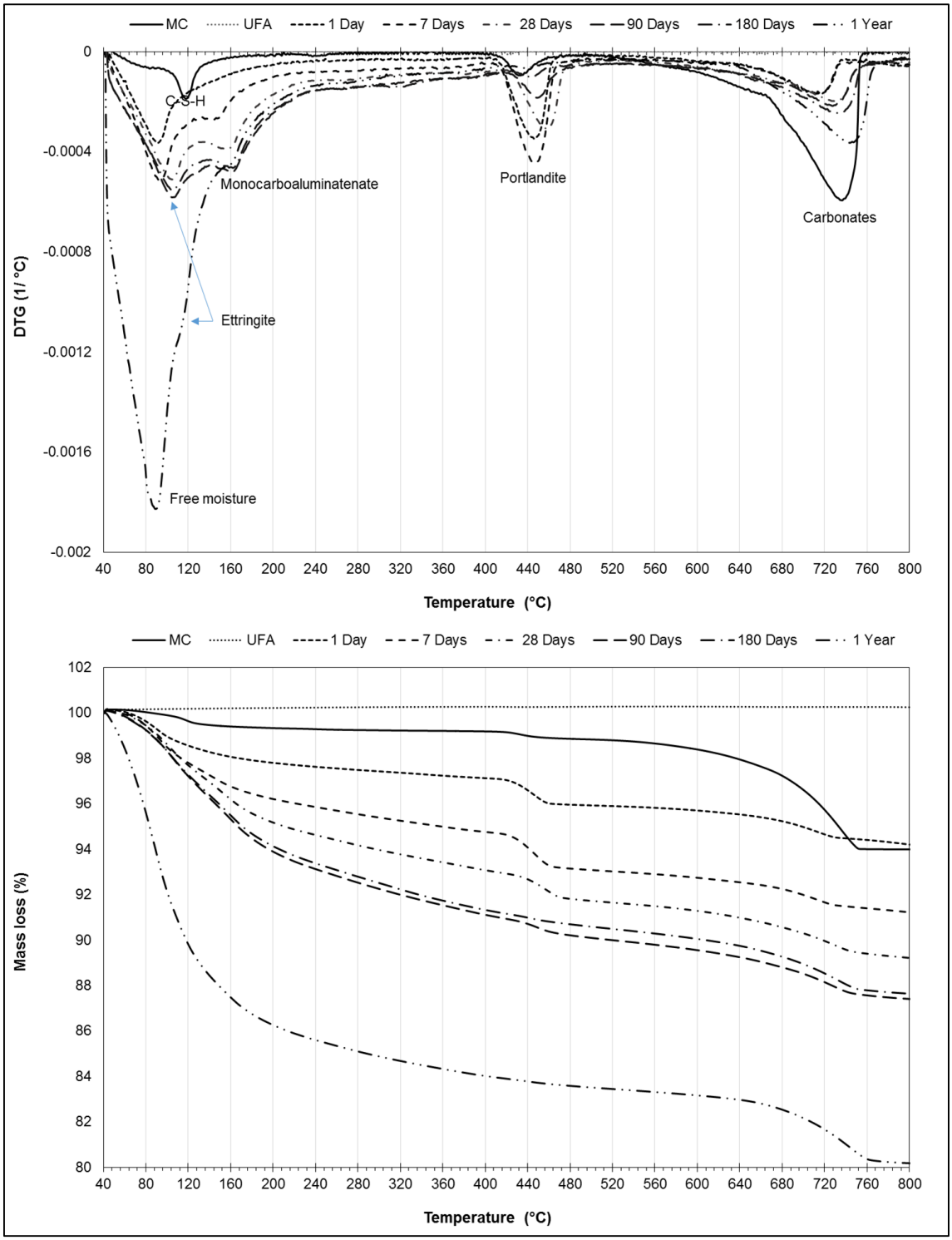

Figure 6.5. DTG and TGA data of anhydrous UFA, cement and hydrated UFA hybrid cement with no chemical activation applied, at all curing ages tested.

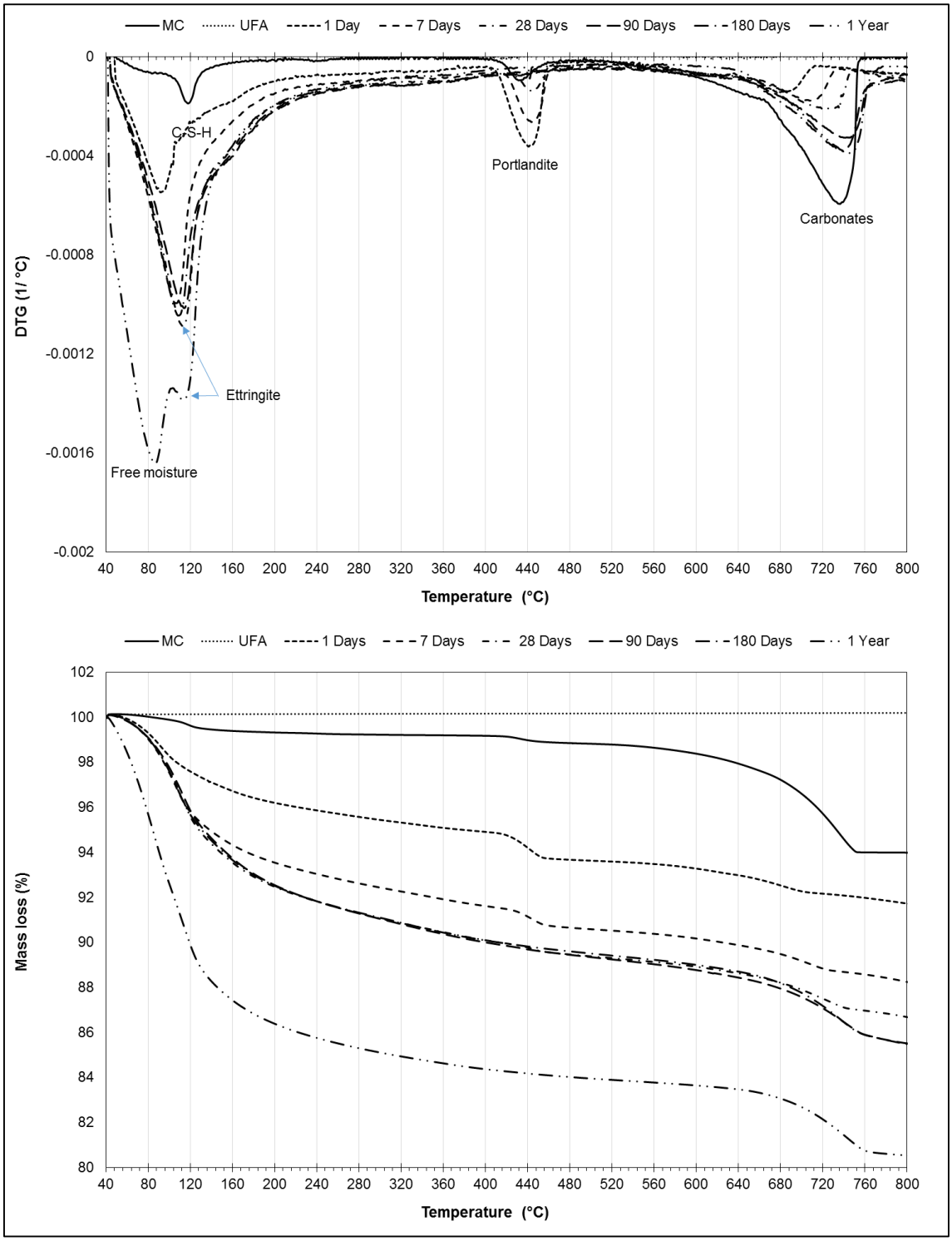

Figure 6.6. DTG and TGA data of anhydrous UFA, cement and hydrated UFA5 hybrid cement with chemical activation applied, at all curing ages tested.

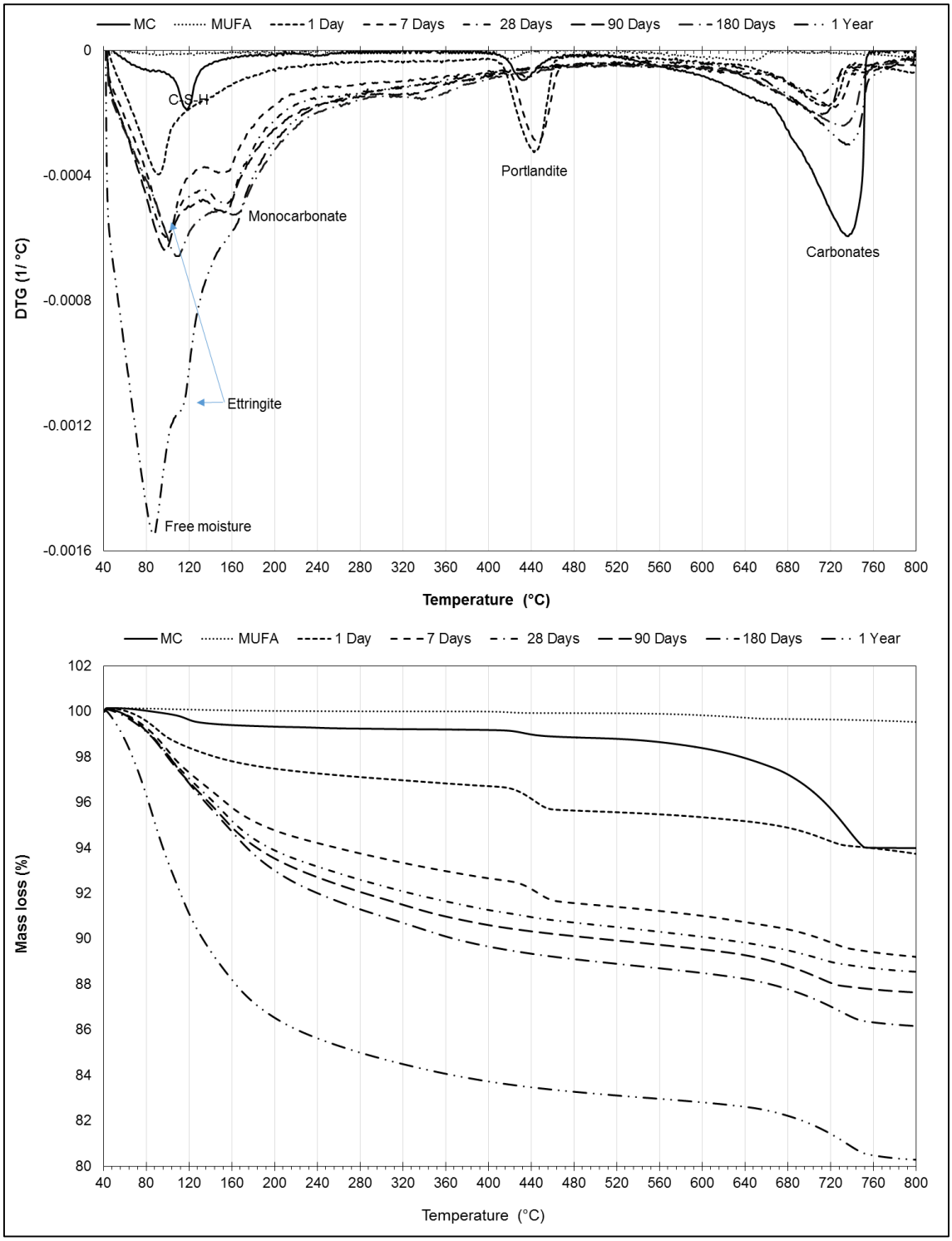

Figure 6.7. DTG and TGA of anhydrous MUFA, cement and hydrated MUFA hybrid cement when mechanical activation is applied, at all curing ages tested.

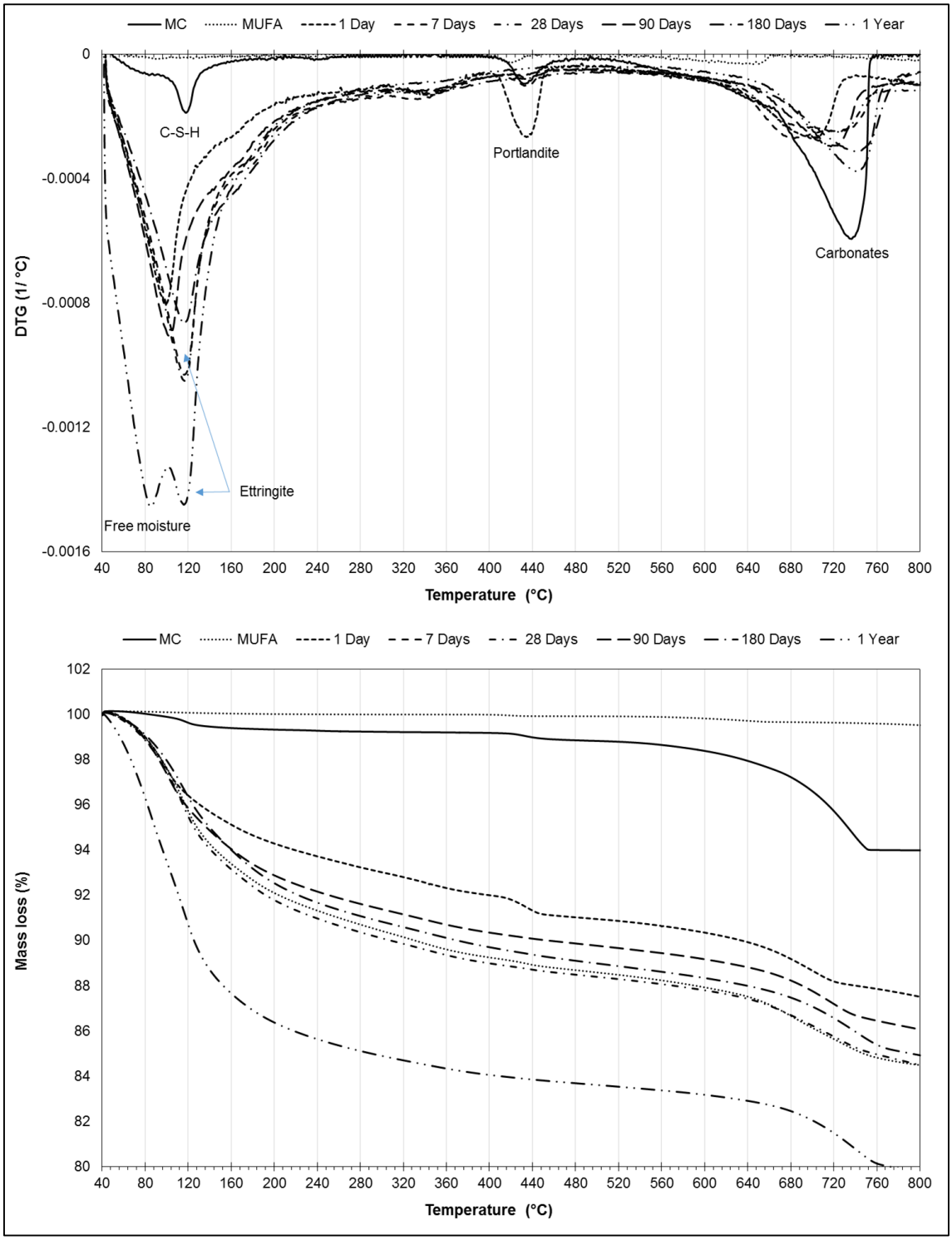

Figure 6.8. DTG and TGA data of anhydrous MUFA, cement and hydrated MUFA5 hybrid cement when combined activation is applied, at all curing ages tested.

From the DTG curve of the UFA hybrid cement paste, presented in Figure 6.5, it can be seen that after 1 day of hydration, mass loss associated with the dehydration of ettringite is evident at around 90°C. This peak shifted to the right (to higher temperatures) with increasing curing age, which is interpreted to be due to ettringite becoming denser and more stable. A secondary peak, due to the loss of water from calcium monocarboaluminate, appears from 7 days of hydration at around 160°C. The peak associated with the dehydration of portlandite at approximately 450 °C is still visible at 90 days of hydration, and to a small extent after 180 days.

When chemical activation (Na_2SO_4) is applied to the UFA hybrid (Figure 6.6), the ettringite peak becomes more prominent compared to the UFA hybrid containing no chemical activation (Figure 6.5). What is also noteworthy is that the AFm peak associated with the dehydration of monocarboaluminate is significantly smaller and less prominent. Portlandite is consumed much quicker, with the last mass loss associated with the dehydration of portlandite only evident up to 28 days.

Once mechanical activation is applied to produce the MUFA hybrid, the DTG curve (Figure 6.7) show that portlandite has already been consumed after 7 days. This is in agreement with the XRD data presented at the start of this chapter. The TGA analysis of the MUFA hybrid paste also presents a clear mass loss associated with the dehydration of calcium monocarboaluminate (approximately 160 °C), which disappears once Na_2SO_4 is added to the hybrid cement paste (MUFA5) and activation methods are combined (chemical and mechanical), as shown in Figure 6.8.

The mass loss associated with the dehydration of portlandite when activation methods are combined, are visible for a shorter period (after 1 day) for the MUFA5 hybrid than for the UFA5 hybrid (after 28 days). The addition of Na_2SO_4 as chemical activator clearly led to an increase in the rate of consumption of portlandite for both UFA5 and MUFA5 hybrids, but more so for the MUFA5 hybrid (when activation methods are combined). This is in agreement with the XRD findings on portlandite consumption and the degree of pozzolanic activity of the fly ash specimens.

6.4.3. Fourier transform infrared spectroscopy (FTIR)

FTIR analysis of the hydration products at different hydration ages obtained for the UFA and UFA5 hybrid is shown in Figure 6.9 a-b. The FTIR spectra for MUFA and MUFA5 is presented in Figure 6.10 a-b. The spectra for the raw cementitious materials (UFA and MC) and (MUFA and MC) are presented at the bottom of Figure 6.9 b and Figure 6.10 b respectively, for comparison with the hybrid cements after hydration. For a complete discussion of the FTIR analysis of the raw cementitious materials, refer to Chapter 4.7.

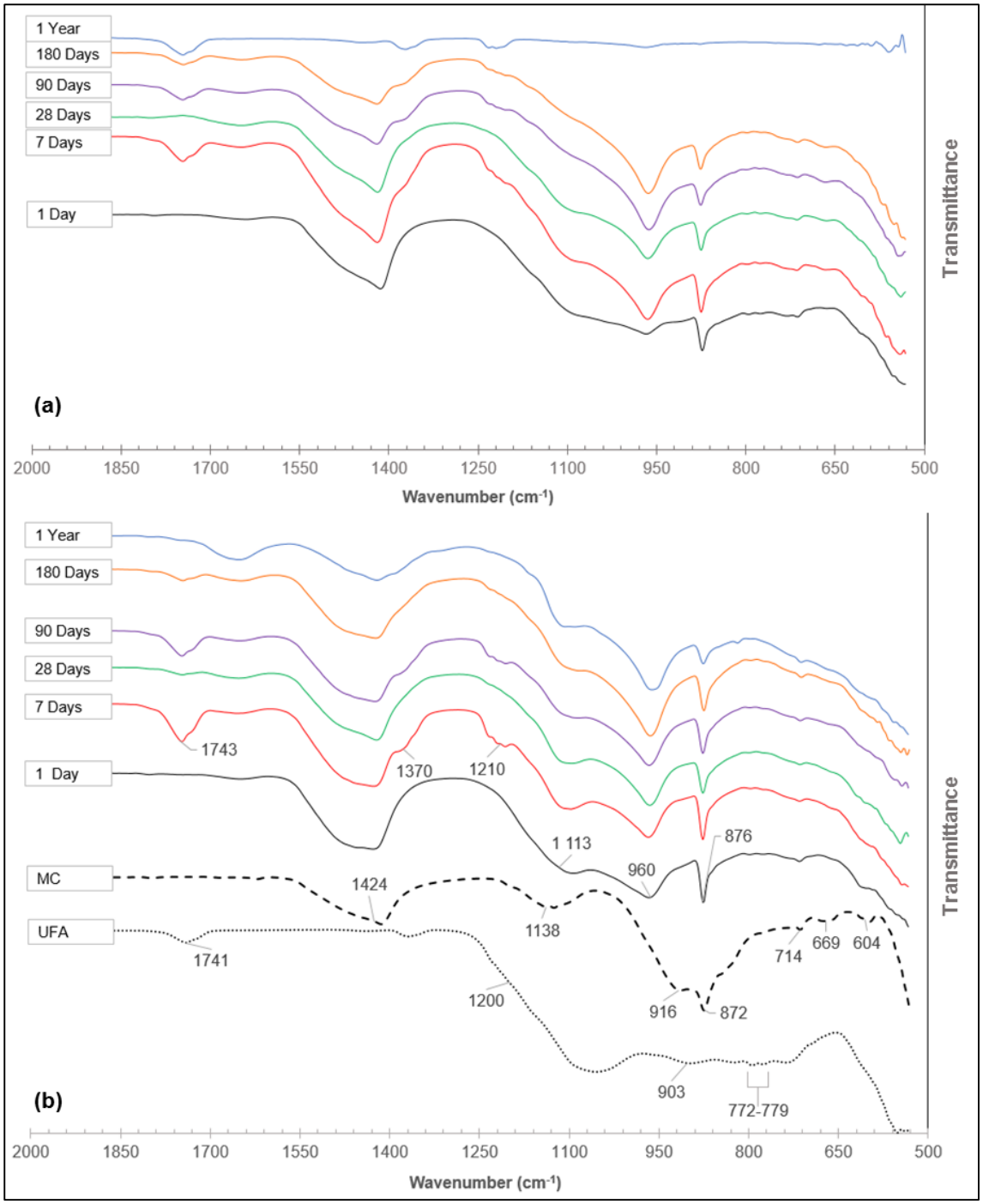

Figure 6.9. FTIR transmission spectra between wavenumbers 530-2000 cm^{-1} obtained for the (a) UFA and (b) UFA5 hybrid cements at all hydration ages tested.

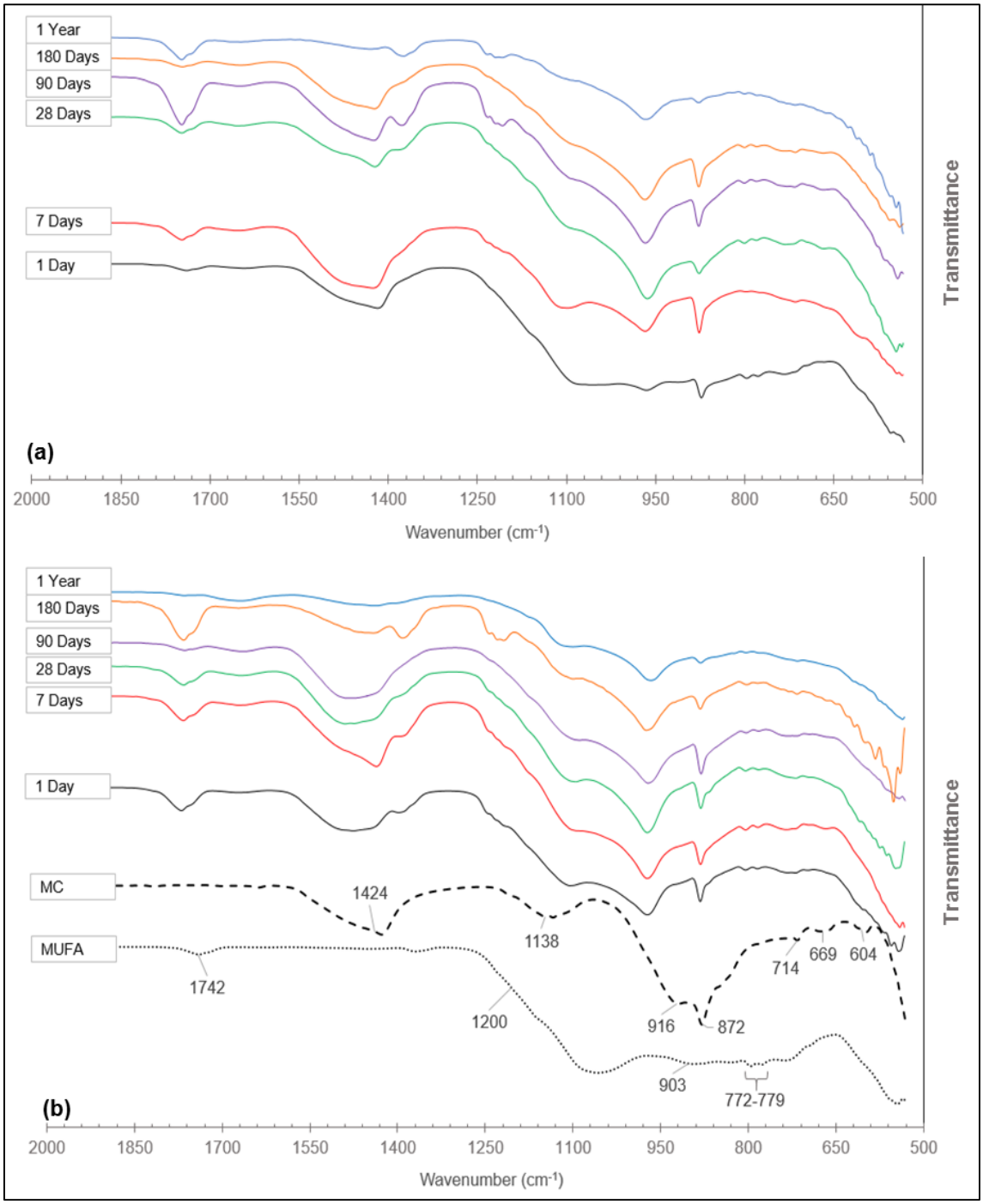

Figure 6.10. FTIR transmission spectra between wavenumbers 530-2000 cm^{-1} obtained for the (a) MUFA and (b) MUFA5 hybrid cements at all hydration ages tested.

In comparison to the transmission spectrum of raw cement (MC) at the bottom of Figure 6.9 a, new transmission band has evolved in the spectrum of both the UFA and UFA5 hybrid cement at around 960 cm^{-1}. The latter is already evident after only 1 day of hydration and occurs through all hydration ages tested. This band (960 cm^{-1}) has been described in literature to represent the Si-O asymmetric stretching vibration (v_3) of the calcium silicate hydration product, also referred to as C-S-H gel, produced during cement hydration. The exact position of the main Si-O band depends on the Ca/Si ratio of the C-S-H gel produced during hydration (Donatello *et al.*, 2014b; Kontoleontos *et al.*, 2013; Palomo *et al.*, 2007).

Another product of cement hydration, ettringite, is visible for both scenarios (UFA and UFA5) at 1113 cm^{-1}. This band is associated with SO_4^{2-} stretching vibrations (v_3) usually found between 1100 and 1170 cm^{-1} (Kontoleontos *et al.*, 2013). Molecular water (O-H bend) is represented by a weak absorption band between 1600 and 1700 cm^{-1}, which is evident at all curing ages.

Once chemical activation, (Na_2SO_4), is added to the UFA hybrid (UFA5) as presented in Figure 6.9 b, the system indicates an increase in the relative intensity of the ettringite band (1113 cm^{-1}) through all curing ages. This phenomena of increased ettringite formation after chemical activation with Na_2SO_4 serves as an indication of the formation of stable, well crystallised ettringite needles, and was also demonstrated by the XRD and TGA findings and discussions. The same can be said for the hybrid cements where the ash has been mechanically activated (MUFA) and a combination of chemical and mechanical activation was applied (Figure 6.10 a an b respectively). Once again, the addition of Na_2SO_4 improved the relative intensity of the ettringite band.

The only gel phase clearly distinguishable in the FTIR data of the four hybrids cements, was C-S-H gel, identified with a band at around 960 cm^{-1}. The position of this band does not appear to move to higher wavenumbers as suggested in literature, indicating the progress of hydration and polymerisation of Si-O (Kontoleontos *et al.*, 2013). It does however appear to increase in relative intensity with increasing curing age, suggesting an increase in the quantity of this specific hydration product.

Apart from the new bands representing C-S-H gel, ettringite and molecular water (O-H bend) that appear after hydration, the remainder of the bands occurring in the FTIR spectra of the

hydrated samples can be attributed to the contributions from the raw starting materials e.g. carbonates (refer to Chapter 4.7 for detail on the FTIR analysis of the raw materials).

The only FTIR transmission band in the 2000 – 4000 cm^{-1} range of significant concern for this study is the small, sharp band at around 3641-3642 $cm^{-1,}$ ascribed to O-H stretching of $Ca(OH)_2$ (portlandite). Figure 6.11 compares this band, associated to portlandite, between the four different hybrid cement pastes after 1 day and 28 days of hydration.

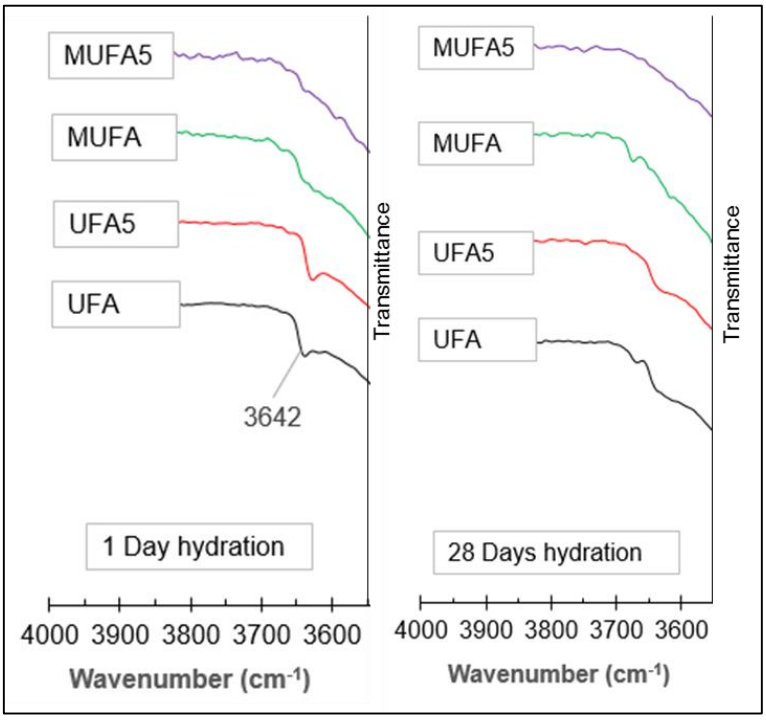

Figure 6.11. FTIR transmission spectra for portlandite between wavenumbers 3600-4000 cm^{-1} presented at 1 day and 28 days of hydration, for UFA, UFA5, MUFA and MUFA5 hybrid cement pastes.

It is evident that after 1 day of hydration, mechanical activation (MUFA), and especially the combination of chemical and mechanical activation (MUFA5) increases the rate of pozzolanic activity of the fly ash, evident by the disappearance of the portlandite band. Once the samples have hydrated for 28 days, there is no more evidence of the small sharp band associated to portlandite. The latter may be due to the portlandite being either completely consumed, or its

quantity being so small that it is not clearly evident on the spectra anymore. This trend of increased pozzolanic activity of fly ash was however also found and supported by the XRD and TGA results.

6.5 The effect of chemical and mechanical activation on the pozzolanic reactivity of fly ash in a high fly ash hybrid cement.

Based on the literature referenced, pozzolanic reactivity of fly ash during this discussion will refer to the rate at which portlandite is consumed within the four different fly ash hybrid scenarios making reference to the applied activation method.

Figure 6.12 summarises the XRD and DTG data presenting the occurrence of portlandite, to serve as indication of the degree of the pozzolanic reaction of hydrated fly ash hybrid cement specimens upon chemical and mechanical activation.

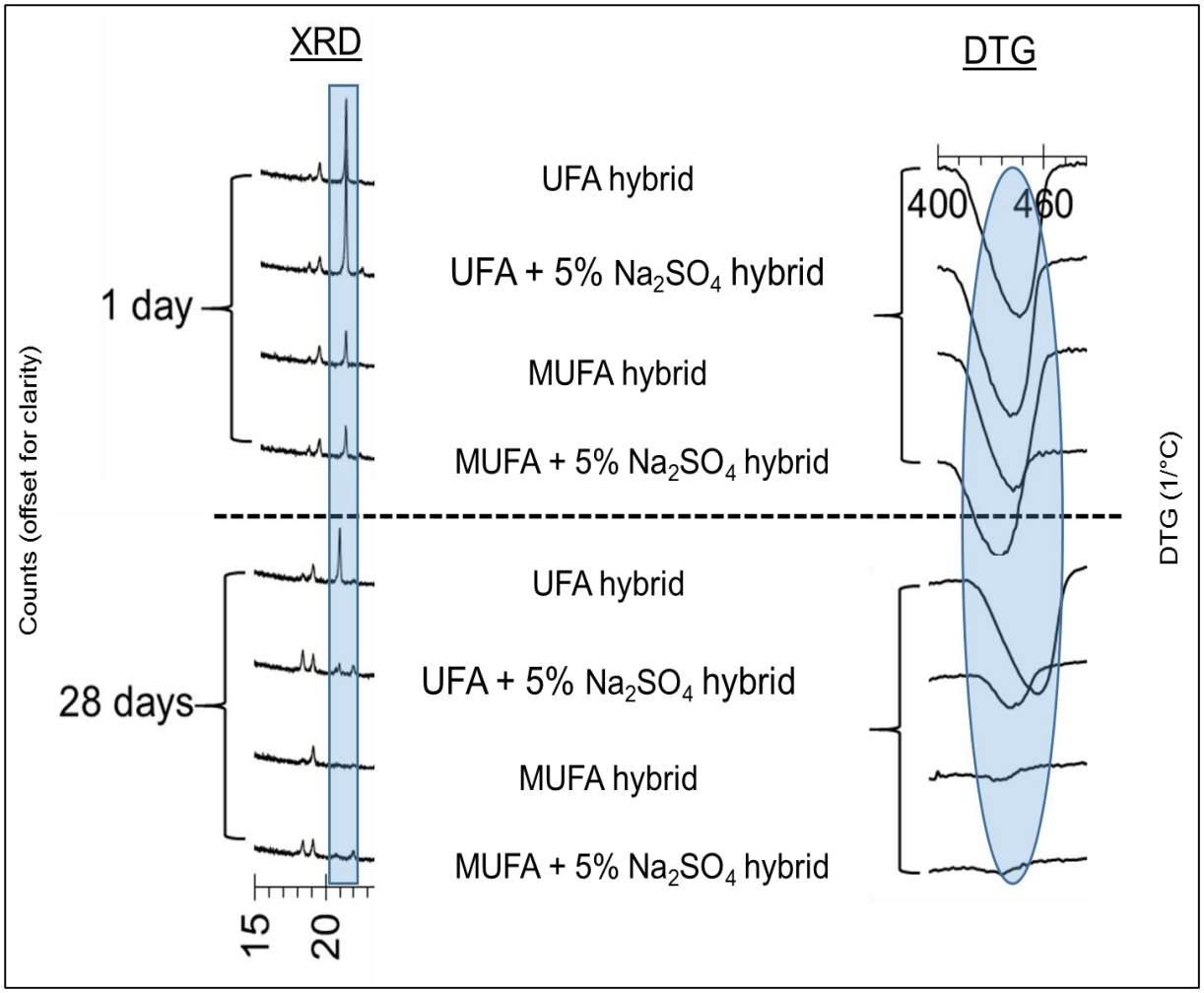

Figure 6.12. Summary of XRD and DTG data presenting the occurrence of portlandite as an indication of the pozzolanic reaction of hydrated fly ash hybrid cement upon chemical and mechanical activation.

With no activation applied to the hybrid cement paste (UFA), portlandite is still evident at 28 days, and a small XRD peak was even identified at 90 days as previously shown in Figure 6.5. Once chemical activation is applied to the hybrid cement paste (UFA5), portlandite was mostly consumed at 28 days. Applying mechanical activation to the unclassified fly ash (MUFA) resulted in an even faster pozzolanic reaction compared to the application of only chemical activation (Na_2SO_4) to the unclassified fly ash. The relative peak intensities significantly reduced, and no portlandite was evident at 28 days.

By combining the activation methods to the hybrid cement paste (MUFA5), the fastest pozzolanic reaction was achieved, with portlandite evident at 1 day, but consumed at the fastest rate compared to the other hybrids.

These results serve as evidence that activation of fly ash, more specifically the combination of chemical and mechanical activation, enhances the reactivity of the hybrid system by improving the rate of initiation of the pozzolanic reaction between fly ash and portlandite.

According to the methods (DTG and XRD) that clearly showed the consumption of portlandite after specific curing ages, the order of pozzolanic reactivity of fly ash for the four hybrid scenarios are as follows:

UFA < UFA + 5% Na_2SO_4 < MUFA < MUFA + 5% Na_2SO_4.

6.6 The effect of chemical and mechanical activation on stable ettringite formation in a high fly ash hybrid cement

It has been reported that the formation of well crystallized, stable ettringite will lend to an increase in paste volume, leading to a denser matrix and hence an increase in compressive strength (Fernández-Jiménez *et al.*, 2011; Qian *et al.*, 2001). The size of the ettringite crystals is also a very important aspect to keep in mind with regard to its stability, i.e. small, poorly crystallized crystals will tend to dissolve more easily compared to large, well-formed crystals (Chrysochoou & Dermatas, 2006). The analytical techniques used in this study which was able to identify ettringite, all agreed on the existence of ettringite for all four hybrid scenarios, at all of the studied curing ages, even up to 1 year.

Figure 6.13 provides a summary of the XRD and DTG data, indicating the presence of ettringite in hydrated fly ash hybrid cement specimens upon chemical and mechanical activation.

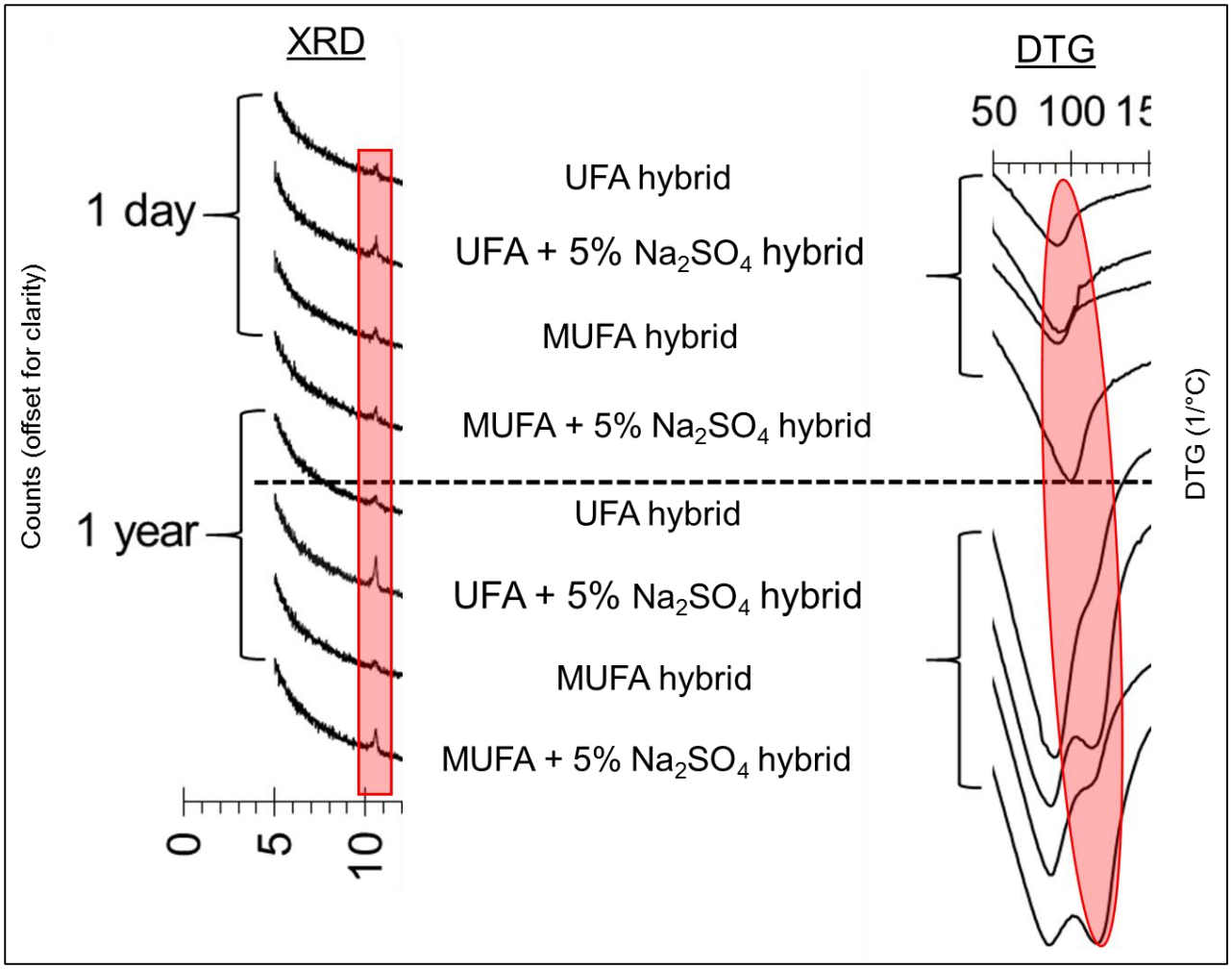

Figure 6.13. Summary of XRD and DTG data presenting the presence of ettringite in hydrated fly ash hybrid cement specimens upon chemical and mechanical activation.

The relative XRD and DTA (Figure 6.13) peak intensities clearly showed that the addition of Na_2SO_4 to the hybrid cement paste (UFA5) promotes ettringite formation when compared to no activation (UFA) (Lee *et al.*, 2003).

Interestingly enough, when the application of mechanical activation without chemical activation (MUFA) is applied and compared, it does not appear to contribute to increased ettringite formation.

From the results presented, it would appear that in comparison to mechanical activation chemical activation (Na_2SO_4) plays a critical role in the formation of well crystallized, stable ettringite within the hydrated hybrid cement. For the purpose of this study, stable ettringite

refers to it not converting to monosulfoaluminate, or "disappearing" after a few hours or days as suggested by some literature (Donatello *et al.*, 2014b; Hewlett, 2004). This is also evident once activation methods are combined (MUFA5). The relative peak intensities for the combined activation methods present similar intensities in comparison to the hybrid which only had chemical activation applied (UFA5), implying no significant additional contribution evident from mechanical activation towards ettringite formation.

Since it was just deliberated that mechanical activation makes little to no contribution to ettringite formation, any favourable physical performance from the combination of activation methods must then be a result of promoted ettringite formation from chemical activation, in combination with other factors and advantages from mechanical activation like an increase in the rate of pozzolanic activity between fly ash and cement. Fly ash hybrid mortar and concrete compressive strengths are presented and discussed in Chapter 7 and Chapter 8 respectively.

The existence of monocarboaluminate was evident for both UFA and MUFA hybrids where Na_2SO_4 was not used as a chemical activator. Once Na_2SO_4 was added to both of these systems, the monocarboaluminate was no longer evident. This would suggest that in specimens with no added Na_2SO_4, the sulfate content was still sufficient to prevent conversion of the ettringite to monosulfoaluminate, and rather produce monocarboaluminate from 7 days onwards. These findings are in agreement with the hydration chemistry of fly ash containing cements as discussed in Chapter 2.3.3. Since ettringite formation is favoured by the presence of sulfates, no AFm phases were evident once Na_2SO_4 was added (Garcia-Lodeiro *et al.*, 2016c). No monosulfoaluminate was detected in any of the four hybrid cases, confirming there was no conversion of ettringite to monosulfoaluminate (Fernández-Jiménez *et al.*, 2011).

It would appear that the reaction conditions in this study, whether chemical or mechanical activation was applied to the system, promoted the production of well crystallized, stable ettringite, which is in agreement with Velandia *et al*. (2016b) who also found ettringite formation to be favoured by Na_2SO_4 addition.

It is also well known that small ettringite crystals can undergo a process called "Ostwald ripening". This is the scenario where small ettringite crystals precipitate in large pores where favourable conditions results in the growth of larger, more stable crystals (Donatello *et al.*, 2014b; Garcia-Lodeiro *et al.*, 2016c). Figure 6.14 is an example of well crystallized ettringite crystals, as well as crystals formed in voids within the hydrated hybrid matrix. All four

micrographs are of the UFA5 hybrid at a very late hydration age (180 days) with 5% Na_2SO_4 added, proving stable ettringite formation within this specific hybrid even at later curing ages.

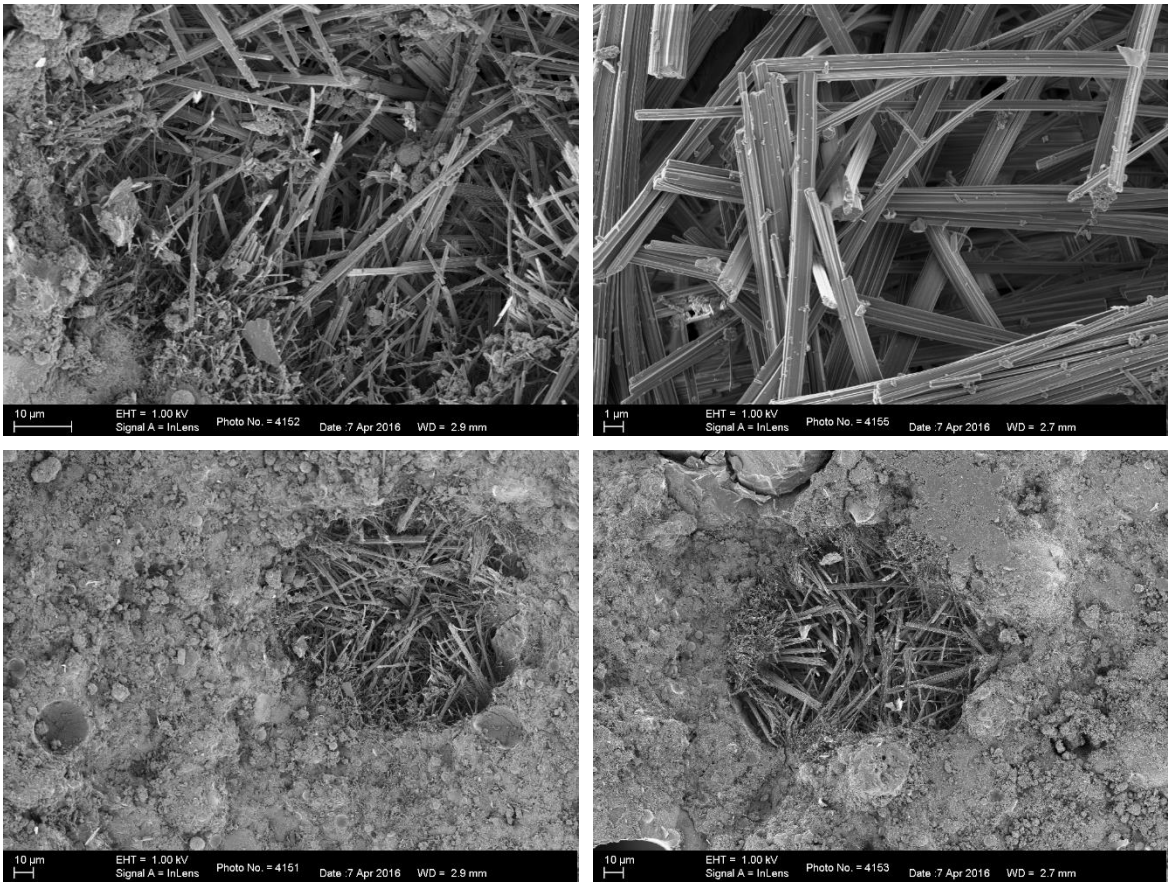

Figure 6.14. Well crystallized ettringite needles in the UFA hybrid with 5% Na_2SO_4 at 180 days of curing.

6.7 Expansion (soundness)

Expansion provides an indication of any unwanted swelling occurring in the cement once hydration takes place. For this study there may be a concern of excess expansion (delayed ettringite formation) due to the addition of sulfates (Na_2SO_4) as a chemical activator.

Expansion testing was only conducted on the extreme scenario where swelling may occur, i.e. the MUFA5 hybrid cement paste. A total of 10 pastes of the same mix design were produced

and measured. Eight of the specimens gave a measurement of 0 mm and the two remaining specimens gave a measurement of 1 mm. This results in an average of 0.2 mm. The South African National Standard for Cement (SANS 50197) specifies a maximum of 10 mm for all of the listed cements (SABS, 2013a). Clearly, the chemical activation used in this study does not pose a risk of unwanted expansion.

Even though it was stipulated in Chapter 1 that a detailed investigation into delayed ettringite formation (DEF) would not form part of this thesis, it is worthwhile making some comments with regards to the available data in comparison to literature.

DEF is a term used to denote the formation of ettringite in hardened concrete, mortar or paste which results in expansion or cracking, and will be detrimental to the integrity of the specimen (Leklou *et al.*, 2008; Taylor, 1997). The reaction mechanism of DEF involves a large number of parameters, the importance of which is not always well understood (Leklou *et al.*, 2008).

According to literature, the most influencial parameters are the temperature and sulfate content in the presence of moisture (Leklou *et al.*, 2008).

- If exceedingly high amounts of gypsum (or other sources of sulfate) are added to cement, and if concrete made with that cement is in a moist service environment, DEF can occur. Abnormal expansions can occur from excessive calcium sulfoaluminate after hardening, and continue until the sulfates become depleted. It has been demonstrated that SO_3 contents of up to 5% had no significant impact on expansion of mortar bars stored in a moist room. However, when high SO_3 content was present (up to 7.5%), excessive expansion was generated (Lerch, 1945; PCA, 2001).

- The temperature conditions for deleterious expansion due to DEF requires curing or in situ temperatures above 70 °C in the presence of moisture. These conditions result in the destruction of primarily formed ettringite in the early stages of hydration, only to recrystallize after a initial delay in the hardened concrete (Hewlett, 2004; PCA, 2001; Taylor, 1997).

Ettringite formed by dissolution and recrystallization in void spaces and cracks is often referred to as “secondary ettringite.” Secondary ettringite is not detrimental to concrete performance

(PCA, 2001). The problem of DEF formation has also not been observed with fly ash or slag concretes (Hewlett, 2004).

Although no detailed SEM study was completed as part of this thesis for the investifation of DEF, none of the above mentioned conditions to promote DEF was apparent in this study.

Sulfate (SO_3) analysis completed on all four of the hybrid scenarios at all of the studied curing ages produced SO_3 percentages well below the concerned 7.5% as reported by Lerch (1945). On average, the hybrids with no added Na_2SO_4 contained less than 1% SO_3, and the hybrids which had 5% Na_2SO_4 added contained less than 3.5% SO_3, which also reduced slightly as the curing age increased. Expansion testing on the "worst case scenario" i.e. the MUFA5 hybrid cement paste showed no reason for concern. Hence, DEF due to excessive sulfates present in the cement is unlikely.

All the specimens were cured at room temperature and had no exposure to extreme heat from external sources. Also, neither of the activation methods caused high internal heat, since all four hybrid scenarios produced heat that would be classified as low heat cement by the European cement standard (EN 197 / SANS 50197) (CEN, 2011), which requires heat evolution of no more than 270 J/g at 41 hours in order to be classified as a low heat common cement. Table 6.3 provides the individual results for the hybrids at 41 hours (taken from the results published earlier in this thesis). From these results it is evident that high temperature would also not be a factor leading to DEF in this study.

Table 6.3. Heat released (Joule/gram) for the 4 hybrid cements at 41 hours of hydration.

UFA	UFA + 5% Na_2SO_4	MUFA	MUFA + 5% Na_2SO_4
79.9	96.5	89.8	147.6

6.8 Conclusion

The test methods applied in this chapter that relate directly to the rate of early age hydration i.e. setting time and heat evolution, provided the similar findings. The FCFA hybrid had the most extended initial setting time and the lowest accumulative heat over a period of 48 hours and 7 days. This is definitely indicative of the slowest reaction rate for hydration at early ages between the three fly ash cement pastes studied. Chemical activation (5% Na_2SO_4) proved to shorten the setting time as well as the induction period. For all three types of hybrids, the addition of Na_2SO_4 accelerated the reaction kinetics by effectively shortening the induction period and raising the maximum rate of heat release. Both of the test methods proved that the combination of chemical activation and mechanical activation had the most favourable effect on hydration rate, which should relate to the highest early age compressive strengths to be discussed in the upcoming two chapters.

Both XRD and TGA showed that the application of chemical activation promoted ettringite formation. Chemical activation as well as mechanical activation increased the rate at which portlandite was consumed, which is furthermore indicative of an increase in the rate of the pozzolanic reaction between portlandite contained in cement and fly ash. It was found that, compared to chemical activation on its own (UFA), the combination of activation techniques (MUFA5) did not result in increased ettringite formation. However, the application of combined chemical and mechanical activation definitely resulted in the fastest rate of portlandite consumption, hence an increased rate of the pozzolanic reaction.

FTIR was the only analytical characterisation technique independent of degree of crystallinity and hence able to identify the hydration-type gels that usually form as part of cement hydration. In this case, all four of the hybrid cement pastes proved to contain C-S-H-type gel, already visible after 1 day of hydration. Evidence of additional types of gel that may have formed, was not evident from the transmission spectra.

An expansion experiment was conducted to confirm that unwanted swelling or delayed ettringite formation (DEF) due to the addition of sulfates would not pose a problem. The highest level of sulfate addition (5% Na_2SO_4) that was added and tested proved that there is no reason for concern since an average of 10 pastes produced an average of 0.2 mm expansion. This is well below the specified value of 10 mm from EN 197 / SANS 50197 (CEN, 2011). A short discussion on delayed ettringite formation (DEF) in conjunction with some of the results

from this study, proved that DEF is not an issue to be considered under the conditions of this study.

~ Chapter 7 ~

Mortar test results and discussion of hybrid fly ash cement

7.1 Introduction

In this part of the thesis the strength development of fly ash hybrid cement is discussed. Blends were prepared by mixing 70% of fine classified fly ash (FCFC), unclassified fly ash (UFA), or mechanically activated unclassified fly ash (MUFA) respectively with 30% cement. Different percentages of Na_2SO_4 at 0%, 1%, 3% and 5% Na_2SO_4, were manually added to the fly ash-cement blends. For a detailed description of the experimental program, refer to Chapter 3.6.

The following notation was used for the hydrated cement blends (hybrids) where applicable:

FCFA hybrid	**No activation applied**
FCFAx hybrid	**Chemical activation applied (x% Na_2SO_4)**
UFA hybrid	**No activation applied**
UFAx hybrid	**Chemical activation applied (x% Na_2SO_4)**
MUFA hybrid	**Mechanical activation applied**
MUFAx hybrid	**Combined activation applied (x% Na_2SO_4 + mechanical activation)**

7.2 Strength of mortars

The fly ash content in blended cement is normally limited by the low initial strength and subsequent slow strength development. This has been ascribed to the delay in pozzolanic activity and was discussed in Chapter 2.3. The strength development of the hybrid specimens produced without chemical activation is given in Figure 7.1.

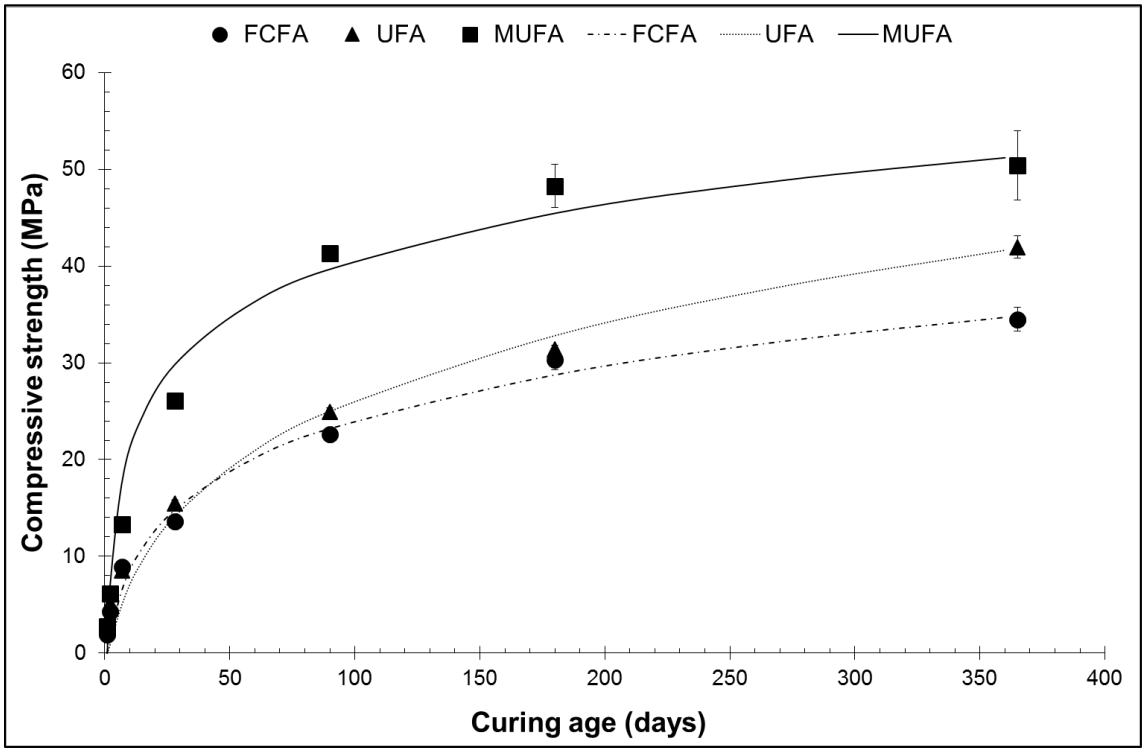

Figure 7.1. Mortar compressive strength of the reference fly ash cement hybrids (without Na_2SO_4) produced from FCFA, UFA and MUFA (n = 6).

The graph shows that the rate at which strength is gained differ significantly for the different ashes. The graph shows the low early strength and slow rate of strength development for both the FCFA and UFA hybrid blends. The rate of strength development for MUFA is somewhat better, since by virtue of the manner in which it was procured (milling of UFA), it has in actual fact been mechanically activated. These results correlate with the observations made on the surface characteristics (Chapter 4.8), which suggests that with FCFA having a larger surface area and being more amorphous, it should markedly improve the strength development characteristics of the hybrid cement. It is noteworthy that for all the hybrids the increase in strength between 1 and 365 days is around 94.5%. The MUFA hybrid gains strength more rapidly and achieves a higher ultimate value. This behaviour is in agreement with the etching of fly ash surfaces exposed to calcium hydroxide (Chapter 5.2). The strengths confirm that, without chemical activation, these 70% fly ash hybrid cements do not meet the minimum strength requirements for a 32,5N cement of 16 MPa after 7 days and 32,5 MPa after 28 days (CEN, 2011). Figure 7.2 shows the different hybrid cement mortars once chemical activation had been applied.

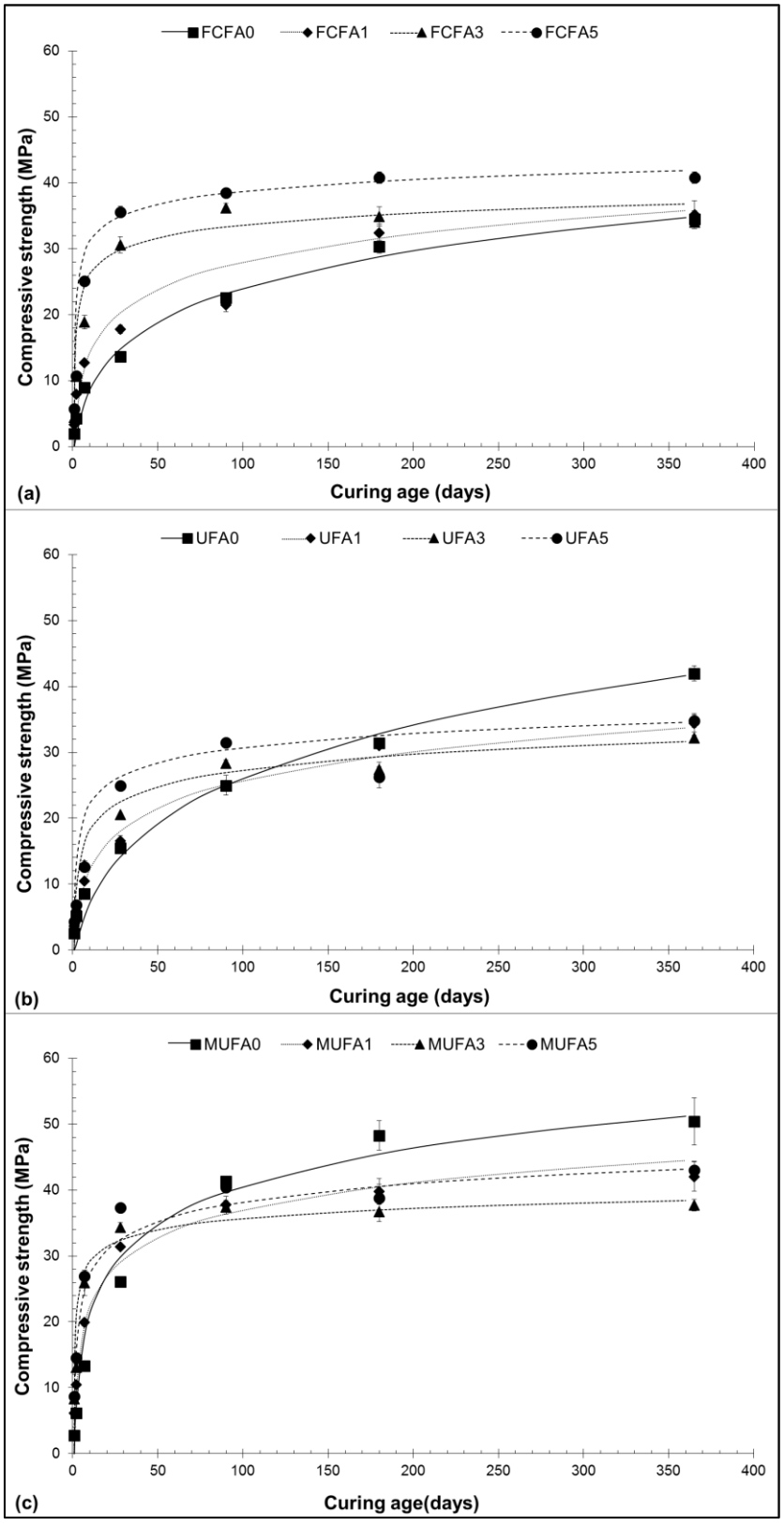

Figure 7.2. Mortar compressive strength of the fly ash cement hybrids (with and without Na_2SO_4) produced from (a) FCFA, (b) UFA and (c) MUFA for up to 1 year of curing (n=6).

The strength of the FCFA (Figure 7.2 a) hybrid cement increases along with increasing sodium sulfate content. This trend is only valid up to 90 days of curing with no significant strength gain for samples containing more than 1% sodium sulfate after 90 days. However, the strength continued to increase for 0% and 1% sodium sulfate addition between 180 days and 1 year of curing. Both the UFA (Figure 7.2 b) and the MUFA hybrid cements (Figure 7.2 c) show similar, but less pronounced initial trends in strength development to that of the FCFA hybrid cement with increasing sodium sulfate addition.

For all curing ages the strength of the MUFA hybrid cement was higher than for both the FCFA and UFA hybrids. This trend also correlates with literature where the combination of grinding and addition of sulfate gave higher strength than any single activation method investigated (Qian *et al.*, 2001).

It should however be noted that for the MUFA hybrid (Figure 7.2 c) the strength reached by the reference specimen (mechanically activated, 0% sodium sulfate) at 180 and 365 days exceeds that reached by the specimens where mechanical and chemical activation are combined. This was also true in the case of UFA at 365 days of curing. Hence, if high long term strength (365 days) is required, mechanical activation of unclassified fly ash, without the addition of chemical activation could be considered.

For a general purpose, normal strength gaining cement (32.5N strength class), the strength development specified by the EN 197 standard requires a minimum strength of 16 MPa at 7 days and 32.5 MPa at 28 days. If rapid early age strength gain is required (32.5R strength class), the EN 197 requires a minimum of 10 MPa at 2 days, no 7 day requirement is specified and the 28 day requirement is the same as for a 32.5 strength class cement. Figure 7.3. illustrates how the different hybrid cements performed physicallly agianst these requirements.

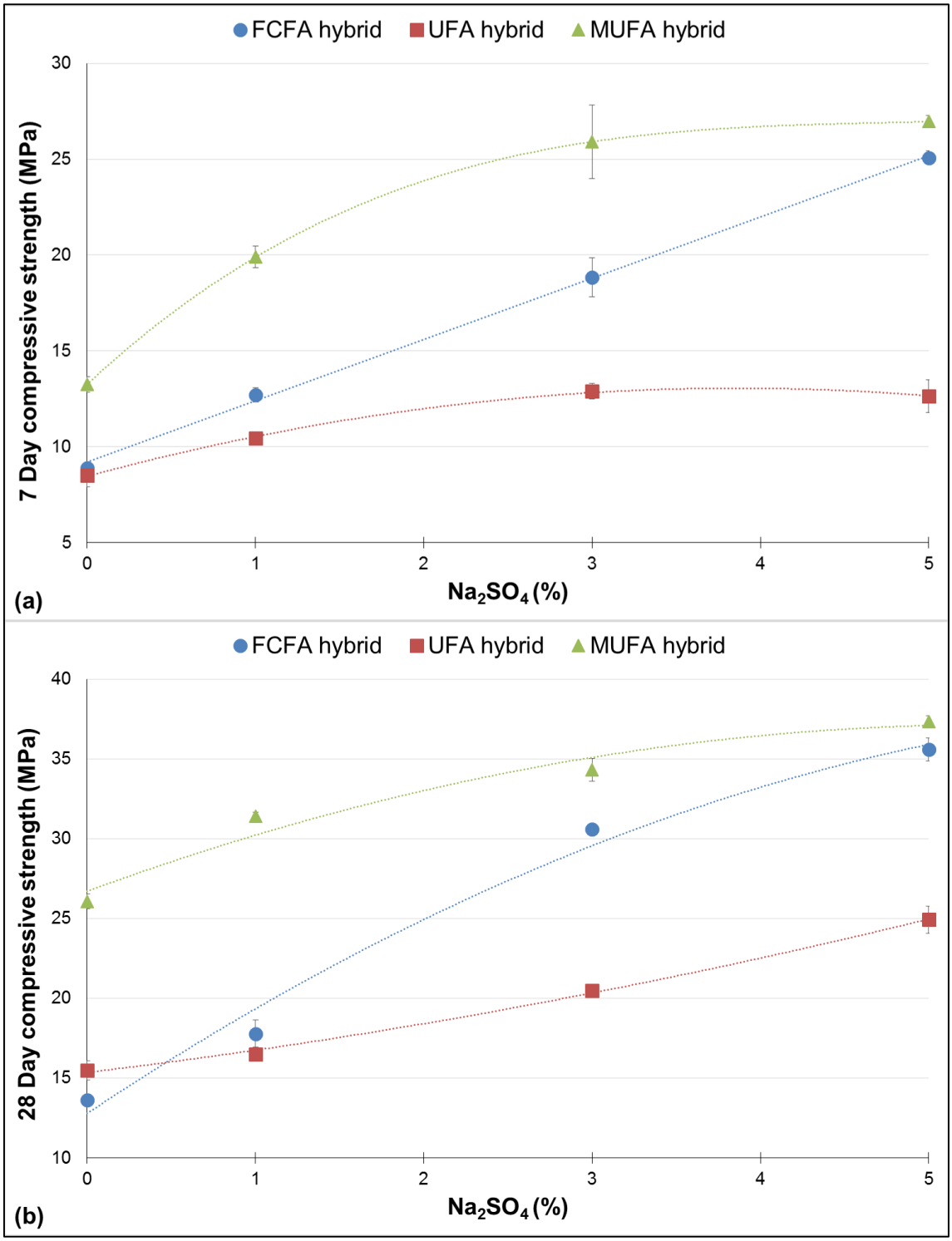

Figure 7.3. The (a) 7 day and (b) 28 day compressive strengths for the FCFA, UFA and MUFA hybrids versus the amount of Na_2SO_4 added to the blend.

From Figure 7.3 it can be seen that the MUFA hybrid was the only blend that produced compressive strengths that complies with a 32.5R (rapid early strength gain) product criteria of EN 197 cement specification, at both 3% and 5% sodium sulfate addition. Even after activation, the unclassified fly ash hybrid cement, did not produce any products complying with this cement specification, affirming once again the rationale behind the combination of chemical and mechanical activation. Figure 7.4 provides a different depiction of the strength gained between 2 day and 28 days.

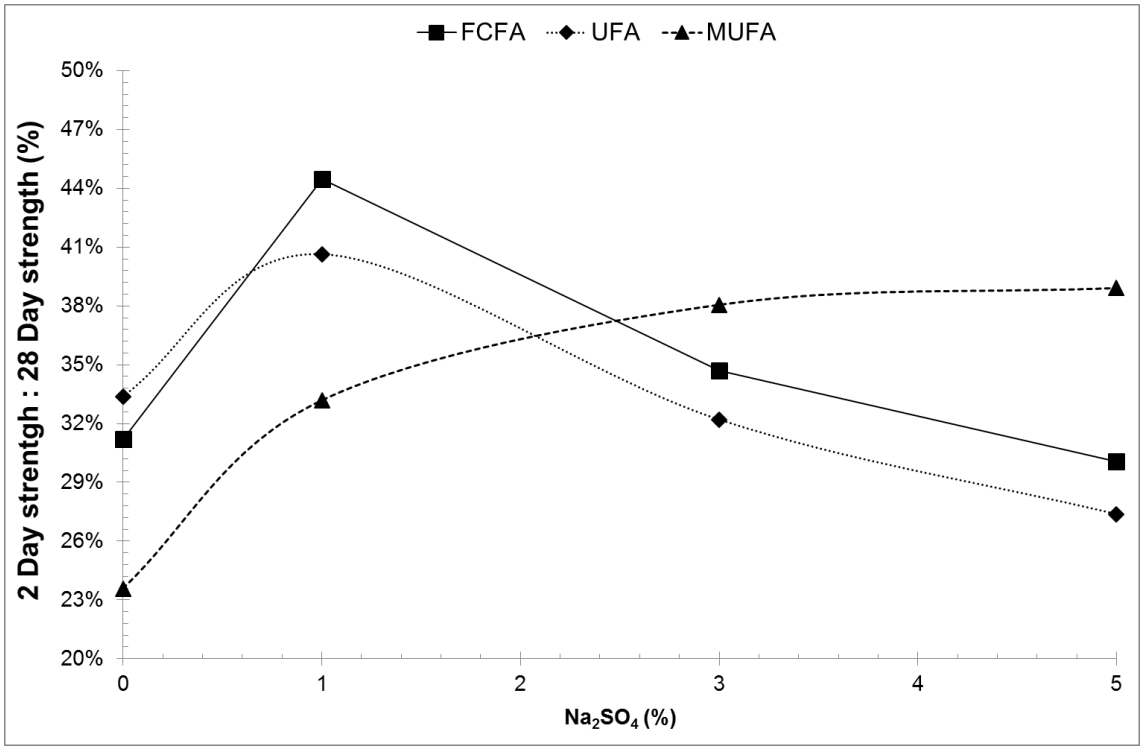

Figure 7.4. The 1 day strength expressed as a percentage of the 28 day strength of the fly ash cement hybrids, produced from FCFA, UFA and MUFA.

This graph expresses the 2 to 28 day strength ratio for each of the hybrids at the four levels of sulfate addition. These results indicate that the addition of sodium sulfate is a suitable activation method for increasing early age strength (after 2 days). For both the FCFA hybrid cement and the UFA hybrid cement, the highest early age strength is achieved when 1% sodium sulfate is added to the mix-formulation. The most significant increase in strength was achieved when 3%

sodium sulfate activator was used in the preparation of the MUFA hybrid cement. This confirms once again that the combination of chemical and mechanical activation yields the best strength results.

From the setting times, heat evolution and conclusion on the rate of increase of the pozzolanic reaction in Chapter 6, as well as the formation of stable ettringite, it was predicted that compressive strength, especially early age strength, should not only be improved, but outperform the FCFA- and UFA hybrid cements, once a combination of activation methods (MUFA5) is applied. The following figure draws a comparison between the total heat obtained for the different hybrid cements and the mortar compressive strength achieved at the same hydration ages. Due to availability of data from the calorimeter, only three data points (hydration ages) are compared in Figure 7.5 i.e. 1 day, 2 days and 7 days.

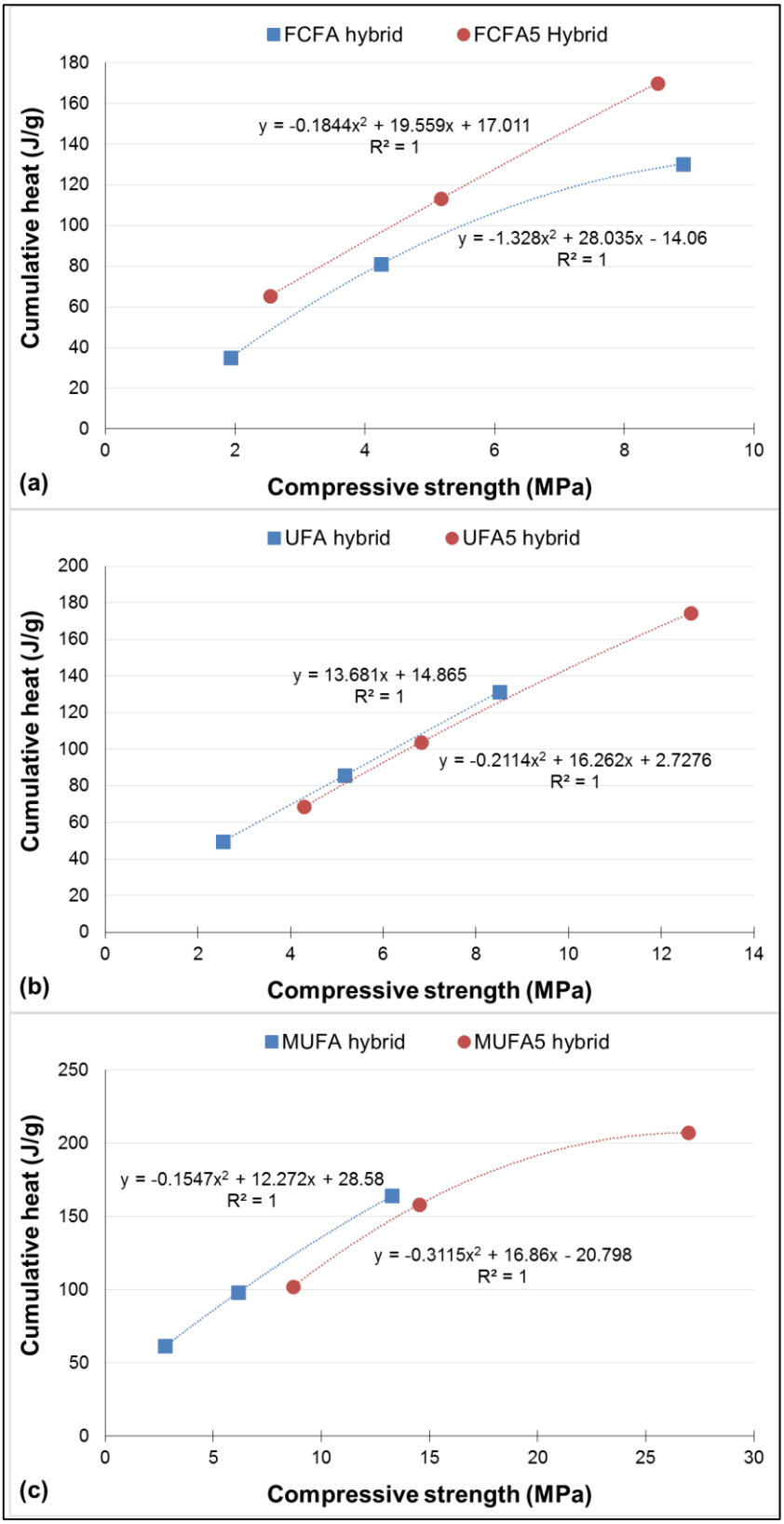

Figure 7.5. Total heat versus strength at 1, 2 and 7 days of hydration for (a) FUFA & FUFA5, (b) UFA & UFA5 and (c) MUFA and MUFA 5 hybrid cement mortars.

It is irrefutable from the data presented in Figure 7.5, that an increase in the total heat output correlates with higher mortar compressive strength, and that the addition of sodium sulfate as chemical activator results in significant increases in initial (1 day) heat output and strength. For all 6 specimens, a logarithmic trend line provided the best fit to describe the relation between total heat output and strength at these curing ages. Once again, the combination of chemical and mechanical activation resulted in superior strength, correlating with the highest total heat of hydration Figure 7.5.

7.3 Conclusion

Despite the favourable particle shape distribution and mineralogy of the fine classified fly ash (FCFA), it proved not to be the most chemically reactive of the three fly ashes considered. Strength development in hybrid cements containing FCFA is likely attributed to physical and not chemical contributions.

The milled unclassified fly ash (MUFA) hybrid achieved the highest compressive strength results at all curing ages considered.

Considering the strength specifications of EN 197, FCFA only produced one product complying with a 32.5N cement when 5% sodium sulfate was added. The unclassified fly ash (UFA) hybrid, even after chemical activation, did not achieve any strengths complying with the EN cement specification. The MUFA hybrid cement was the only blend that produced compressive strengths complying with a 32.5R (rapid early strength gain) product according to EN 197, at both 3% and 5% sodium sulfate addition. The lower sulfate content would however yield a more cost effective hybrid cement.

The combination of mechanical and chemical activation (sodium sulfate) can be considered a valuable technique to address low early strengths and slow strength development, resulting in hybrid cements that comply with the EN 197 cement strength requirements.

It has been proven, as was predicted from the setting time and heat evolution data in Chapter 6 that, the combination of chemical (Na_2SO_4) and mechanical activation (MUFA5) of fly ash results in superior performance of fly ash hybrid cement.

~ Chapter 8 ~

Concrete test results and discussion of hybrid fly ash cement

8.1 Introduction

In this part of the thesis the workability (slump retention) and compressive strength of concrete containing fly ash hybrid cement is investigated. Hybrid cement blends were prepared by mixing 70% of dry unclassified fly ash (UFA), fine classified fly ash (FCFC), or mechanically activated unclassified fly ash (MUFA) respectively with 30% cement. Different percentages of Na_2SO_4 at 0%, 1%, 3% and 5% Na_2SO_4, were manually added to the fly ash-cement blends. For detail on the experimental program and mix design, refer to Chapter 3.

The following notation was used to identify the hydrated concrete blends (hybrids):

FCFA hybrid	**No activation applied**
FCFAx hybrid	**Chemical activation applied (x% Na_2SO_4)**
UFA hybrid	**No activation applied**
UFAx hybrid	**Chemical activation applied (x% Na_2SO_4)**
MUFA hybrid	**Mechanical activation applied**
MUFAx hybrid	**Combined activation applied (x% Na_2SO_4 + mechanical activation)**

8.2 Slump retention of concrete

The slump retention (workability) achieved for the three different hybrids at different additions of Na_2SO_4 are presented in Table 8.1.

Table 8.1. Slump retention (mm) at different Na_2SO_4 additions for FCFA, UFA and MUFA hybrids.

	0% Na_2SO_4	1% Na_2SO_4	3% Na_2SO_4	5% Na_2SO_4
FCFA	150	155	160	170
UFA	160	170	175	170
MUFA	70	70	75	75

Keeping in mind the considerable tolerances in slump from Table 3.8 in Chapter 3, it is evident from the results obtained that neither the addition nor the increase in Na_2SO_4 content make a significant difference on the slump retention achieved. When considering the slump retention results (Table 8.1) for the three fly ashes studied, it is evident that by breaking the fly ash spheres via mechanical activation, the slump retention is affected significantly. The values obtained for slump retention once the ash is milled (MUFA) is almost half of that achieved from using FCFA and UFA. This means that the MUFA hybrids are significantly less workable (stiff) at the same water:cement ratio compared to the FCFA and UFA hybrids.

8.3 Strength of concrete

The control hybrid concrete results are presented in Figure 8.1 and Figure 8.2 a-c portraying the concrete compressive strength results for the respective curing ages.

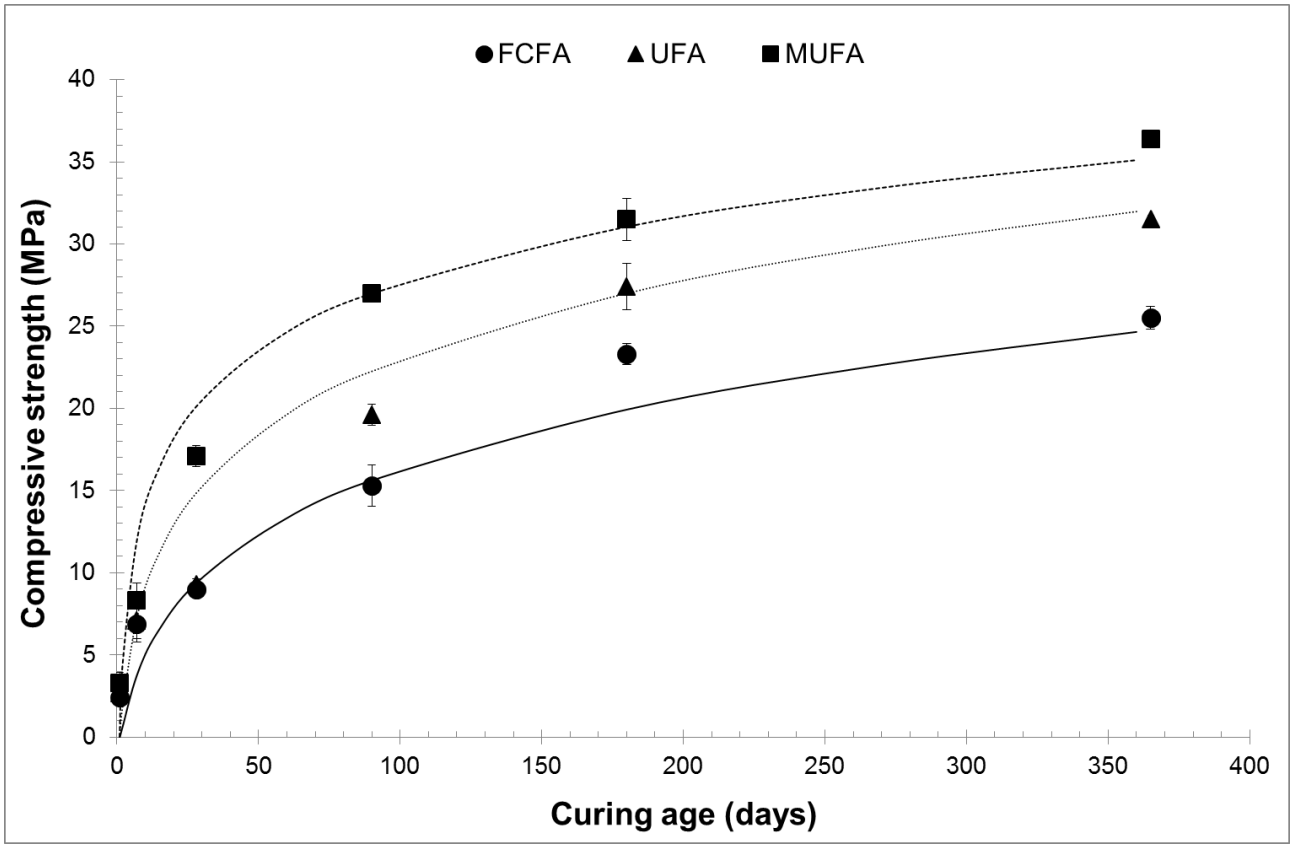

Figure 8.1. Concrete compressive strength of the reference fly ash concrete hybrids (without Na_2SO_4) produced from FCFA, UFA and MUFA (n = 2).

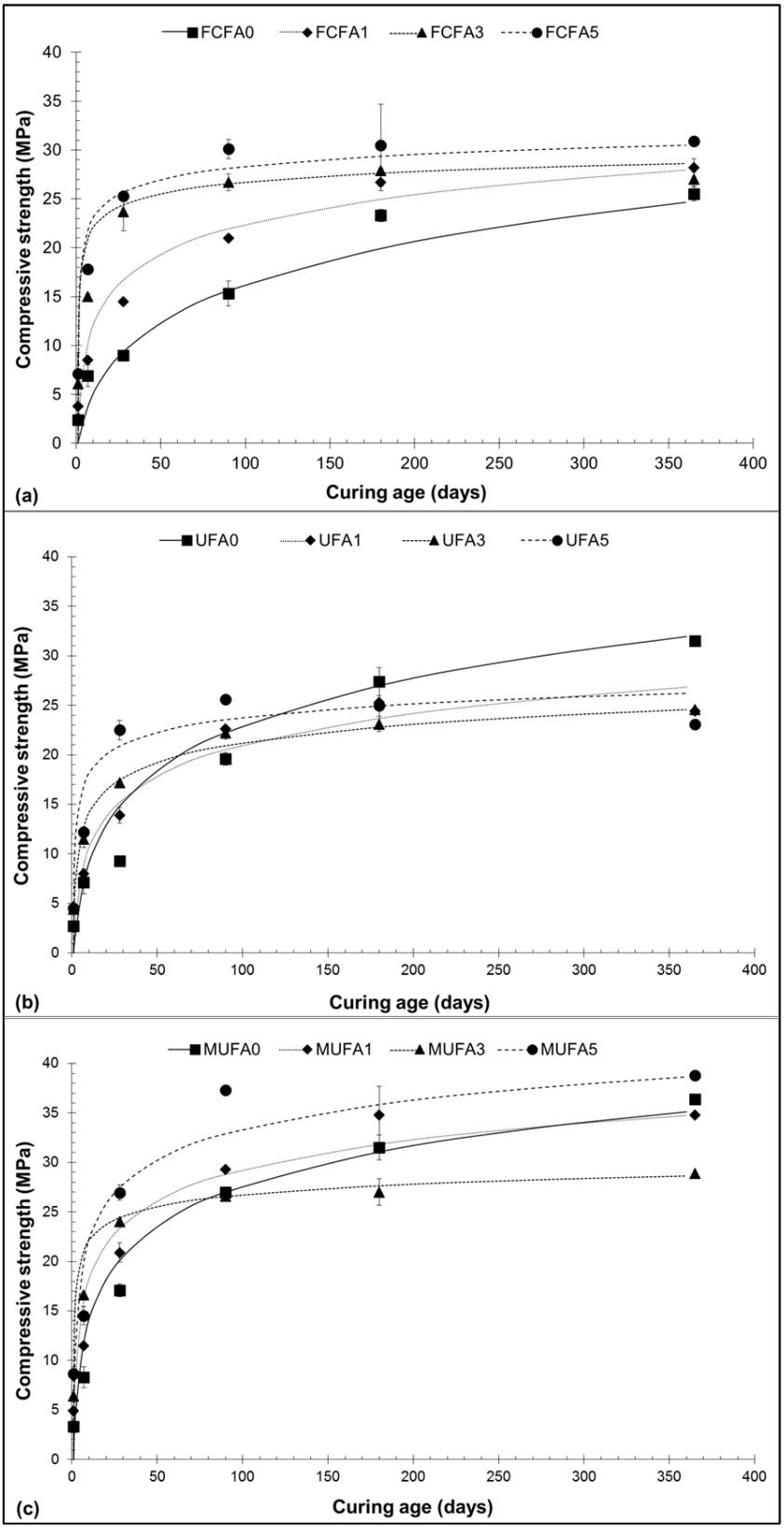

Figure 8.2. Concrete compressive strength of the fly ash concrete hybrids (with and without Na_2SO_4) produced from (a) FCFA, (b) UFA and (c) MUFA for up to 1 year of curing (n=2).

It can be seen that the same trend is evident for concrete as for mortar. Irrespective of the amount of chemical activator added or fineness of fly ash used, the samples always indicate an increase in concrete compressive strength, with an increase in chemical activation up to 28 days of curing when compared to the respective control samples (Figure 8.1).

If the fine classified fly ash is considered (Figure 8.2 a), the activation effect is evident for all five curing ages presented on the graph. It is possible that the consistent enhancement in strength may be due to the very fine nature of the classified fly ash, which can result in enhanced "filler effect" in the concrete. The filler effect of the fine spherical particles can result in improved particle packing and workability, as well as the provision of additional nucleation sites on the surface of the fly ash for the cement hydrates (seeding effect), and the increase of effective water-to-cement ratio (w/c), when the water-to-solid ratio is kept constant whereby the hydration of cement is promoted (Deschner *et al.*, 2012).

Regarding the chemical activation of unclassified fly ash (Figure 8.2 b), little activation takes place in 24 hours for different sulfate additions when compared to the control sample.

The concrete strength for the MUFA hybrid blends are presented in Figure 8.2 c. The benefit of combined chemical and mechanical activation is clearly evident, especially at early concrete ages.

It is only when samples reach the 90 day curing mark and onwards, that results become somewhat erratic and deviate from the abovementioned trend for both the UFA and MUFA hybrids. However, unlike the findings for the mortar testing, the results obtained for fine classified fly ash samples still indicate definite increases in compressive strength with an increase in chemical activation up to 180 days of curing. All three hybrid systems seem to reach a natural plateau for concrete compressive strength around 1 year.

Figure 8.3 presents the 7 and 28 day concrete compressive strength results versus the different Na_2SO_4 additions, as was done for mortar strengths in section 7.2

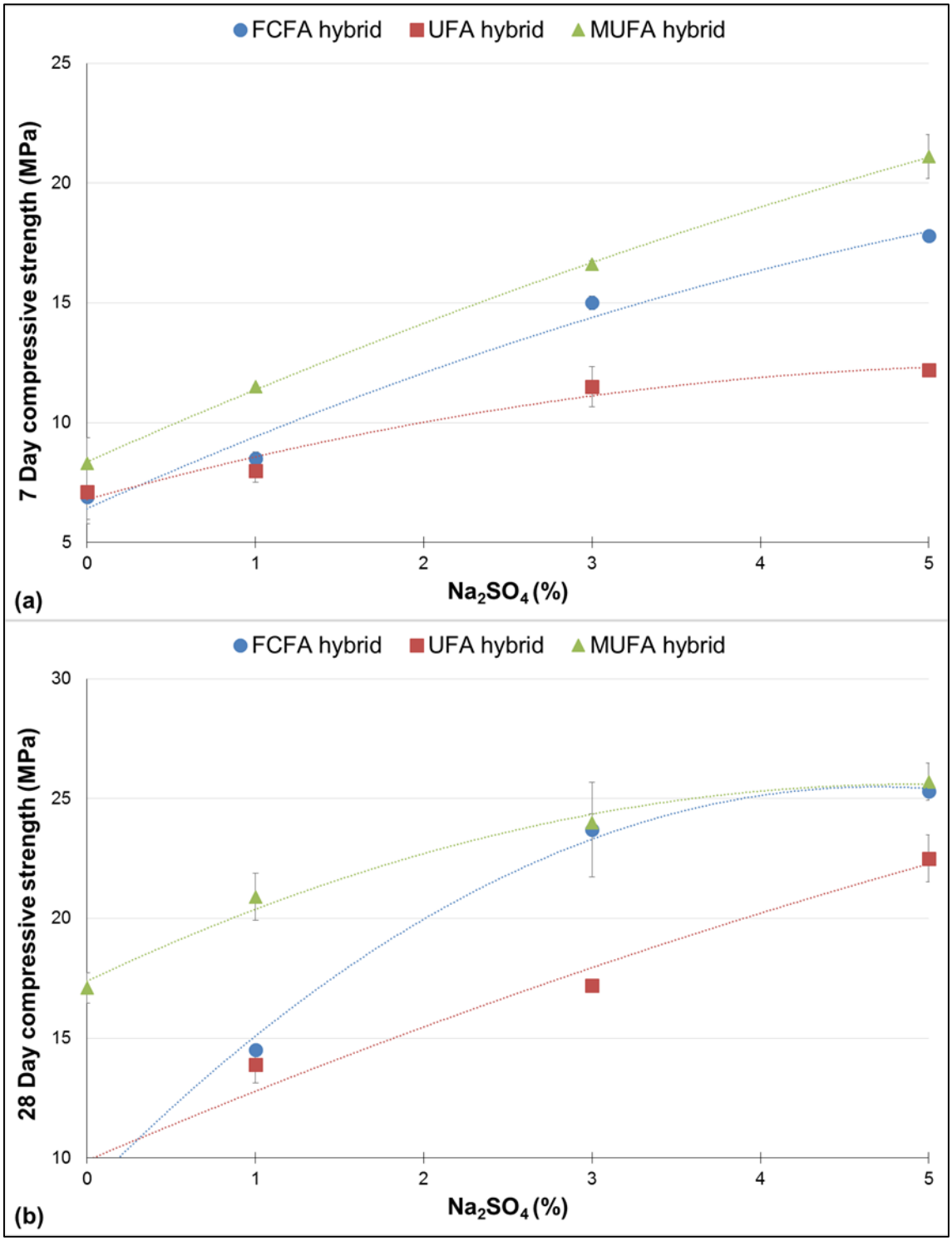

Figure 8.3. The (a) 7 day and (b) 28 day compressive strengths for the FCFA, UFA and MUFA concrete hybrids versus the amount of Na_2SO_4 added to the blend.

From Figure 8.3 it can be seen that the MUFA hybrid once again outperformed the other two hybrids, especially at both 7 days and 28 days. Similar to the mortar strengths, the UFA hybrid was outperformed by both the FCFA and the MUFA hybrid, affirming once again the rationale behind the combination of chemical and mechanical activation.

8.4 Conclusion

The advantage of chemical activation in any of the three fly ash scenarios, is evident in the concrete strengths. It could also be seen that FCFA may be the least chemically reactive, but it could enhance strength by possibly improving the packing density of the specimens be means of the filler effect. Hence, the strength advantages realised from use of FCFA may be attributed to its physical nature, rather than its chemical reactivity.

Although mechanical activation reduced workability of the concrete mix, it is imperative to remember that these mixes were not optimised with regards to binder:water ratio. The latter could significantly improve workability.

~ Chapter 9 ~

Conclusions and recommendations for future work

9.1. Introduction

Globally, cement companies are producing nearly two billion tons of CO_2 per annum, approximately 7% of the planet's total CO_2 emissions. Should this trend continue, the cement industry will be emitting CO_2 at an alarming rate by the year 2025. Immediate global replacement of Portland cement is currently not possible due to technical concerns around paste, mortar and concrete rheology or the supply of universally available, consistent quality supplementary cementitious materials. However, partial replacement i.e. hybrid cements that contain 30% or less cement clinker, are deemed to be technologically viable materials for contemporary construction.

This thesis contributes to the development of new environmentally friendly binders in concrete, specifically for application in the South African market. The effect of combined chemical and mechanical activation on the formation of hydration products and the properties of high fly ash containing cementitious systems is poorly understood and literature in this regard exceedingly limited.

In this thesis, the hybrid cement produced consists of 70% siliceous fly ash and 30% Portland cement to which a combination of chemical and mechanical activation methodologies were applied. For convenience, the graphical layout (Chapter 3) of the experimental program is presented again in Figure 9.1.

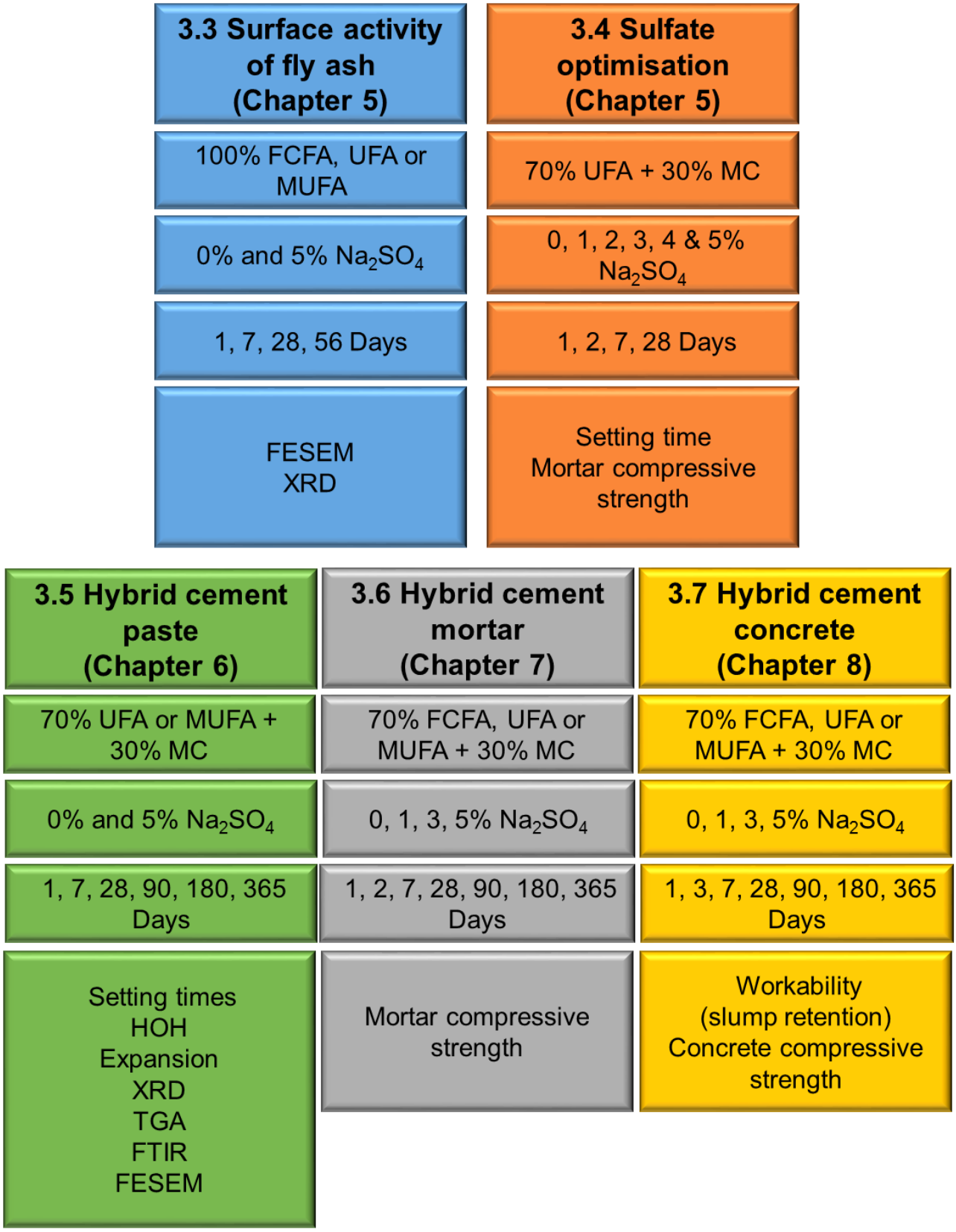

Figure 9.1. Overview of the experimental program.

9.2. Conclusions

Objective 1

Evaluation and comparison of the physical surface effect of chemical activation at four different curing ages, on three different siliceous fly ashes, differentiated by fineness and/or particle shape (due to mechanical activation) (Chapter 5).

Curing fly ash in a saturated calcium hydroxide solution serves as a viable, easy and cost effective method to evaluate surface properties of fly ash.

Despite its favourable particle shape distribution and mineralogy, the fine classified fly ash (FCFA) proved not to be the most chemically reactive of the three fly ashes considered. Strength development in hybrid cement containing FCFA is likely attributed to physical as well as chemical contributions.

The surface reactivity of the three fly ashes according to the presented results can be listed as follows: FCFA < UFA < MUFA, whereby the fine classified fly ash showed the least surface reactivity, and mechanically activated (milled) fly ash indicated the most surface reactivity.

The presence of increased amorphous phase within the fly ash specimens did not automatically result in superior surface reactivity upon activation for the respective fly ash products. The combination of activation methods (mechanical and chemical) proved to be the most effective in increasing the surface reactivity of the fly ash.

Objective 2

Determination of the effect of the quantity of sodium sulfate addition (chemical activation) on fly ash-based hybrid cement specimens, with regard to mortar compressive strength gain at three different curing ages. The effect of dry addition of Na_2SO_4 to the hybrid specimens as well as addition of the Na_2SO_4 in solution form was studied (Chapter 5).

Chemical activation (Na_2SO_4) is unquestionably effective in improving mortar compressive strength at all curing ages, irrelevant of the method of sulfate addition when compared to the control sample which contains no sulfate~~s~~.

It is also evident that compressive strength data obtained for early curing age specimens (1 day and 2 days) indicate evidence of an optimum amount of sulfate addition. For these specimens, the compressive strength results indicate some degree of decline with increasing SO_4^{2-} content. The dry- and wet addition of sulfates produced maximum additions of 2.9% Na_2SO_4 and 2.8% Na_2SO_4 respectively after 1 day of hydration, and 2.9% Na_2SO_4 and 2.8 % Na_2SO_4 respectively after 2 days of hydration. The results suggest that between 1 day and 2 days of hydration, the addition of more sulfates to the system is not necessarily the contributing factor to higher compressive strength in mortar specimens, indicating a possible saturation point for sulfates within the system at this stage of hydration.

Regarding the later curing ages, 7 day strength development seems to reach a plateau with increasing sulfate addition, whereas 28 day mortar compressive strength continues to increase as the percentage of sulfate increases.

Both initial and final setting times decreased with the addition of sulfates in comparison to the control sample (0% Na_2SO_4), however, very little change in setting was observed for Na_2SO_4 contents above 2%.

Objective 3

Evaluation of the setting times and heat evolution of fly ash hybrid pastes containing 70% of fly ash , as well as expansion on the hybrid cement containing the highest amount (5%) of Na_2SO_4 (Chapter 6).

The test methods applied in this chapter that relate directly to the rate of early age hydration rate i.e. setting time and heat evolution, provided the same findings.

The FCFA hybrid exhibited the most extended initial setting time and the lowest accumulative heat over a period of 48 hours and 7 days. This is indicative of the reaction rate at early ages being slower than that of the other two fly ash cement pastes. Chemical activation (5% Na_2SO_4) proved to reduce setting times as well as the induction periods in the heat flow diagrams.

For all three types of hybrid cements, the addition of Na_2SO_4 accelerated the rate of hydration by effectively shortening the induction period and raising the maximum rate of heat release. Both test methods applied proved that the combination of chemical activation and mechanical

activation had the most favourable effect on hydration rate, which should relate to the highest early age compressive strengths

The expansion experiment confirmed that unwanted swelling or delayed ettringite formation (DEF) due to the addition of sulfate would not pose a problem. The highest level of sulfate addition (5% Na_2SO_4) that was added and tested proved no reason for concern seeing that an average of 10 pastes produced an average of 0.2 mm expansion. This is well below the specified maximum allowable value of 10 mm from EN 197 / SANS 50197 (CEN, 2011).

Objective 4

Characterisation and discussion of the hydration products resulting from combined (chemical and mechanical) activation of fly ash, when used to produce hybrid cement paste containing 70% fly ash, at different curing ages over a period of one year (Chapter 6).

Both XRD and TGA showed that the addition of chemical activation (Na_2SO_4) promoted ettringite formation. Chemical activation as well as mechanical activation increased the rate at which portlandite was consumed which is indicative of an increase in the reaction rate between cement and fly ash.

It was found that the combination of activation techniques (MUFA5) did not result in more ettringite formation than chemical activation on its own (UFA). However, the combined activation resulted in the highest rate of portlandite consumption, hence an increased rate of the pozzolanic reaction.

FTIR was the only characterisation technique independent of degree of crystallinity of the hydration products, and hence FTIR could be used to identify the gels that usually form as part of cement hydration. In this case, all four of the hybrid cement pastes proved to contain C-S-H-type gel, already visible after 1 day of hydration. The presence of additional types of gel that may have formed, were not evident from the transmission spectra.

Objective 5

Reporting and discussion of the strength behaviour of fly ash-based hybrid mortar cements containing 70% of the three fly ashes, differentiated by fineness and/or particle shape (due to mechanical activation), at different sulfate additions and curing ages (up to one year) (Chapter 7).

Despite its favourable particle shape distribution and mineralogy, the fine classified fly ash (FCFA) proved not to be the most chemically reactive of the three fly ashes considered. Strength development in hybrid cement containing FCFA is likely attributed to physical rather than chemical contributions.

The milled unclassified fly ash (MUFA) hybrid achieved the highest compressive strength results at all curing ages considered.

Considering the strength specifications of EN 197 / SANS 50197, FCFA only produced one product complying with a 32.5N cement when 5% sodium sulfate was added. The unclassified fly ash (UFA) hybrid, even after chemical activation, did not produce any strengths complying with the cement specification. The MUFA hybrid was the only blend that produced compressive strengths that comply with a 32.5R (rapid early strength gain) product according to EN 197 / SANS 50197, at both 3% and 5% sodium sulfate addition. The lower sulfate content would however be the more cost effective option.

The combination of mechanical and chemical activation (sodium sulfate) can be considered a valuable technique to address low early strengths and slow strength development, resulting in hybrid cements that comply with the EN 197 / SANS 50197 cement strength requirements.

It has been proven, as was predicted from the setting time and heat evolution data in Chapter 6 that, the combination of chemical (Na_2SO_4) and mechanical activation (MUFA5) of fly ash results in a superior performing fly ash hybrid cement.

Objective 6

Reporting and discussion of the slump retention and strength behaviour of concrete made with fly ash-based hybrid cement containing 70% of the three fly ashes, differentiated by fineness and/or particle shape (due to mechanical activation), at different sulfate additions and curing ages (up to one year) (Chapter 8).

Even in concrete compressive strength, the advantage of chemical activation in any of the three fly ash scenarios, is evident. It could also be seen that FCFA may be the least chemically reactive, but it is possible that it is enhancing strength by possibly improving the packing density of the specimens be means of the filler effect. Hence, the strength advantages realised from use of FCFA may be attributed to its physical nature, rather than its chemical reactivity.

Although mechanical activation reduced workability of the concrete mix, it is imperative to remember that these mixes were not optimised with regards to binder:water ratio. The latter could significantly improve workability.

9.3. Recommendations for future work

Due to the millions of tons of ash stockpiled in South Africa, more research on this local resource as a supplementary cementitious material needs to be conducted.

It is imperative to understand different behavioural properties of the fly ashes produced from varying qualities of coal. Hence, future work may investigate fly ash from all of the different sources in South Africa when used for the production of fly ash hybrid cement.

For more definitive characterisation of the amorphous-type gels that are produced during hydration of the discussed hybrids cements, it would be of value to include solid state nuclear magnetic resonance (solid state NMR) as a characterisation tool.

It will be imperative to optimise concrete mixes with regard to water:binder ratio in order to improve workability of the MUFA hybrid. Hence, a study whereby different water:binder ratios are investigated will be of great value towards the application of these types of hybrid cements in concrete.

Seeing that the type of hybrid studied in this thesis falls outside of the scope of EN 197 for allowable cements and fly ash contents, and should it ever be included in the scope, it will be imperative to do more comprehensive work on the durability properties of such a product.

It will also be worthwhile to investigate the possibility of alkali silica reaction (ASR).

References

ACAA. 2014. *American Coal Ash Association. 2014 Coal Combustion Product (CCP) Production & Use Survey Report.* [Online]. Available: https://www.acaa-usa.org/ [Accessed 04-03-2016].

ADAA. 2014. *Ash Development Association of Australia (ADAA). Annual Membership Survey Results.* [Online]. Available: http://www.adaa.asn.au/home.php [Accessed 03-04-2016].

Al-Zahrani, M.M., Al-Tayyib, A.-H.J., Al-Dulaijan, S.U. & Osei-Twum, E. 2006. 29Si MAS-NMR study of hydrated cement paste and mortar with varying content of fly ash. *Advances in Cement Research,* 18(1):27-34.

Alexander, M.G., Barnard, J.L., Bennie, I.M., Burch, B., Callaghan, B.G., Dutton, A.R., Glauber, I., Hodgkiss, J.E., Kaplan, M.F., Keene, P.W., Kruger, J.E., Lane, J.W., Oberholster, R.E., Thompson, C.J., Dijk, J.V., Aardt, J.H.P.V. & Vasarhelyi, M.A. 1986. *Fulton's Concrete Technology.* South Africa: The Natal Witness (Pty) Ltd.

Baert, G., Hoste, S., Schutter, G.D. & Belie, N.D. 2008. Reactivity of fly ash in cement paste studied by means of thermogravimetry and isothermal calorimetry. *Journal of Thermal Analysis and Calorimetry,* 94(2):485-492.

Balaz, P. 2008. *Mechanochemistry in Nanoscience and Minerals Engineering.* Springer.

Bentur, A. 1976. Effect of Gypsum on the Hydration and Strength of C3S Pastes. *Journal of the American Ceramic Society,* 59(5-6):210-213.

Blanco, F., Garcia, M.P., Ayala, J., Mayoral, G. & Garcia, M.A. 2006. The effect of mechanically and chemically activated fly ashes on mortar properties. *Fuel,* 85(14-15):2018-2026.

Blissett, R.S. & Rowson, N.A. 2012. A review of the multi-component utilisation of coal fly ash. *Fuel,* 97:1-23.

CEN 2011. Cement - Part 1: Composition, specifications and conformity criteria for common cements. *EN 197-1.* Brussels: European Committee for Standardization.

CEN 2016. Methods of testing cement - Part 1: Determination of strength. *EN 196-1:2016.* European Committee for Standardization.

Choudhary, H.K., Anupama, A.V., Kumar, R., Panzi, M.E., Matteppanavar, S., Sherikar, B.N. & Sahoo, B. 2015. Observation of phase transformations in cement during hydration. *Construction and Building Materials,* 101:122-129.

Chrysochoou, M. & Dermatas, D. 2006. Evaluation of ettringite and hydrocalumite formation for heavy metal immobilization: literature review and experimental study. *J Hazard Mater,* 136(1):20-33.

Criado, M., Fernandez-Jimenez, A. & Palomo, A. 2007. Alkali activation of fly ash: Effect of the SiO2/Na2O ratio Part I: FTIR study. *Microporous and Mesoporous Materials,* 106 180–191.

Criado, M., Jiménez, A.F. & Palomo, A. 2010. Effect of sodium sulfate on the alkali activation of fly ash. *Cement & Concrete Composites 32,* 32:589–594.

Deschner, F., Winnefeld, F., Lothenbach, B., Seufert, S., Schwesig, P., Dittrich, S., Goetz-Neunhoeffer, F. & Neubauer, J. 2012. Hydration of Portland cement with high replacement by siliceous fly ash. *Cement and Concrete Research,* 42(10):1389-1400.

Dilnesa, B.Z. *APPLICATION OF THERMOGRAVIMETRIC METHOD IN CEMENT SCIENCE.* [Online]. Available: [Accessed 23-01-2016].

Domone, P.L. 2003. Fresh concrete. In: Newman, J. & Choo, B.S. (eds.). *Advanced Concrete Technology.* Burlington: Elsevier.

Donatello, S., Fernández-Jimenez, A., Palomo, A. & Jantzen, C. 2013. Very High Volume Fly Ash Cements. Early Age Hydration Study Using Na2SO4 as an Activator. *Journal of the American Ceramic Society,* 96(3):900-906.

Donatello, S., Garcia-Lodeiro, I., Fernandez-Jimenez, A. & Palomo, A. 2014a. Some durability aspects of hybrid alkaline cements. *MATEC Web of Conferences,* 11:01008.

Donatello, S., Maltseva, O., Fernandez-Jimenez, A., Palomo, A. & Klein, L. 2014b. The Early Age Hydration Reactions of a Hybrid Cement Containing a Very High Content of Coal Bottom Ash. *Journal of the American Ceramic Society,* 97(3):929-937.

Duchesne, J., Duong, L., Bostrom, T. & Frost, R. 2010. Microstructure Study of Early In Situ Reaction of Fly Ash Geopolymer Observed by Environmental Scanning Electron Microscopy (ESEM). *Waste and Biomass Valorization,* 1(3):367-377.

Fanghui, H., Qiang, W. & Jingjing, F. 2015. The differences among the roles of ground fly ash in the paste, mortar and concrete. *Construction and Building Materials,* 93:172-179.

Fernández-Jiménez, A. & Palomo, A. 2003. Characterisation of fly ashes. Potential reactivity as alkaline cements☆. *Fuel,* 82(18):2259-2265.

Fernández-Jiménez, A., Sobrados, I., Sanz, J. & Palomo, A. 2011. Hybrid cements with very low OPC content. International Congress on the Chemistry of Cement ICCC XIII. Madrid.

Garcia-Lodeiro, I., Carcelen-Taboada, V., Fernández-Jiménez, A. & Palomo, A. 2016a. Manufacture of hybrid cements with fly ash and bottom ash from a municipal solid waste incinerator. *Construction and Building Materials,* 105:218-226.

Garcia-Lodeiro, I., Donatello, S., Fernández-Jiménez, A. & Palomo, Á. 2016b. Hydration of Hybrid Alkaline Cement Containing a Very Large Proportion of Fly Ash: A Descriptive Model. *Materials,* 9(8):605.

Garcia-Lodeiro, I., Fernández-Jimenez, A. & Palomo, A. 2015. Cements with a low clinker content: versatile use of raw materials. *Journal of Sustainable Cement-Based Materials,* 4(2):140-151.

García-Lodeiro, I., Fernández-Jiménez, A. & Palomo, A. 2013a. Hydration kinetics in hybrid binders: Early reaction stages. *Cement and Concrete Composites*, 39:82-92.

García-Lodeiro, I., Fernández-Jiménez, A. & Palomo, A. 2013b. Variation in hybrid cements over time. Alkaline activation of fly ash–portland cement blends. *Cement and Concrete Research*, 52:112-122.

Garcia-Lodeiro, I., Taboada, V.C., Fernández-Jiménez, A. & Palomo, Á. 2016c. Recycling Industrial By-Products in Hybrid Cements: Mechanical and Microstructure Characterization. *Waste and Biomass Valorization*.

Heidrich, C., Feuerborn, H.-J. & Weir, A. 2013. Coal Combustion Products: a Global Perspective. 2013 World of Coal Ash (WOCA) Conference Lexington, KY.

Heinz, D., Göbel, M., Hilbig, H., Urbonas, L. & Bujauskaite, G. 2010. Effect of TEA on fly ash solubility and early age strength of mortar. *Cement and Concrete Research,* 40(3):392-397.

Hewlett, P. 2004. *Lea's Chemistry Of Cement And Concrete (4th Ed).* Elsevier Science & Technology Books.

Horgnies, M., Chen, J.J. & Bouillon, C. 2013. Overview about the use of Fourier Transform Infrared spectroscopy to study cementitious materials. *Materials Characterisation VI,* 1:251-262.

Hu, J., Ge, Z. & Wang, K. 2014. Influence of cement fineness and water-to-cement ratio on mortar early-age heat of hydration and set times. *Construction and Building Materials,* 50:657-663.

Hughes, T.L., Methven, C.M., Jones, T.G.J., Pelham, S.E., Fletcher, P. & Hall, C. 1995. Determining Cement Composition by Fourier Transform Infrared Spectroscopy. *Advn Cem Bas Mat,* 2:91-104.

IEA 2015. IEA Statistics: Key Coal Trends - Excerpt from Coal Information. 2015 ed.: International Energy Agency.

Inés García-Lodeiro, O.M., Ángel Palomo, Ana Fernández-Jiménez. 2012. Hybrid Alkaline Cements. Part I: Fundamentals. *Romanian Journal of Materials*, 42(4):330-335.

Institute, C.a.C. 2009. *Fulton's concrete technology, 9.* South Africa: Intrepid Printers (Pty) Ltd.

Iyer, R.S. & Scott, J.A. 2001. Power station fly ash — a review of value-added utilization outside of the construction industry. *Resources, Conservation and Recycling,* 31:217–228.

Kaur, A., Bishnoi, S. & Bhattacharjee, B. 2017. Characteristics of fly ashes in India for use in cement and concrete. *Advances in Cement Research*:1-11.

Kearsley, E.P. & Wainwright, P.J. 2003. Effect of fly ash properties on concrete strength. *Journal of the South African Institution of Civil Engineers,* 45(1):19-24.

Kocaba, V. 2009. *Development and Evaluation of Methods to Follow Microstructural Development of Cementitious Systems Including Slags.* Ecole Polytechnique Federale de Lausanne.

Kontoleontos, F., Katsiotisa, N., Tsakiridisb, P., Kaloidasc, V., Marinosa, A. & Katsiotia, M. 2013. Dry-grinded Ultrafine Cements Hydration. Physicochemical and Microstructural Characterization. *Materials Research,* 16(2):404-416.

Kovtun, M., Kearsley, E.P. & Shekhovtsova, J. 2015. Dry powder alkali-activated slag cements. *Advances in Cement Research,* 27(8):447-456.

Krüger, J.E. 2003. South African fly ash: a cement extender. South Africa: South African Coal Ash Association (SACAA).

Kruger, R.A. 1997. Fly ash beneficiation in South Africa: creating new opportunities in the market-place. *Fuel,* 76(8):777-779.

Kruger, R.A. 2013. Coal ash in South Africa : Production, Utilisation and Research. . South African Coal Ash Association.

Kruger, R.A. & Krueger, J.E. 2005. Historical Development of Coal Ash Utilisation in South Africa. 2005 World of Coal Ash. Kentucky, USA.

Kumar, R., Kumar, S. & Mehrotra, S.P. 2007. Towards sustainable solutions for fly ash through mechanical activation. *Resources, Conservation and Recycling,* 52(2):157-179.

Kumar, S. & Kumar, R. 2011. Mechanical activation of fly ash: Effect on reaction, structure and properties of resulting geopolymer. *Ceramics International,* 37(2):533-541.

Kumar, S., Kumar, R. & Bandopadhyay, A. 2006. Innovative methodologies for the utilisation of wastes from metallurgical and allied industries. *Resources, Conservation and Recycling,* 48(4):301-314.

Lee, C.Y., Lee, H.K. & Leeb, K.M. 2003. Strength and microstructural characteristics of chemically activated fly ash–cement systems. *Cement and Concrete Research,* 33:425-431.

Leklou, N., Aubert, J.-E. & Escadeillas, G. 2008. Microscopic observations of samples affected by delayed ettringite formation (DEF). *Materials and Structures,* 42(10):1369-1378.

Lerch, W. 1945. Effect of SO_3 Content of Cement on Durability of Concrete. Illinois: Portland Cement Association.

Lothenbach, B., Durdzinski, P. & De Weerdt, K. 2016. Thermogravimetric analysis. In: Scrivener, K.L., Snellings, R. & Lothenbach, B. (eds.). *A Practical Guide to Microstructural Analysis of Cementitious Materials.* UK: CRC Press.

Mejía, J.M., Rodríguez, E., Mejía De Gutiérrez, R. & Gallego, N. 2015. Preparation and characterization of a hybrid alkaline binder based on a fly ash with no commercial value. *Journal of Cleaner Production,* 104:346-352.

Mingard, K., R, M., Jackson, P., Lawson, S., Patel, S. & Buxton, R. 2009. Measurement Good Practice Guide No. 111. *Improving the consistency of particle size measurement.* Scotland: National Physical Laboratory.

Mollah, M.Y.A., Yu, W., Schennach, R. & Cocke, D.L. 2000. A Fourier transform infrared spectroscopic investigation of the early hydration of Portland cement and the influence of sodium lignosulfonate. *Cement and Concrete Research* 30:267–273.

Olivier, J.G.J., Janssens-Meanhout, G., Muntean, M. & Peters, J.a.H.W. 2015. Trends in global CO2 emissions: 2015 Report. *In:* Jrc, P.A. (ed.). The Hague: PBL Nethrelands Environmental Assessment Agency; Ispra: European Commission Joint Research Centre.

Pacheco-Torgal, F., Labrincha, J.A., Leonelli, C., Palomo, A. & Chindaprasirt, P. 2015. *Handbook of Alkali-activated Cements, Mortars and Concretes.* United Kingdom: Woodmead Publishing.

Palomo, A., Fernández-Jiménez, A., Kovalchuk, G., Ordoñez, L.M. & Naranjo, M.C. 2007. Opc-fly ash cementitious systems: study of gel binders produced during alkaline hydration. *Journal of Materials Science,* 42(9):2958-2966.

Palomo, A., Krivenko, P., Garcia-Lodeiro, I., Kavalerova, E., Maltseva, O. & Fernández-Jiménez, A. 2014. A review on alkaline activation: new analytical perspectives. *Materiales de Construcción,* 64(315):e022.

PCA 2001. Ettringite Formation and the Performance of Concrete. Portland Cement Association

PCA. 2004. *Innovations in Portland Cement Manufacturing.* U.S.A: Portland Cement Association.

Qian, J., Shi, C. & Wang, Z. 2001. Activation of blended cements containing fly ash. *Cement and Concrete Research,* 31:1121–1127.

Qiao, X.C., Poon, C.S. & Cheung, E. 2006. Comparative studies of three methods for activating rejected fly ash. *Advances in Cement Research,* 18(4):165-170.

Rashad, A.M. 2014. A comprehensive overview about the influence of different admixtures and additives on the properties of alkali-activated fly ash. *Materials & Design,* 53:1005-1025.

Reynolds-Clausen, K. & Singh, N. 2017. Eskom's revised Coal Ash Strategy and Implementation Progress. World of Coal Ash (WOCA) Conference. Lexington, Kentucky. .

SABS 1982. Standardized Specification for Civil Engineering Construction. *G : CONCRETE (STRUCTURAL)* Pretoria: South African Bureau of Standards.

SABS 2006a. Concrete tests — Compressive strength of hardened concrete. *SANS 5863:2006 Edition 2.1.* Pretoria, South Africa: SABS Standards Division.

SABS 2006b. Concrete tests — Consistence of freshly mixed concrete — Slump test. *SANS 5862-1:2006 Edition 2.1.* Pretoria, South Africa: SABS Standards Division.

SABS 2006c. Methods of testing cement - Part 3: Determination of setting times and soundness. *SANS 50196-3:2006 Edition 2* Pretoria, South Africa: SABS Standards Division.

SABS 2013a. Cement - Part 1: Composition, specifications and conformity criteria for common cements. *SANS 50197-1.* Pretoria: SABS Standards Division.

SABS 2013b. Fly ash for concrete - Part 1: Definition, specifications and conformity criteria. *SANS 50450-1.* Pretoria, South Africa: SABS Standards Division.

Sarkar, A., Rano, R., Mishra, K.K. & Sinha, I.N. 2005. Particle size distribution profile of some Indian fly ash—a comparative study to assess their possible uses. *Fuel Processing Technology,* 86(11):1221-1238.

Shekhovtsova, J., Kovtun, M. & Kearsley, E.P. 2016. Temperature rise and initial shrinkage of alkali-activated fly ash cement pastes. *Advances in Cement Research,* 28(1):3-12.

Shi, C. 1996. Early Microstructure Development of Activated Lime-Fly Ash Pastes. *Cement and Concrete Research,* 26(9):1351-1359.

Shi, C. & Day, R.L. 1995. Acceleration of the reactivity of fly ash by chemical activation. *Cement and Concrete Research,* 25(1):15-21.

Shi, C., Jiménez, A.F. & Palomo, A. 2011. New cements for the 21st century: The pursuit of an alternative to Portland cement. *Cement and Concrete Research,* 41(7):750-763.

Snellings, R. 2016. X-ray powder diffraction applied to cement. In: Scrivener, K.L., Snellings, R. & Lothenbach, B. (eds.). *A Practical Guide to Microstructural Analysis of Cementitious Materials.* UK: CRC Press.

Snellings, R., Salze, A. & Scrivener, K.L. 2014. Use of X-ray diffraction to quantify amorphous supplementary cementitious materials in anhydrous and hydrated blended cements. *Cement and Concrete Research,* 64:89-98.

Tangpagasit, J., Cheerarot, R., Jaturapitakkul, C. & Kiattikomol, K. 2005. Packing effect and pozzolanic reaction of fly ash in mortar. *Cement and Concrete Research,* 35(6):1145-1151.

Taylor, H.F.W. 1997. *Cement Chem Taylor 2nd ed.* London: Thomas Telford Publishing.

Temuujin, J., Williams, R.P. & Van Riessen, A. 2009. Effect of mechanical activation of fly ash on the properties of geopolymer cured at ambient temperature. *Journal of Materials Processing Technology,* 209(12-13):5276-5280.

Tomeczec, J. & Palugniok, H. 2002. Kinetics of mineral matter transformation during coal combustion. *Fuel,* 81:1251-1258.

UKQAA. 2014. *UK Quality Ash Association. Ash Statistics for 2014.* [Online]. Available: http://www.ukqaa.org.uk/ [Accessed 04-03-2016].

Van Der Merwe, E.M., Prinsloo, L.C., Mathebula, C.L., Swart, H.C., Coetsee, E. & Doucet, F.J. 2014. Surface and bulk characterization of an ultrafine South African coal fly ash with reference to polymer applications. *Applied Surface Science,* 317:73-83.

Velandia, D.F., Lynsdale, C.J., Provis, J.L., Ramirez, F. & Gomez, A.C. 2016. Evaluation of activated high volume fly ash systems using Na_2SO_4, lime and quicklime in mortars with high loss on ignition fly ashes. *Construction and Building Materials,* 128:248-255.

Wadso, L., Winnefeld, F., Ridingt, K. & Sandberg, P. 2016. Calorimetry. In: Scrivener, K.L., Snellings, R. & Lothenbach, B. (eds.). *A Practical Guide to Microstructural Analysis of Cementitious Materials.* UK: CRC Press.

Wee, J.-H. 2013. A review on carbon dioxide capture and storage technology using coal fly ash. *Applied Energy,* 106:143-151.

Winter, N.B. 2009. *Understanding Cement* United Kingdom: WHD Microanalysis Consultants Ltd.

Yao, Z.T., Ji, X.S., Sarker, P.K., Tang, J.H., Ge, L.Q., Xia, M.S. & Xi, Y.Q. 2015. A comprehensive review on the applications of coal fly ash. *Earth-Science Reviews,* 141:105-121.

Ylmén, R., Jäglid, U., Steenari, B.-M. & Panas, I. 2009. Early hydration and setting of Portland cement monitored by IR, SEM and Vicat techniques. *Cement and Concrete Research,* 39(5):433-439.

Zhang, Y. & Zhang, X. 2008. Research on effect of limestone and gypsum on C_3A, C_3S and PC clinker system. *Construction and Building Materials,* 22(8):1634-1642.

Zhao, J., Wang, D., Wang, X., Liao, S. & Lin, H. 2015. Ultrafine grinding of fly ash with grinding aids: Impact on particle characteristics of ultrafine fly ash and properties of blended cement containing ultrafine fly ash. *Construction and Building Materials,* 78:250-259.